Coupled Fluid Flow, Deformation, Heat Transport & Mineral Reactions in Hydrothermal Mineralising Systems

热液成矿系统中流体流动，变形，热传递&矿物反应的耦合过程

Alison Ord

Centre for Exploration Targeting,
University of Western Australia

MULTISCALE DYNAMICS OF ORE BODY FORMATION

Bruce Hobbs, Weronika Gorczyk, Alison Ord and Klaus Gessner

成矿多尺度动力学

Thanks to Ian Tyler, Catherine Spaggiari and Hugh Smithies

MULTISCALE DYNAMICS OF HYDROTHERMAL MINERAL SYSTEMS
热液成矿系统多尺度动力学

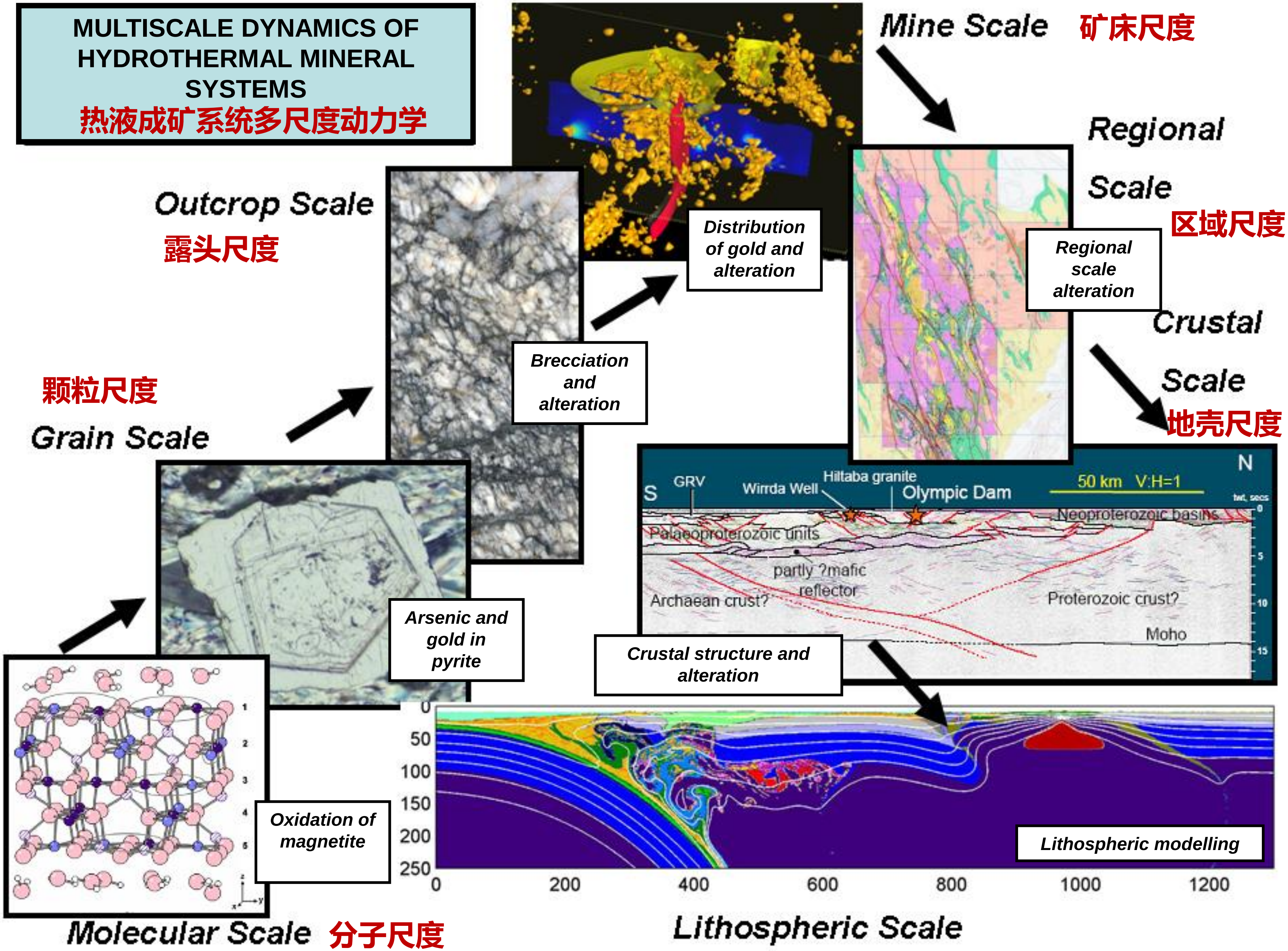

Approach

Hydrothermal mineralising systems are open flow thermodynamic systems held away from thermodynamic equilibrium by the flow of heat, chemical species, fluids, and momentum.

热液成矿系统是一个开放的流动热力学系统，由于热流，化学反应，流体以及动力而远离热力学平衡

These processes are coupled so that non-linear behaviour is expected.

这些过程是耦合的，所以有望呈现非线性特征

We explore a systems approach to hydrothermal mineralising systems, providing computational examples of interacting processes at various scales.

介绍对热液成矿系统的系统研究方法，以及在不同尺度下的相互作用的计算实例

The challenge for geologists is to develop robust models for the formation of high quality resources (large tonnage, high grade, and suitable metallurgical properties) that will impact significantly on global and local exploration strategies.

地质学家致力于开发一种形成高质量资源的稳健模型（储量大，高品位，利于冶炼），这些显著的影响全球和地区的勘探策略

It will be increasingly possible to formulate detailed models at the local, regional and lithospheric scale.

构建局部，区域，岩石圈尺度的精细模型愈发可能

This will drive a shift in perspective away from the traditional deposit-oriented and class-oriented approaches to ore deposit research towards understanding the basic and common processes that are involved in hydrothermal systems.

这将带来从传统的矿床导向，类型导向方法到了解热液系统的基础和普遍过程的转变

Arising from this systems, or holistic approach to ore deposit localisation, our goal is to develop a scenario testing methodology that enables the exploration team to test a range of hypotheses concerning an exploration model with the aim of decreasing the time and cost to discovery of significant mineral deposits.

我们的目标是建立一种基于场景测试的方法体系，能够对关于勘探模型的一系列假设进行验证，以减少发现大型矿床的时间和资金消耗

If one is to develop a quantitative, rather than qualitative approach to the modelling of hydrothermal ore processes then it is clear from the start that a number of difficulties arise from the uncertainties involved in precisely defining or understanding, at the time of mineralisation,

采取定量方法去对热液成矿过程进行模拟，一些难题应运而生，在成矿发生时

- the geometry and dimensions of the ore system,
- 矿床系统的几何形状和尺寸
- the physical and chemical characteristics of the system, 矿床系统的物理和化学特征
- the geodynamic history, 地球动力学历史
- the processes responsible for fluid flow and
- 流体流动过程
- the processes involved in transport and deposition of the metal species. 金属成分的运移和沉淀过程

We chose to adopt a scenario approach similar to that used by the Royal Dutch Shell Group of Companies over the past 40 years.

我们采用了一套场景方法，类似于

Royal Dutch Shell公司在过去的40年里采用的方法

Scenarios regarding the formation of hydrothermal ore deposits are plausible and challenging stories.

They may not necessarily be correct.

关于热液矿床形成的故事似乎合理且赋有挑战，但可能并不是必然正确

They are meant to offer several alternative stories that describe how a particular ore body formed.

可能具有几种故事去解释某种矿体的形成

Each story must be plausible,

that is, internally consistent with all available data, & also challenging in that there is a deep dependence on the intuition & geological experience of the people developing the scenarios.

每一种故事都是可能的，也就是说，已知数据内在统一，这也挑战着于人们在构建场景时具有的直觉的地质经验的深度依赖

The development of these scenarios by a team helps to create a common culture and language through which a rigorous series of exploration models may be developed and explored. They challenge the mental maps held by the team.

构建这样的场景，可以通过构建一系列勘探模型帮助创造一种通用的文化和语言。

Models, Scenarios, & Stories

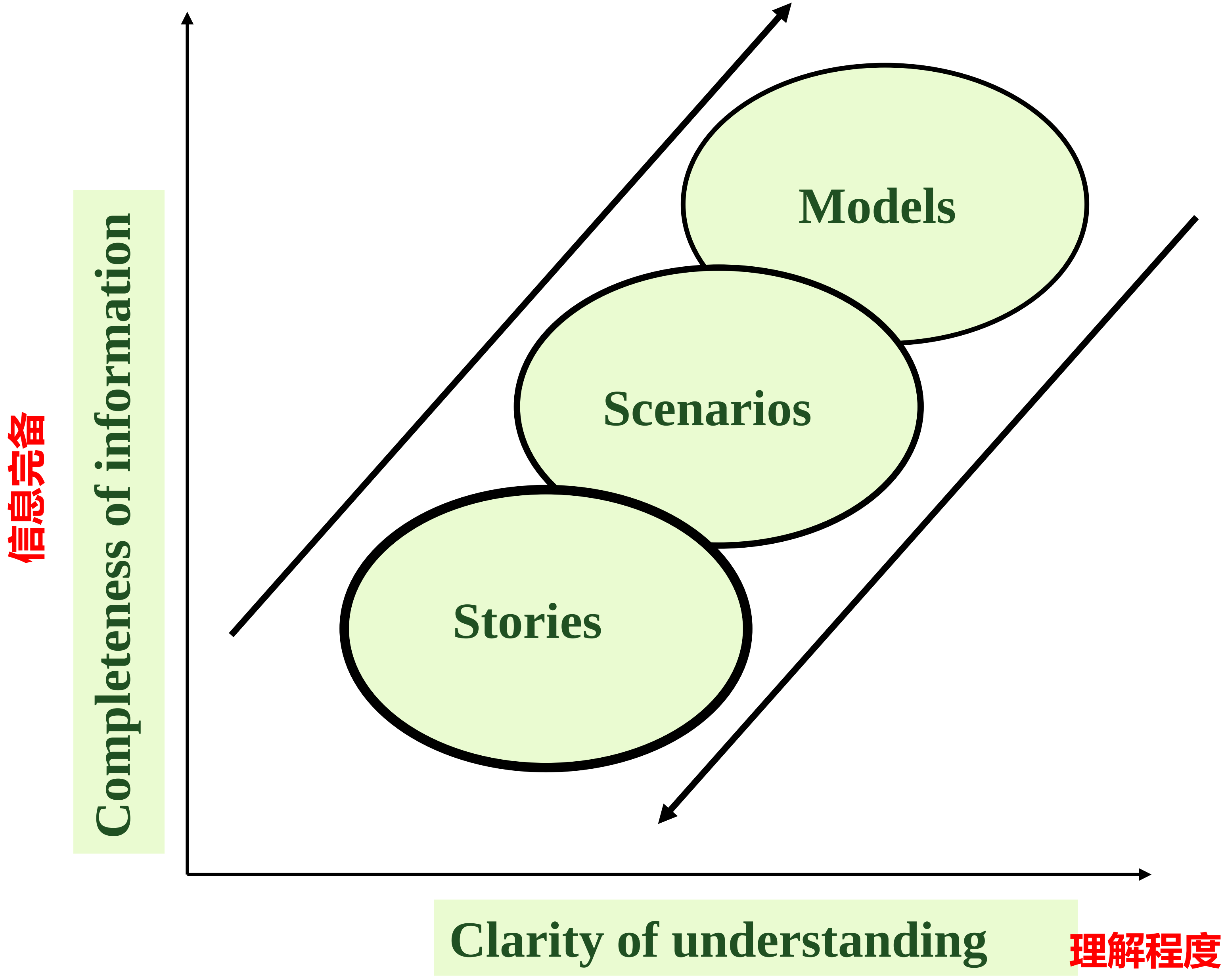

MOST FEATURES IN MINERALISED ROCKS FORM THROUGH INTERACTIONS BETWEEN FOUR TYPES OF PROCESSES.

矿化岩石中四种过程相互作用的显著特点

1. Deformation. 变形
2. Heat. 热
3. Fluid Flow. 流体流动
4. Chemical Reactions. 化学反应

HENCE OUR APPROACH OVER THE PAST DECADE HAS BEEN TO ASSEMBLE COMPUTER CODES THAT ENABLE THE SIMULATION OF THESE FOUR PROCESSES,

我们的方法集合了相关计算机代码，能够对这四种过程进行模拟。

FIRST
AS SINGLE PROCESSES AND PROGRESSIVELY, AS COMPLETELY COUPLED PROCESSES.

首先是对单一过程进行模拟，之后渐进的对四种过程进行全耦合模拟。

The approach allows industry to have greater confidence in its exploration programs

可以充分相信这些方法并应用于实际勘探项目，

CHEVRON FOLDS吉尔斯式褶皱

OTHER STYLES OF FOLDS其他类型褶皱

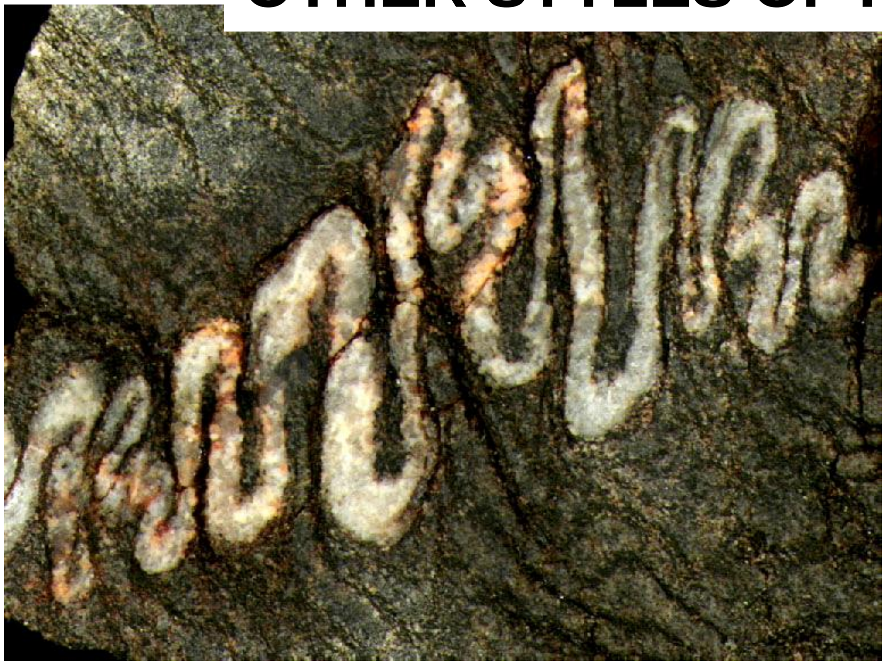

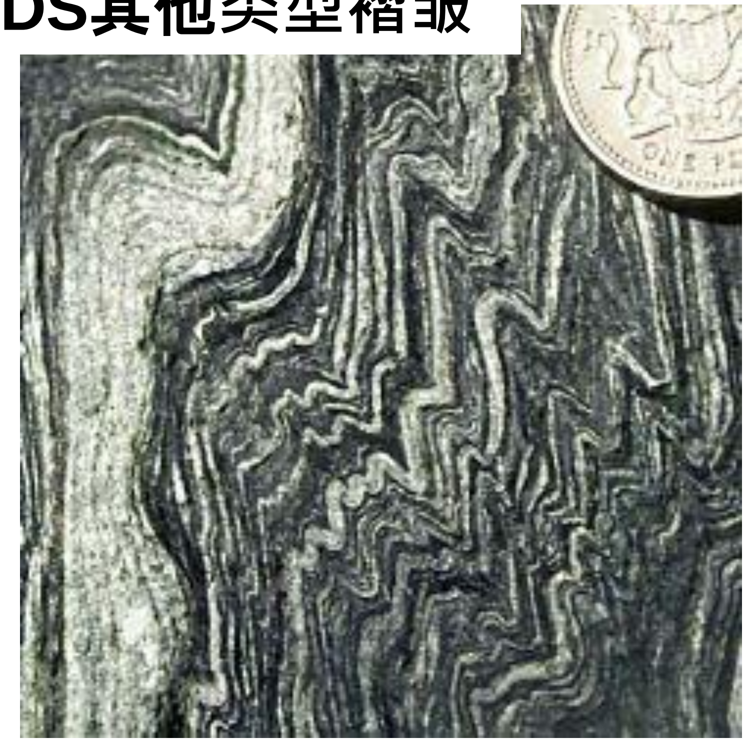

Micro-scale chemical reactions 微观化学反应

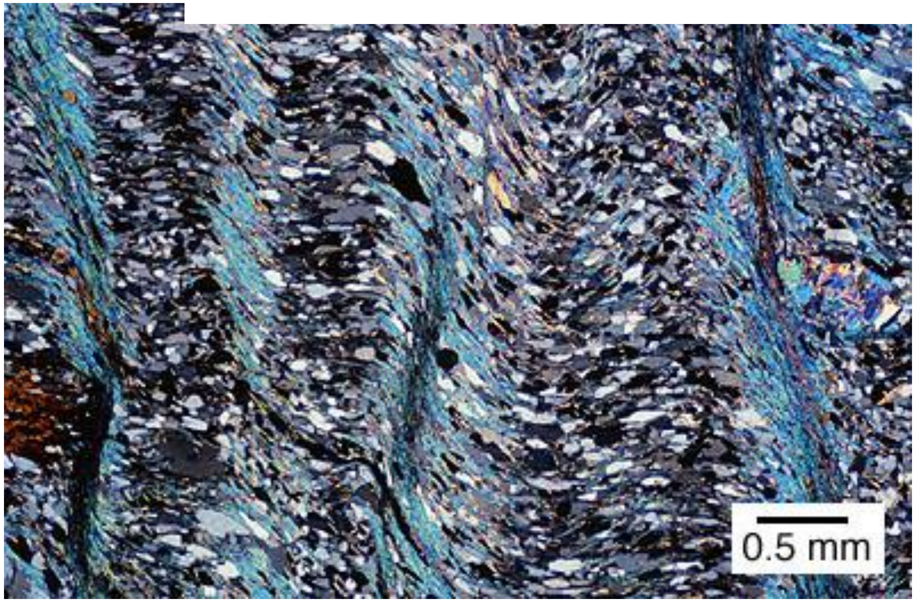

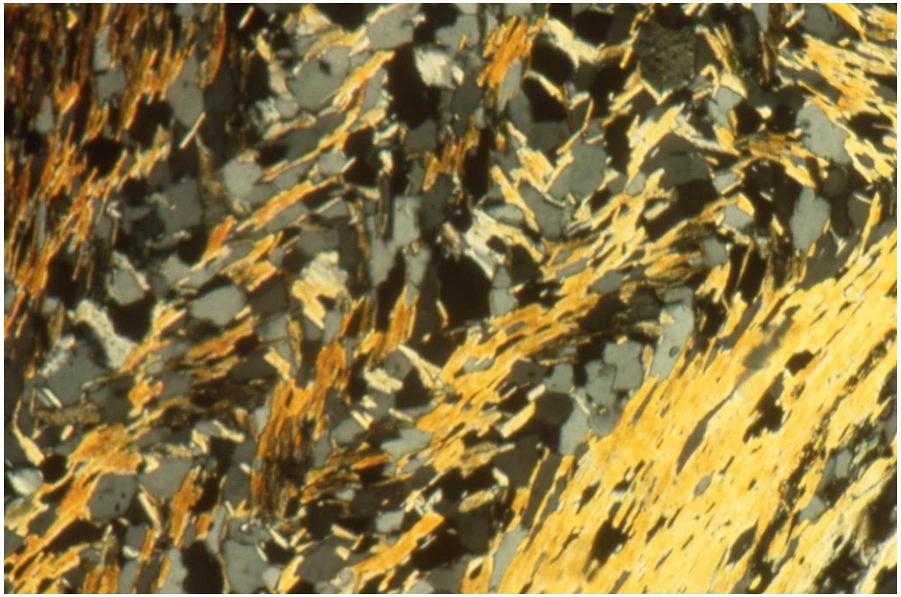

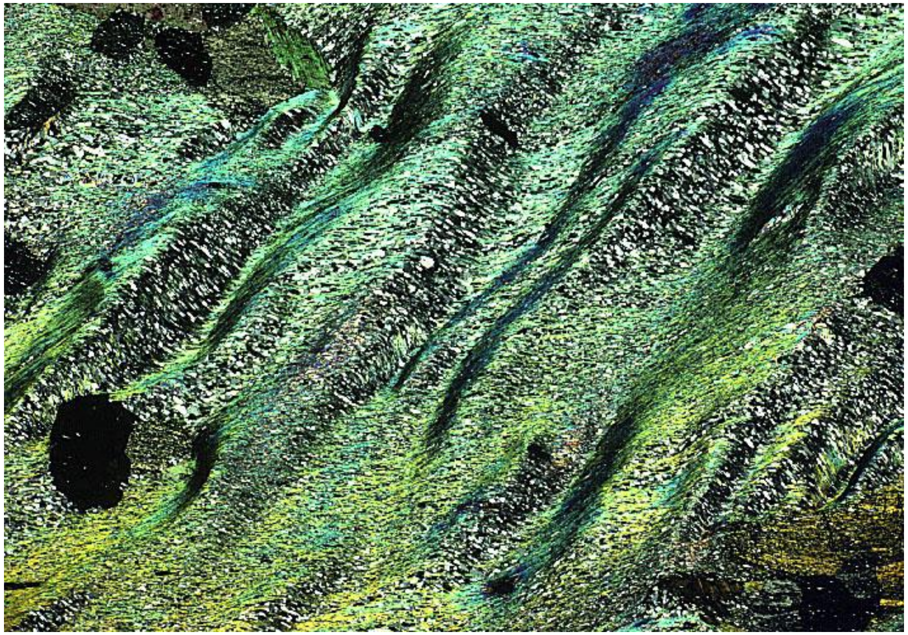

10 km

SCALE INVARIANCE IN STRUCTURAL GEOLOGY

构造地质中的标度不变性

1m

SIMILAR STRUCTURES AT ALL SCALES

各种尺度下相似结构

Photos: J-P. Burg

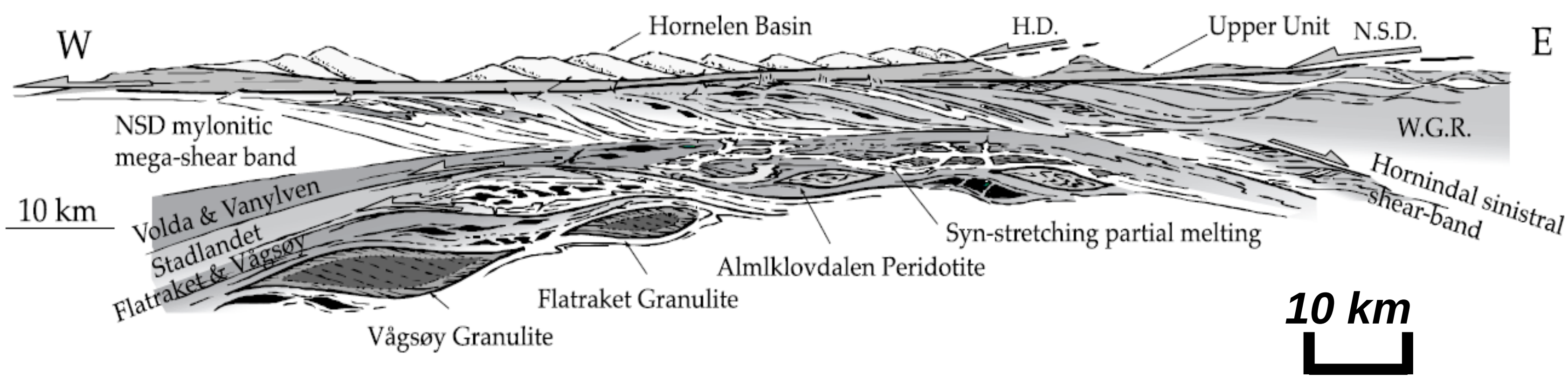

Fig. 3 Unscaled schematic cross-section showing the different areas and structural relations on a restored vertical profile. The core of the crustal boudin contains granulites and eclogites (black pods), Stadlandet, Vanylven and Volda are partly migmatized rims sheared to the west with amphibolitized eclogites. The Hornindal shear band is the symetrical limit of the boudin. On top, the ductile shear band associated to the NSD crosscuts these structures to the west.

各尺度下石香肠构造与局部熔融

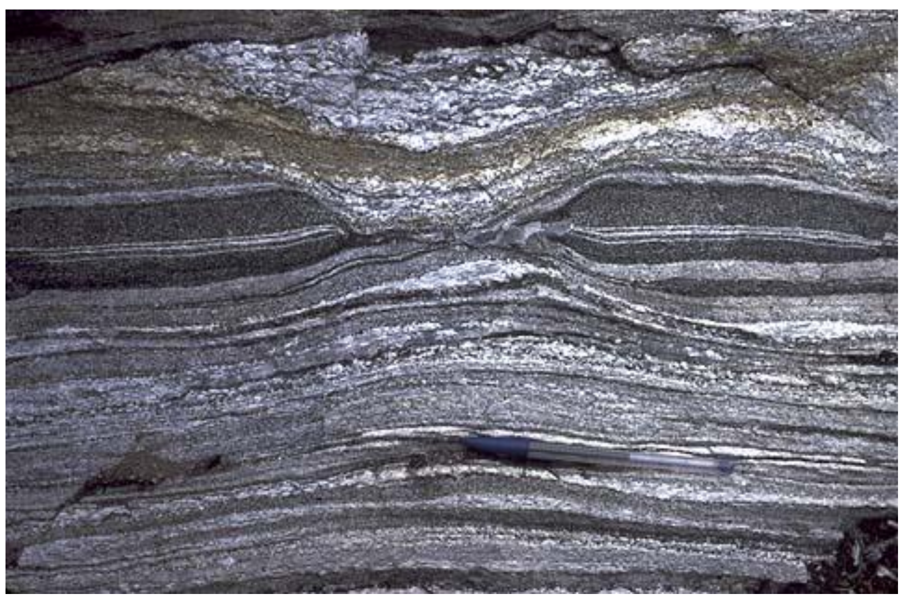

Boudinage and partial melting at all scales

10 cm

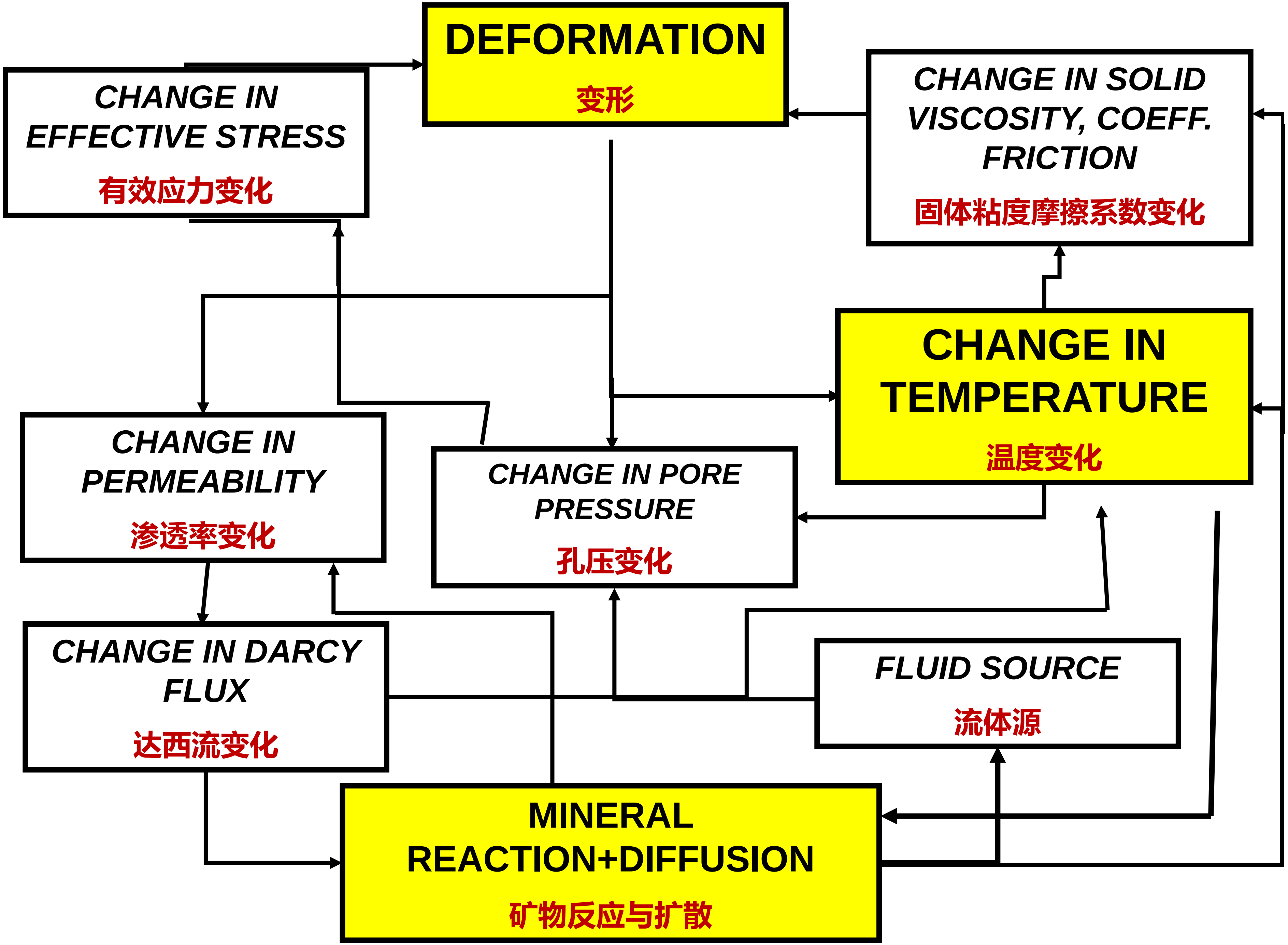
DEFORMATION
变形
CHANGE IN EFFECTIVE STRESS
有效应力变化
CHANGE IN SOLID VISCOSITY, COEFF. FRICTION
固体粘度摩擦系数变化
CHANGE IN TEMPERATURE
温度变化
CHANGE IN PERMEABILITY
渗透率变化
CHANGE IN PORE PRESSURE
孔压变化
CHANGE IN DARCY FLUX
达西流变化
FLUID SOURCE
流体源
MINERAL REACTION+DIFFUSION
矿物反应与扩散

热-力学褶皱

初始粘度比=5

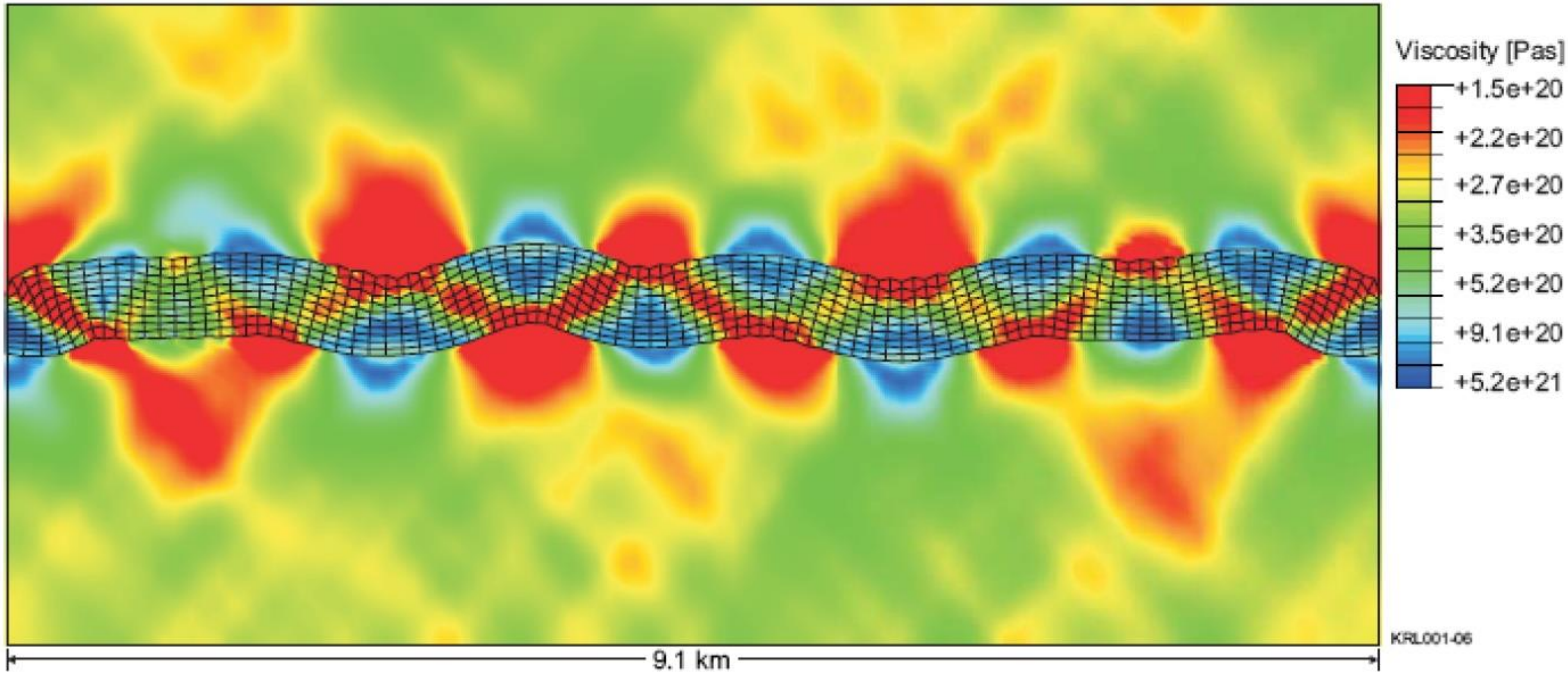

THERMAL-MECHANICAL FOLDING

INITIAL VISCOSITY RATIO = 5

热应变

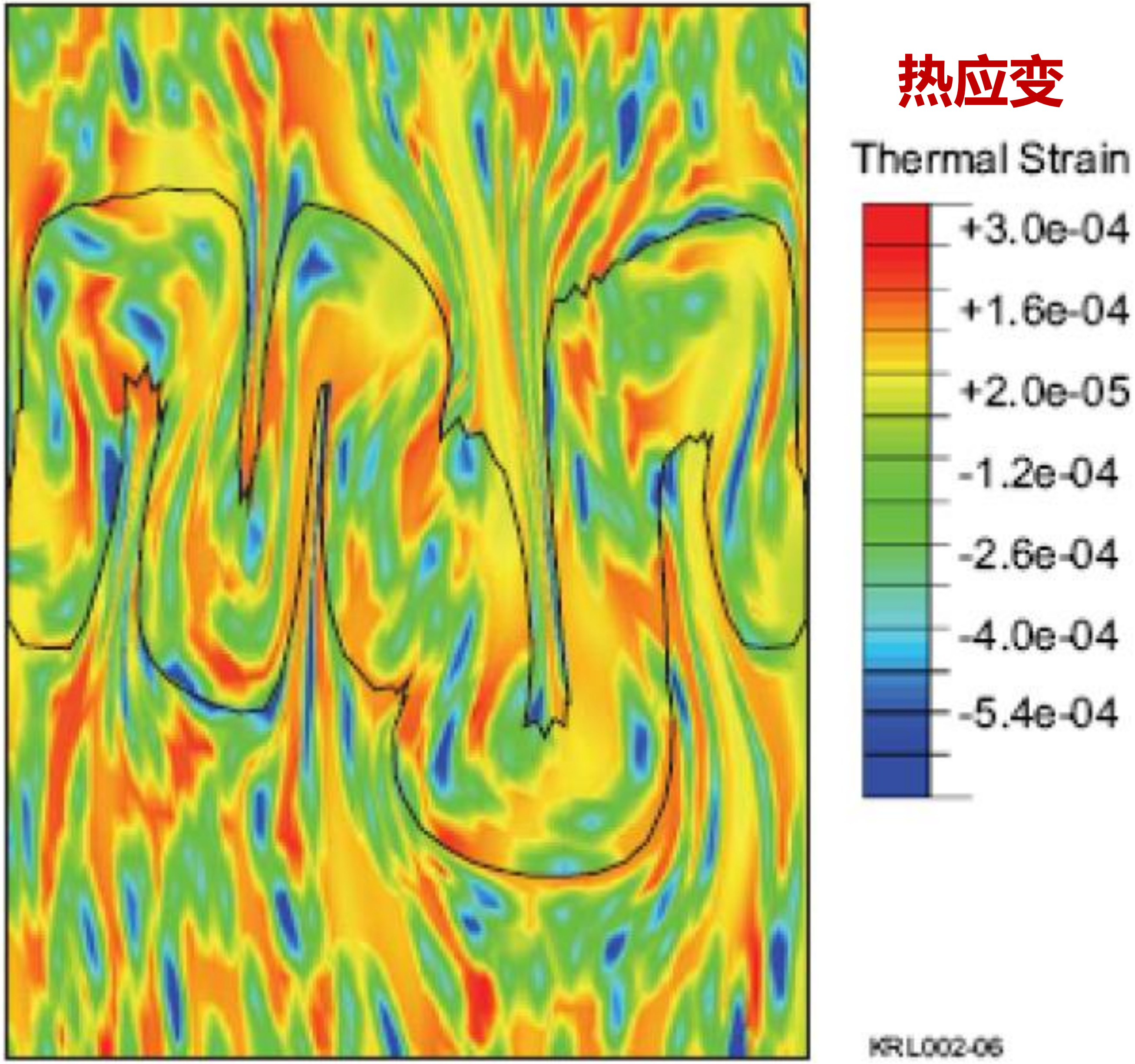
Thermal Strain
+3.0e-04
+1.6e-04
+2.0e-05
-1.2e-04
-2.6e-04
-4.0e-04
-5.4e-04
KRL002-06

Thermal
Mechanical
Coupling

热-力学耦合

无耦合

No
Coupling

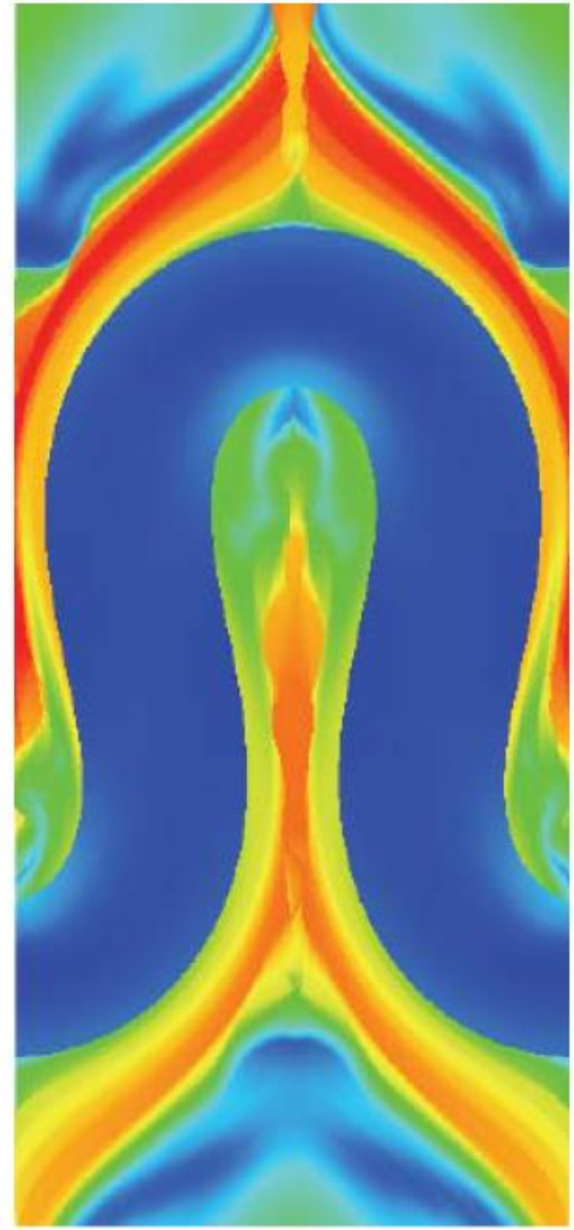

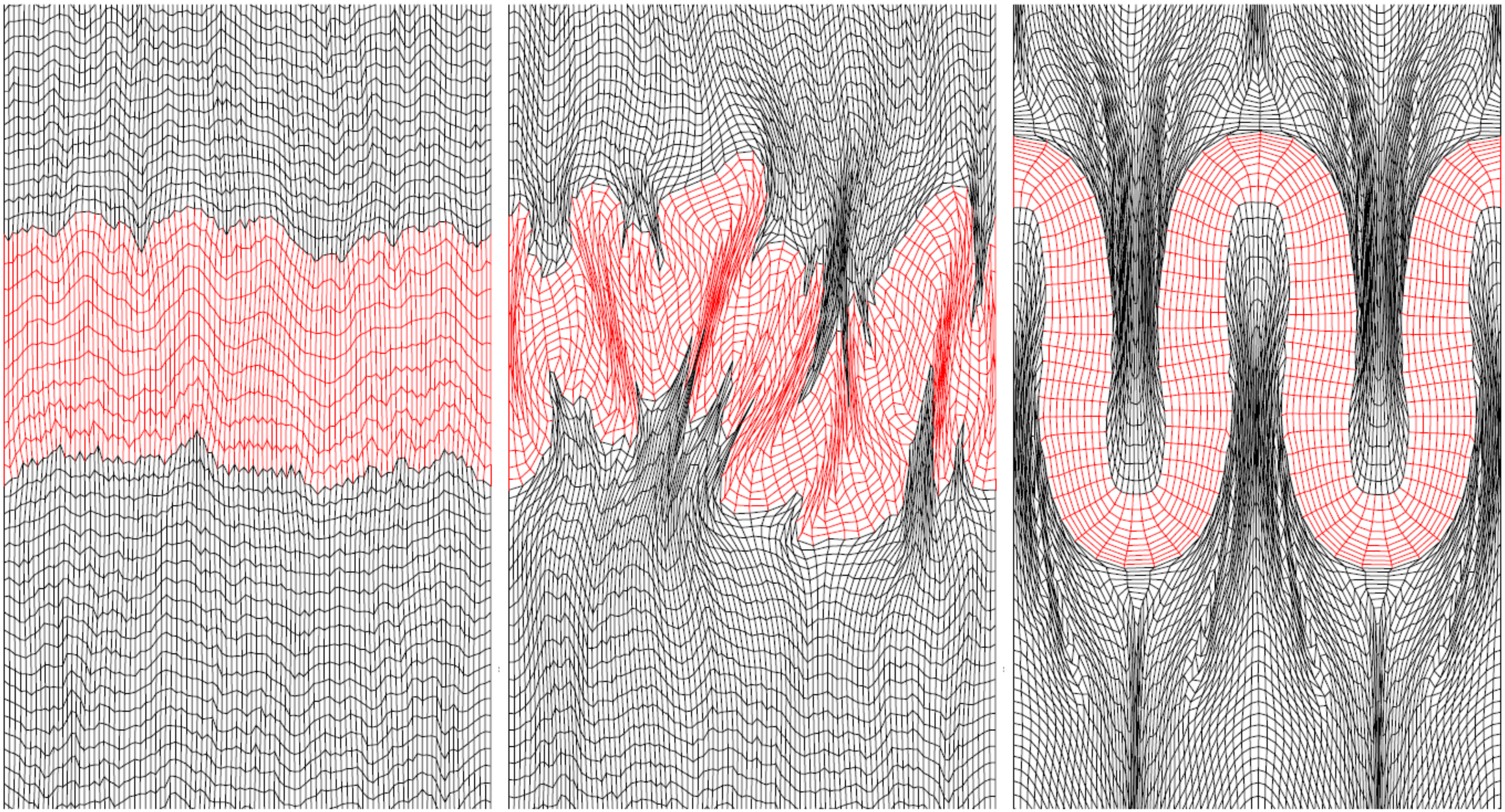

510 Kelvin 550 Kelvin 710 Kelvin

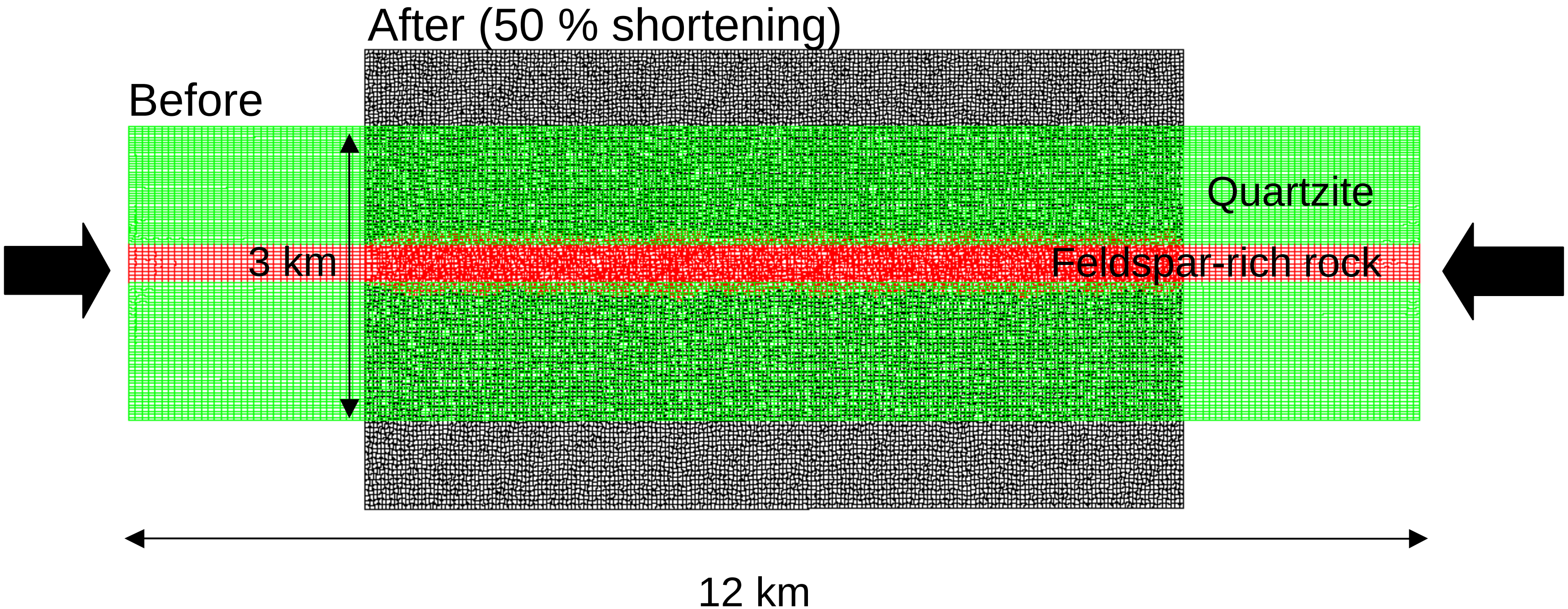

Thermal expansion included

MODEL SETUP

Length scale associated with shear zone development = (thermal diffusivity/strain-rate)$^{1/2}$

= $(10^{-6}/10^{-12})^{1/2}$ m = 1km

SENSITIVITY OF DEFORMATION TO TEMPERATURE.

变形对温度敏感程度

THE “BRITTLE-DUCTILE” TRANSITION.

脆-韧性转换

510 K

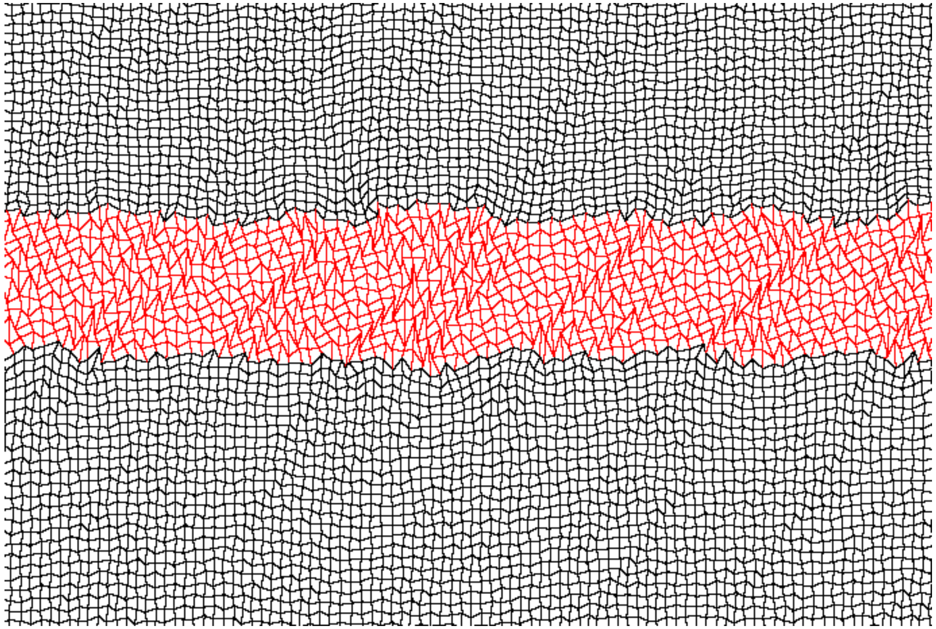

530 K

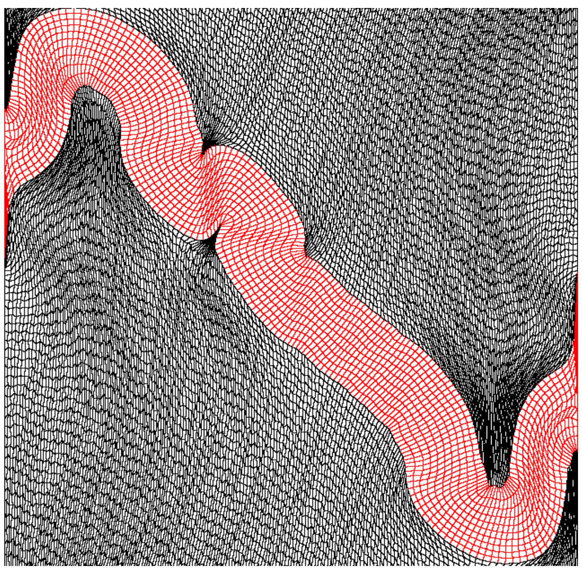

550 K

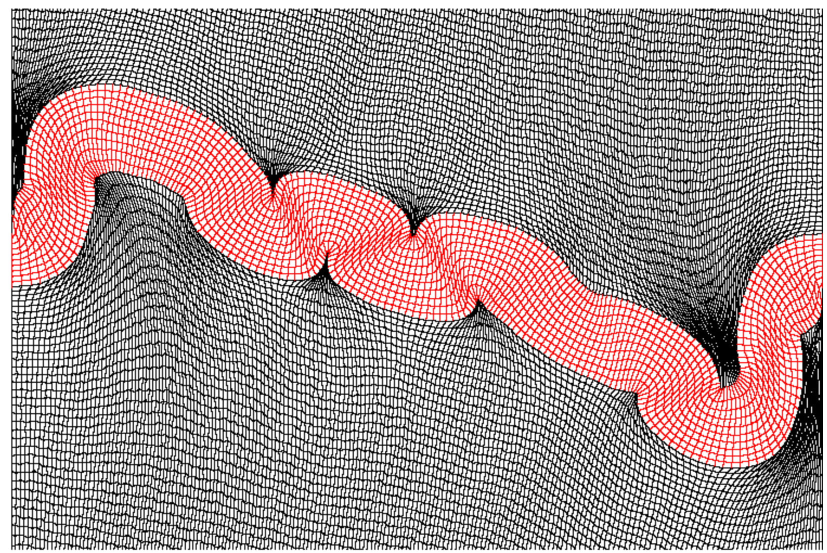

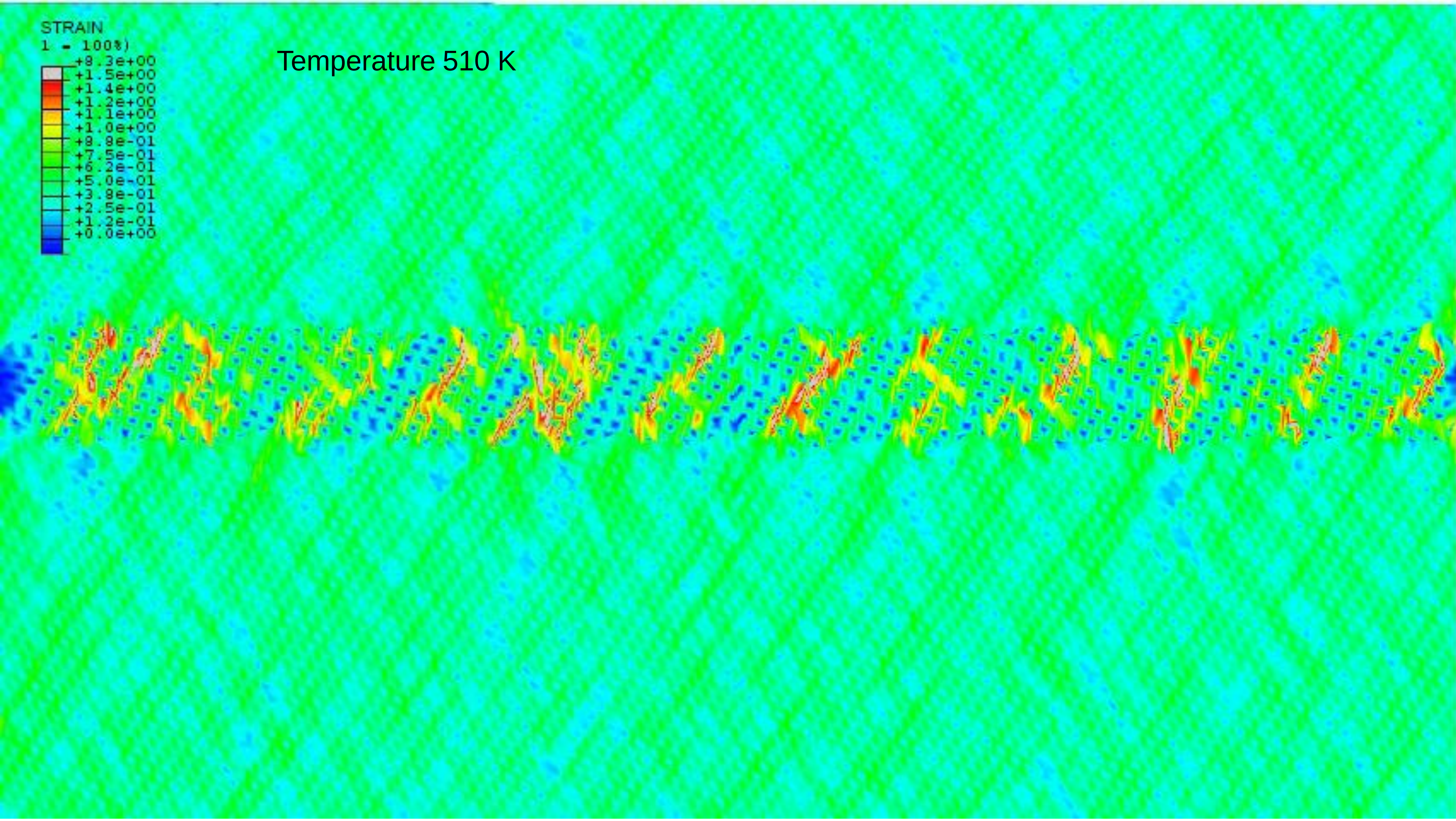
STRAIN
1 = 100%)
+8.3e+00
+1.5e+00
+1.4e+00
+1.2e+00
+1.1e+00
+1.0e+00
+8.8e-01
+7.5e-01
+6.2e-01
+5.0e-01
+3.8e-01
+2.5e-01
+1.2e-01
+0.0e+00
Temperature 510 K

510 K STRAIN

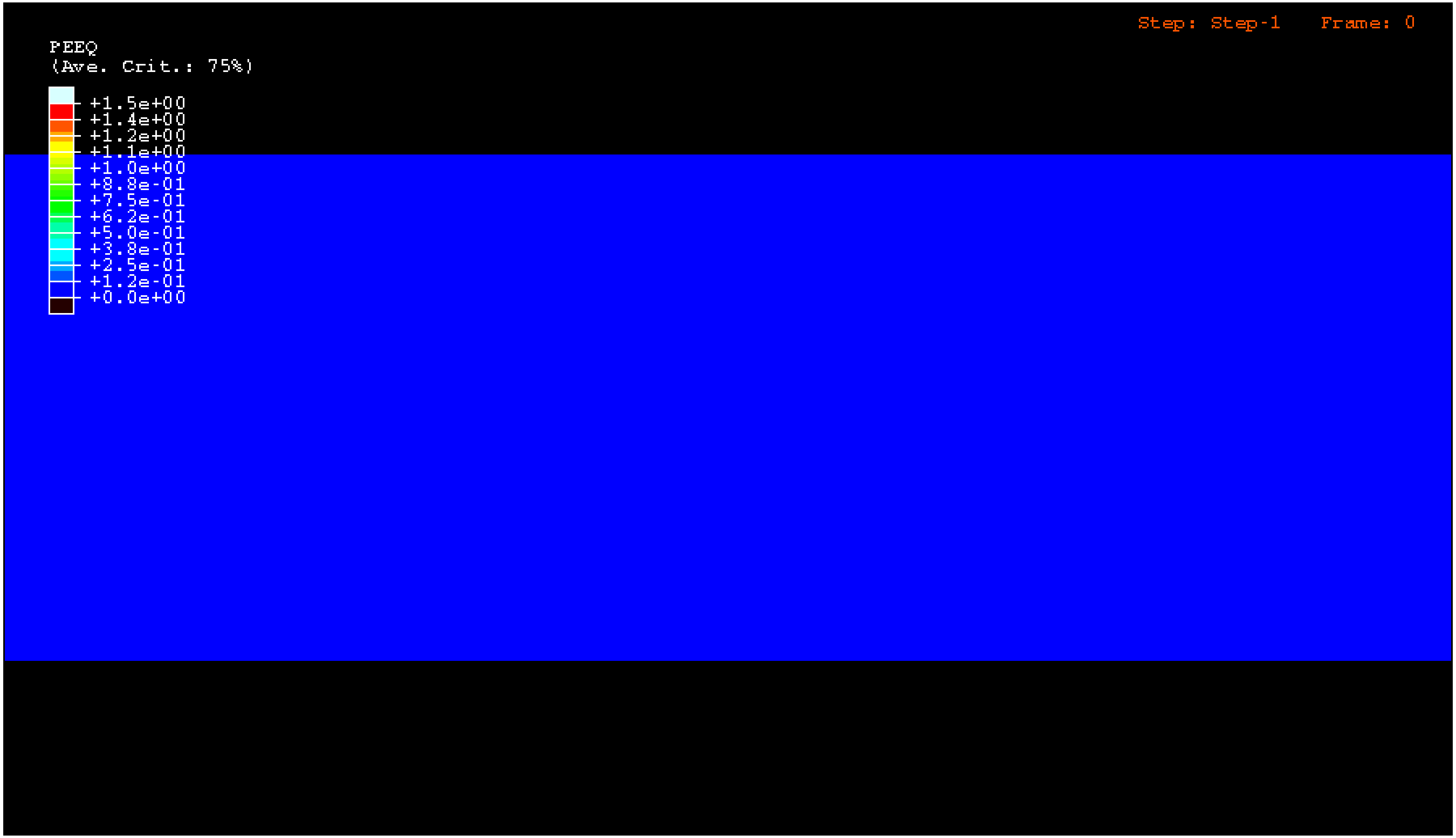

Step: Step-1 Frame: 0
PEEQ
(Ave. Crit.: 75%)
+1.5e+00
+1.4e+00
+1.2e+00
+1.1e+00
+1.0e+00
+8.8e-01
+7.5e-01
+6.2e-01
+5.0e-01
+3.8e-01
+2.5e-01
+1.2e-01
+0.0e+00

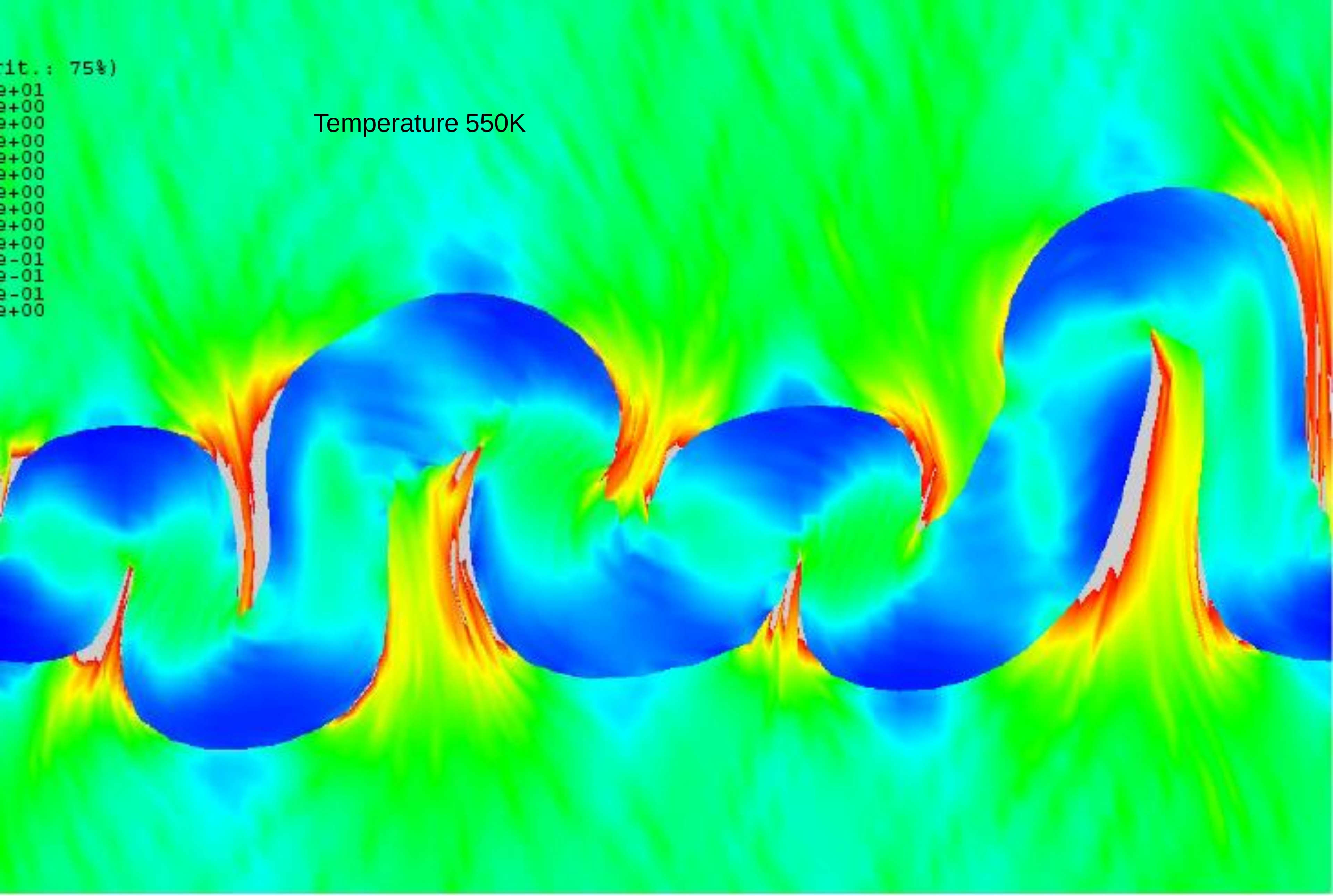
rit.: 75%)
Temperature 550K

550 K STRAIN

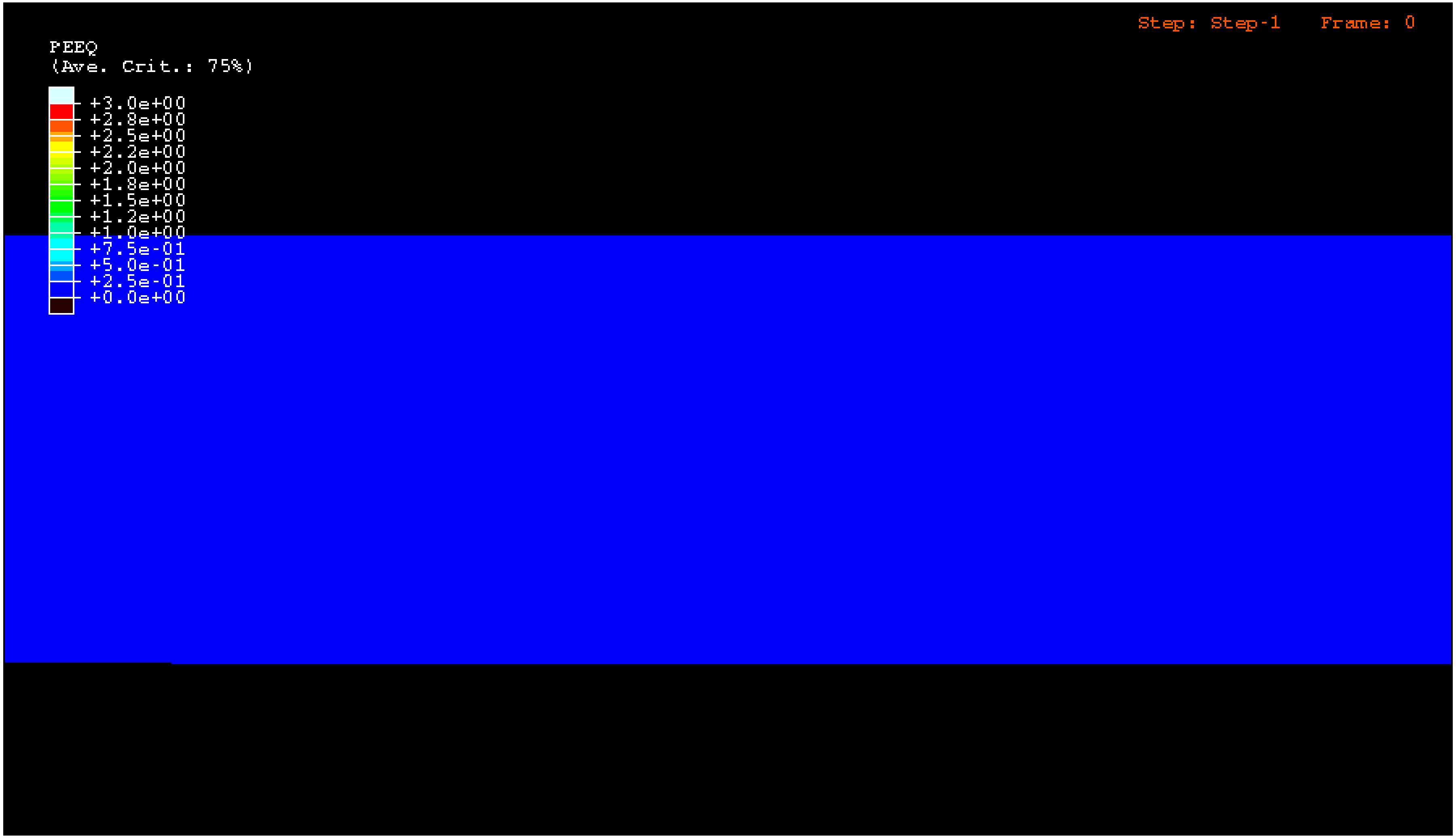
Step: Step-1 Frame: 0
PEEQ
(Ave. Crit.: 75%)
+3.0e+00
+2.8e+00
+2.5e+00
+2.2e+00
+2.0e+00
+1.8e+00
+1.5e+00
+1.2e+00
+1.0e+00
+7.5e-01
+5.0e-01
+2.5e-01
+0.0e+00

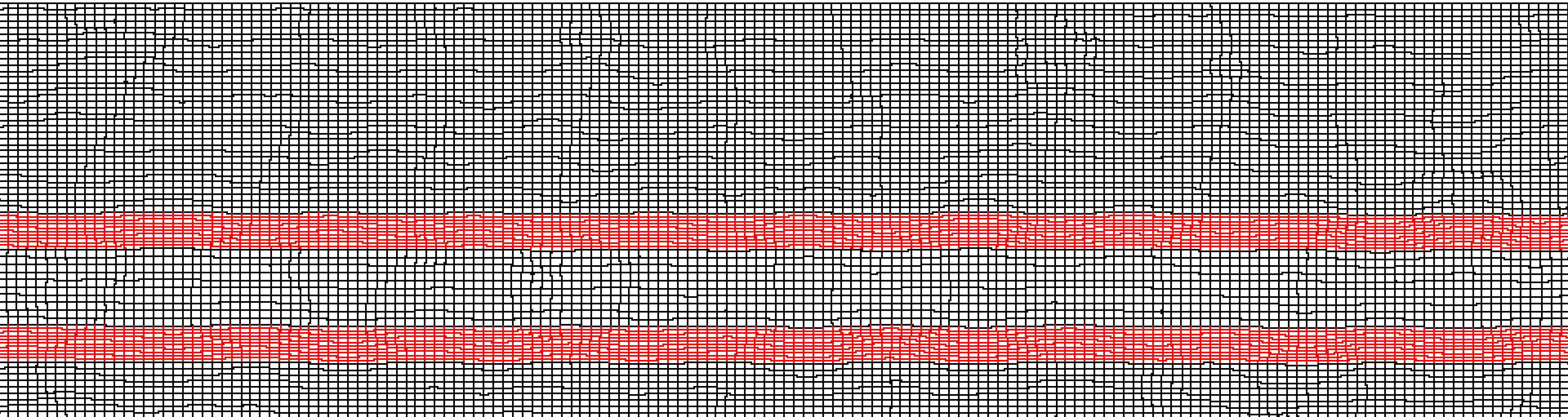

doublemesh1

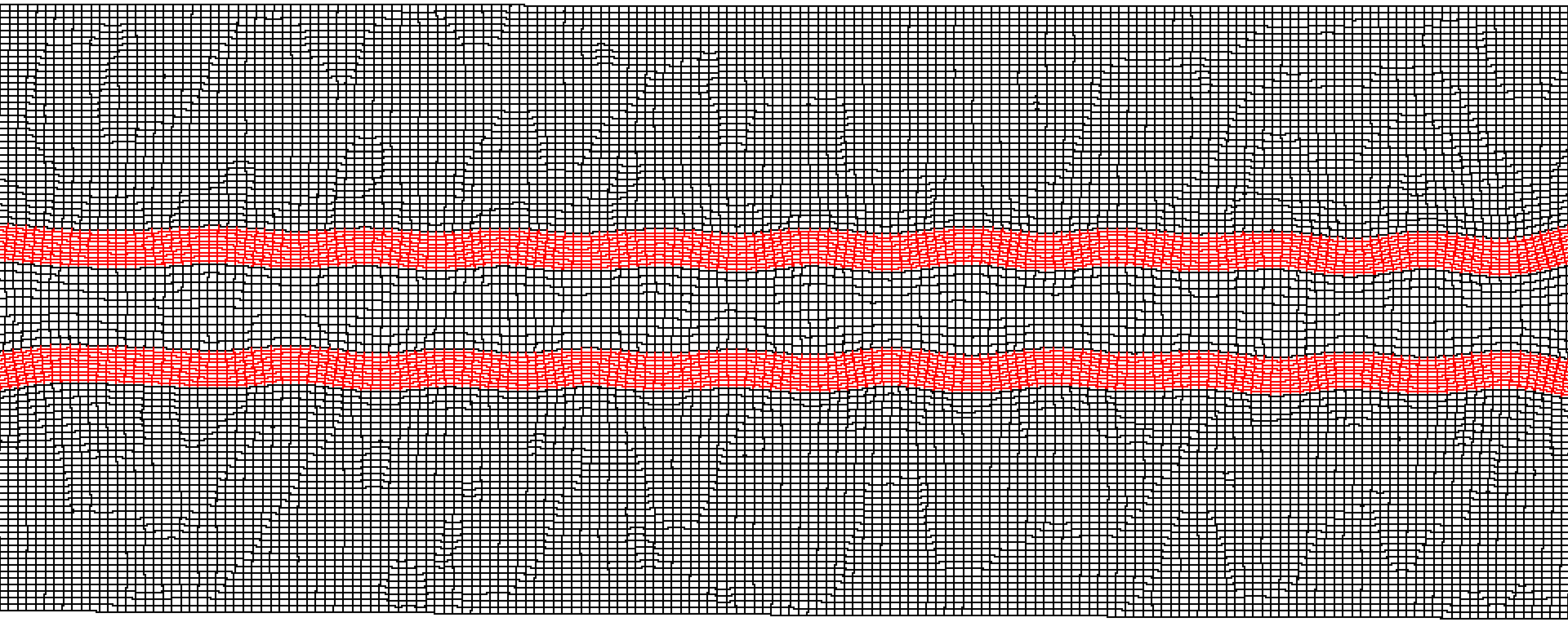

doublemesh2

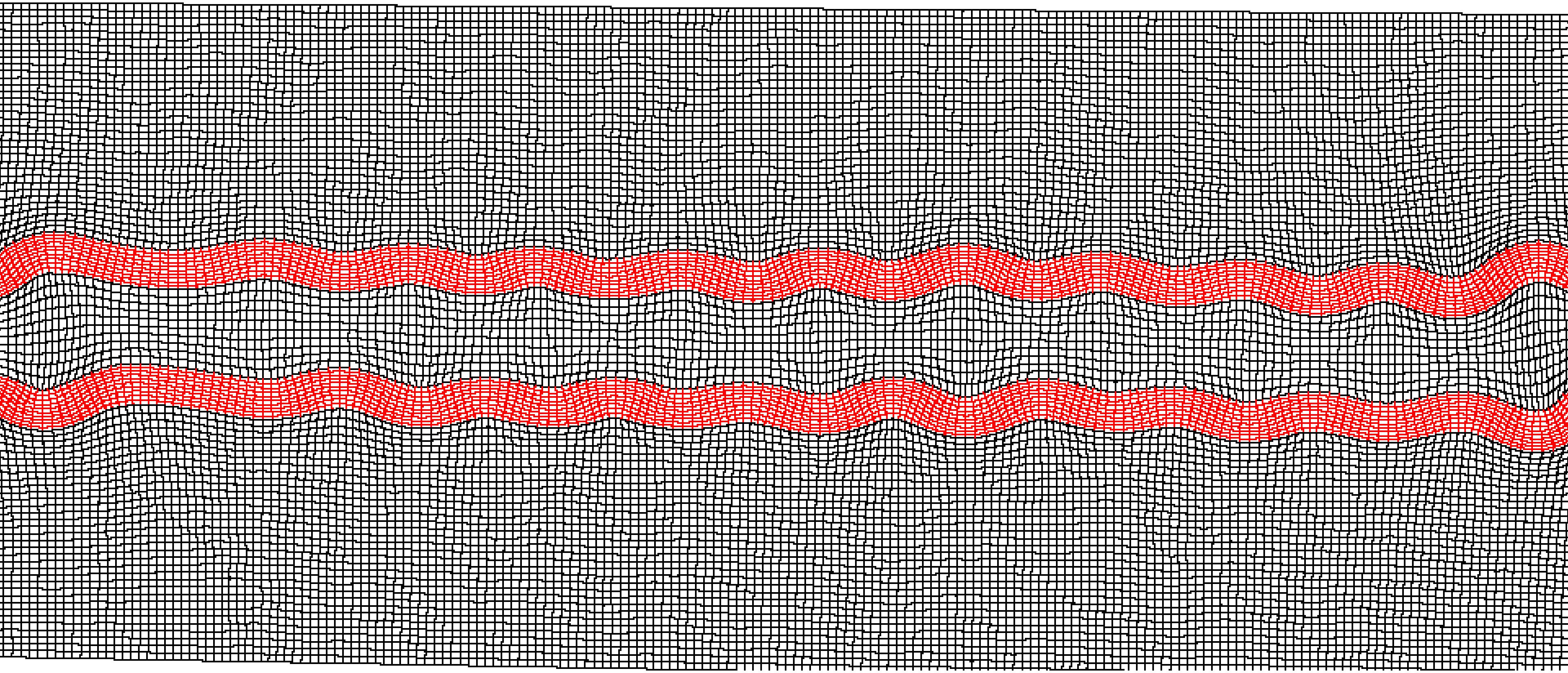

doublemesh3

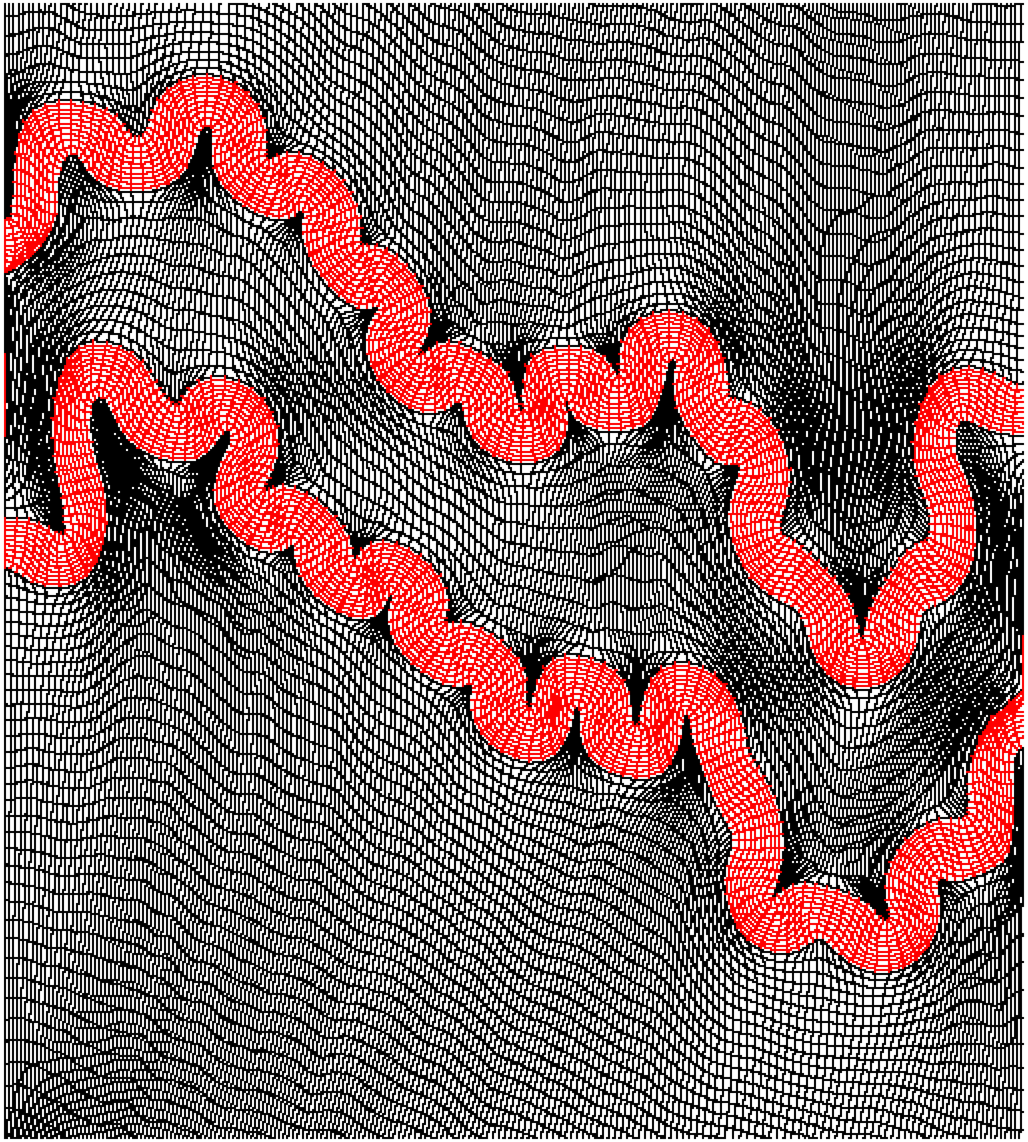

doublemesh4

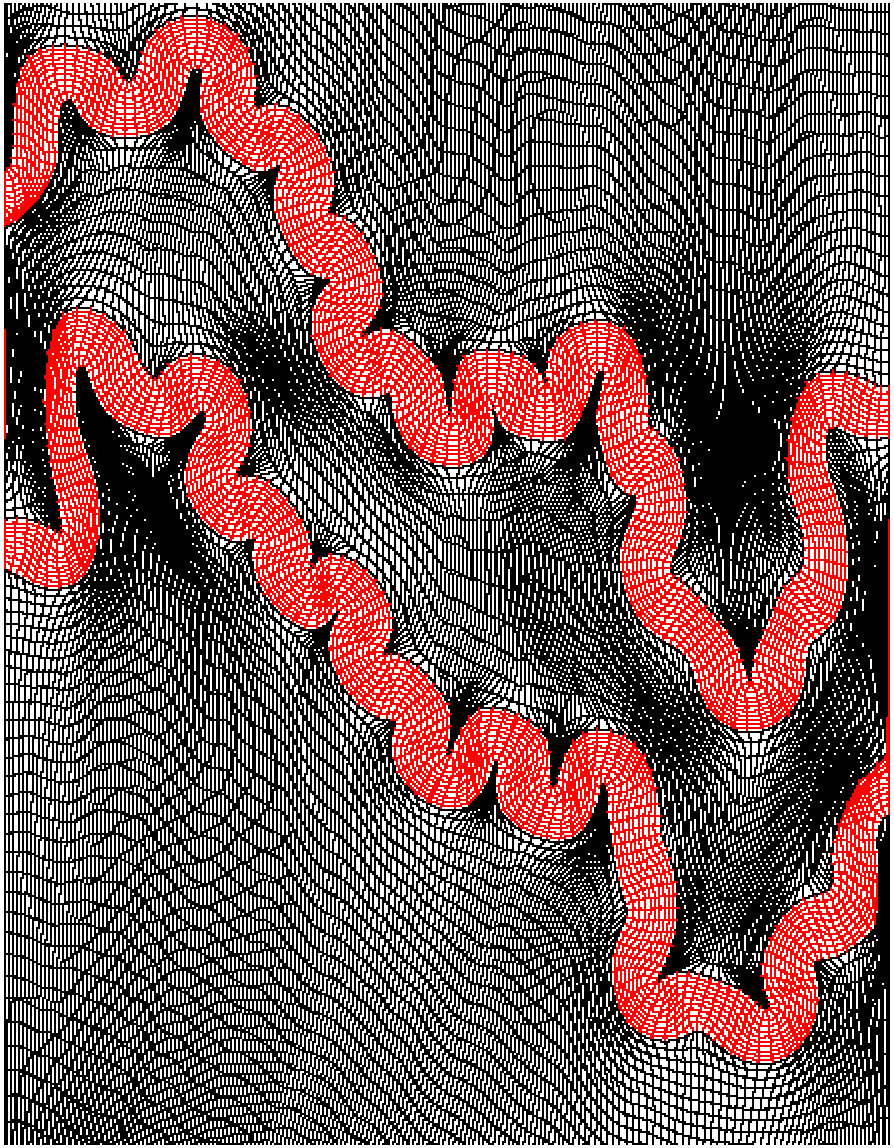

doublemesh5

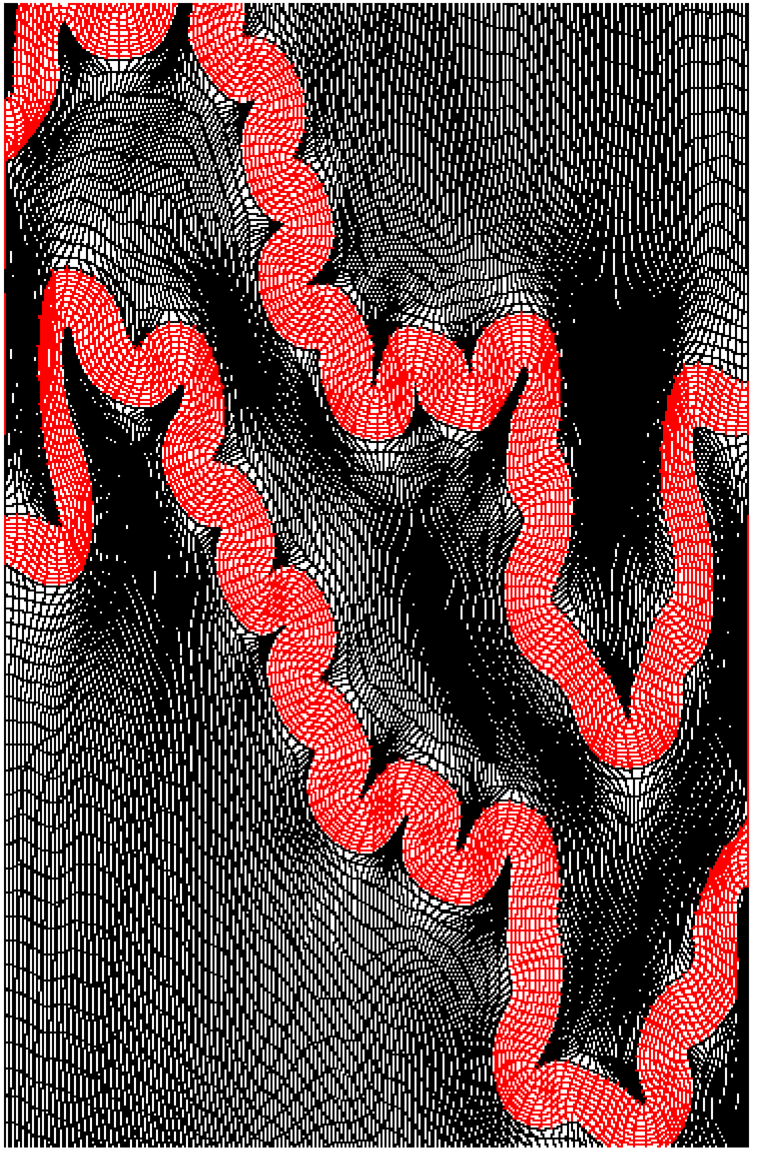

doublemesh7

doublemesh8

doublemesh10

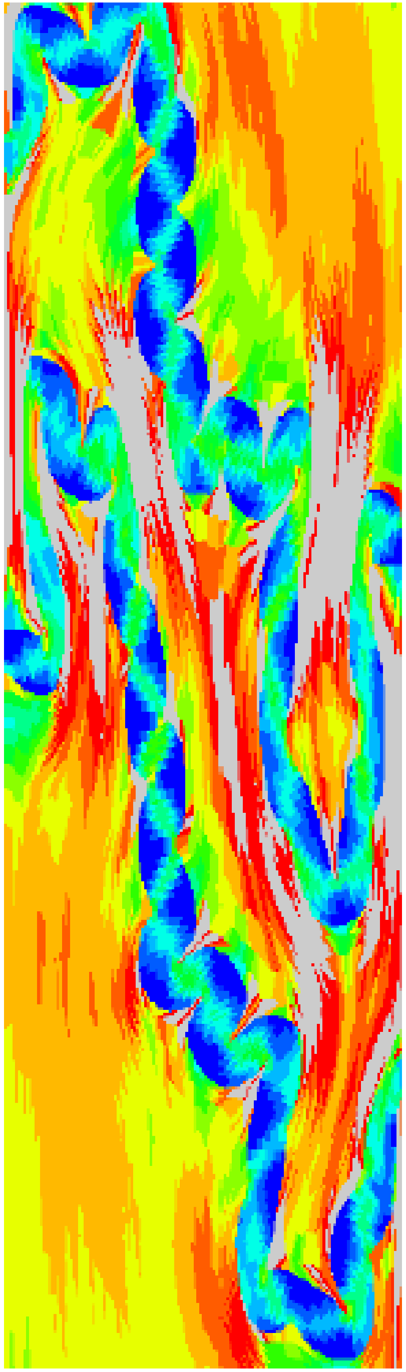

Plot of strain

Note zones of localisation
in folded layer

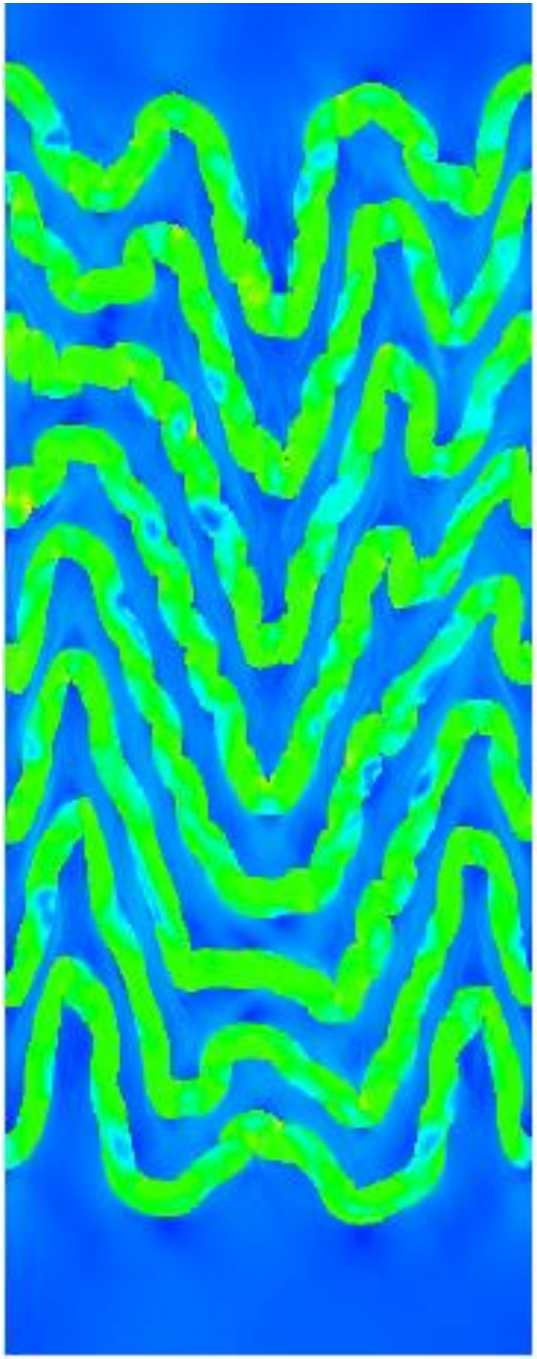
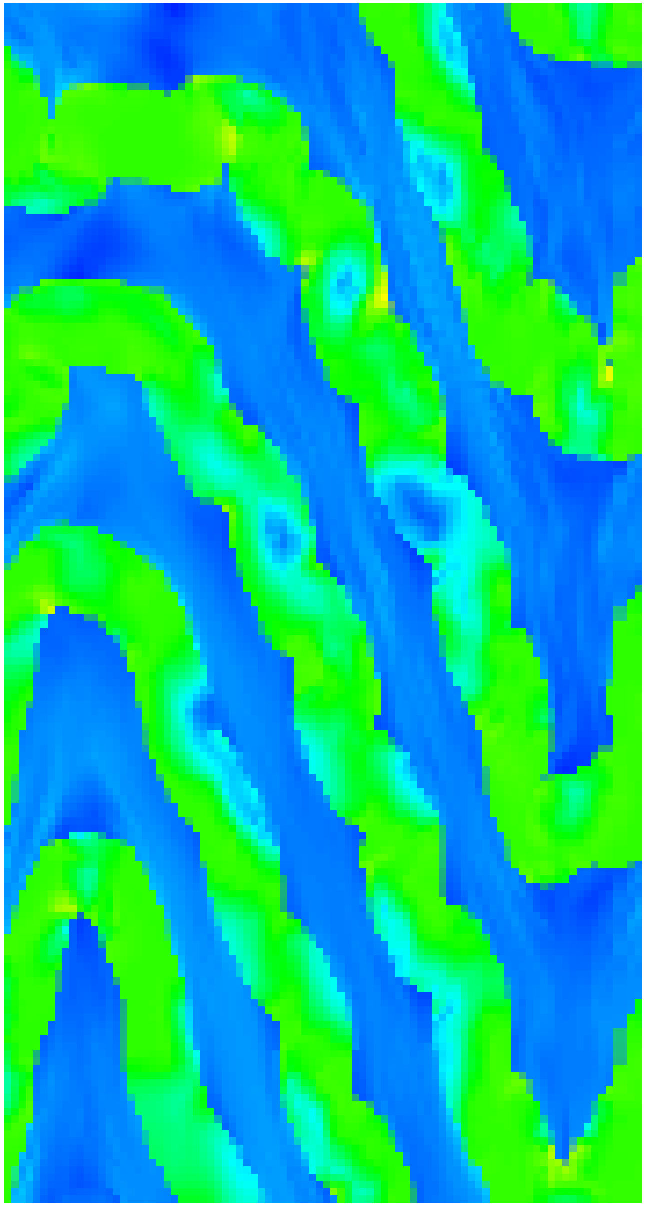

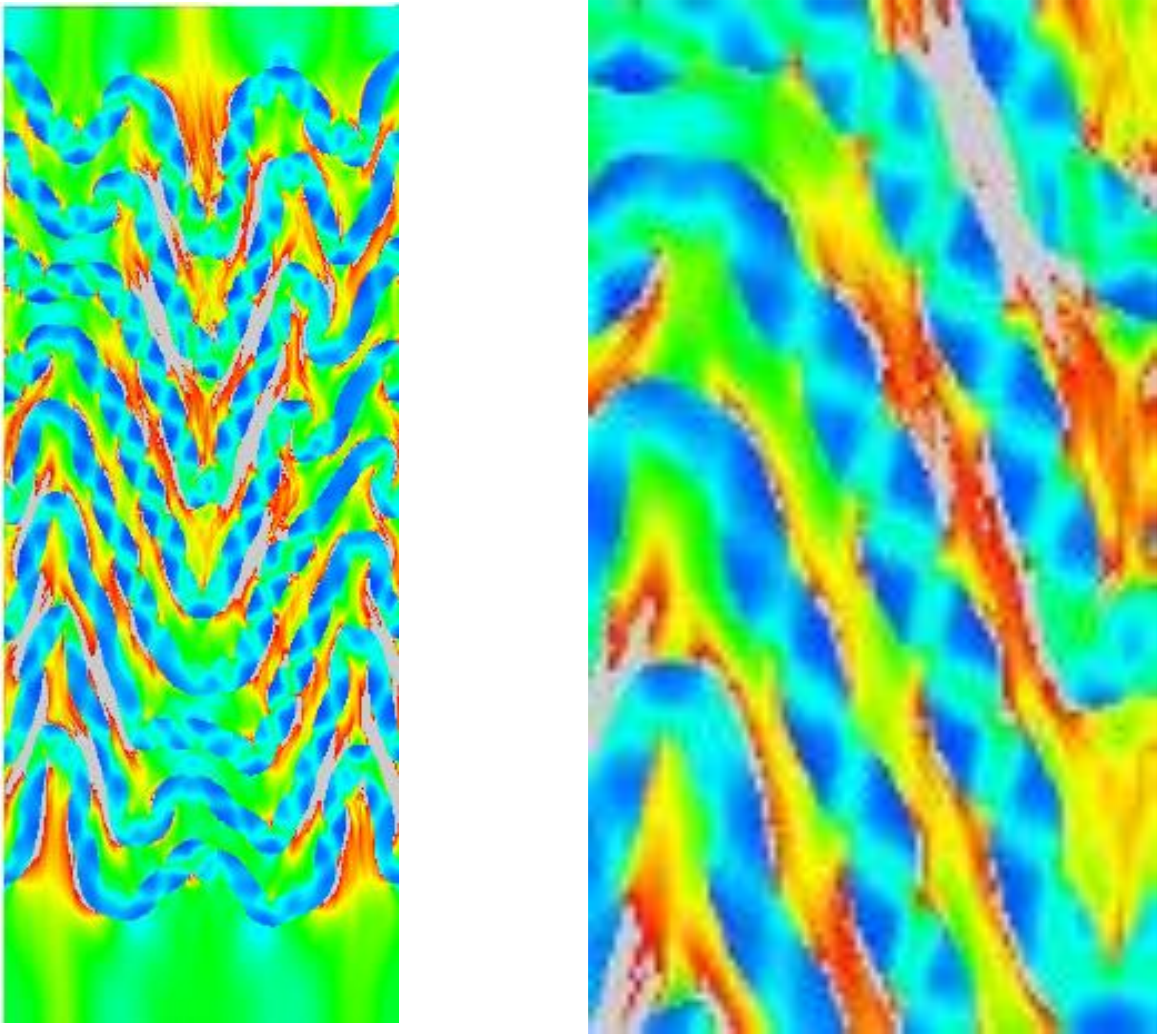

A Extension of a Feldspar layer in Quartz (before: 3.3x12 km; after: 13.2x3 km)

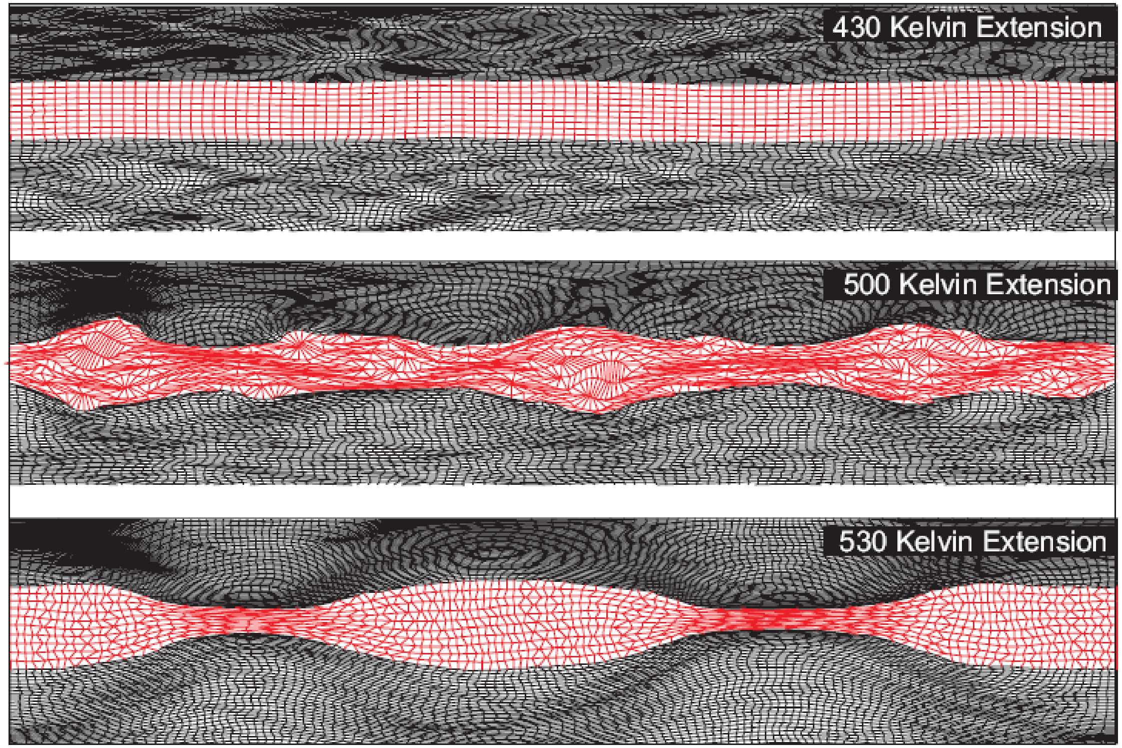

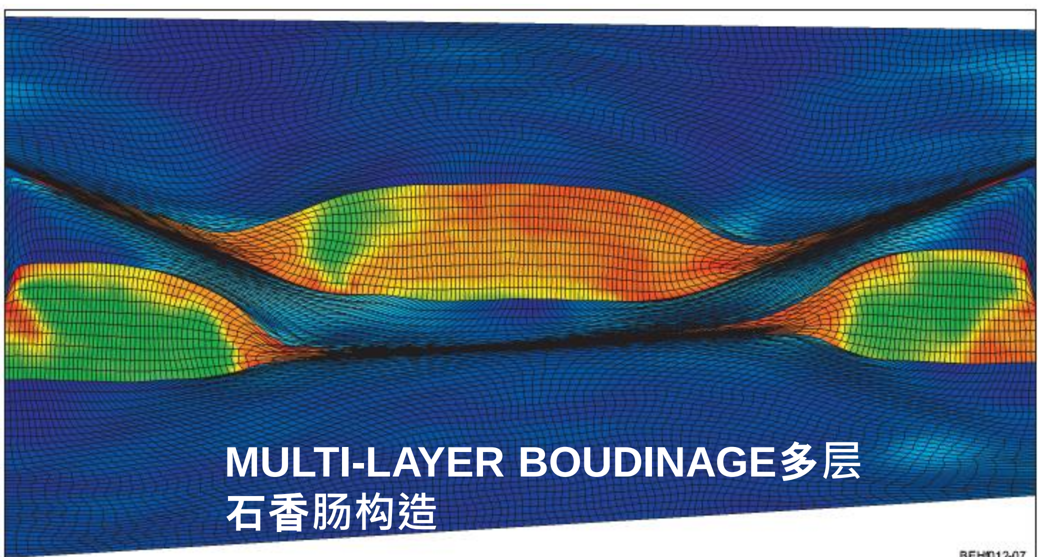

BIOT THEORY PREDICTS NO BOUDINAGE IN THESE MATERIALS

基于毕奥理论在这些材料中无法产出石香肠构造

Deformation of multi-layer sequence; Newtonian viscosity

多层层序：牛顿粘度

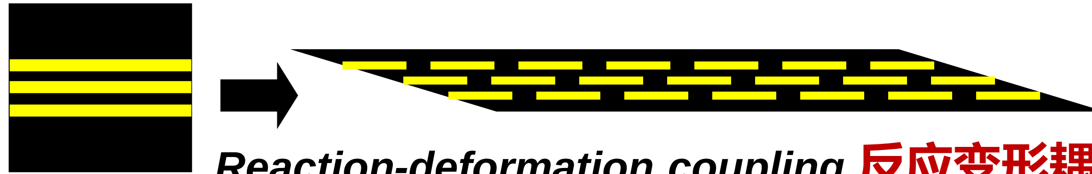

***Reaction-deformation coupling* 反应变形耦合**

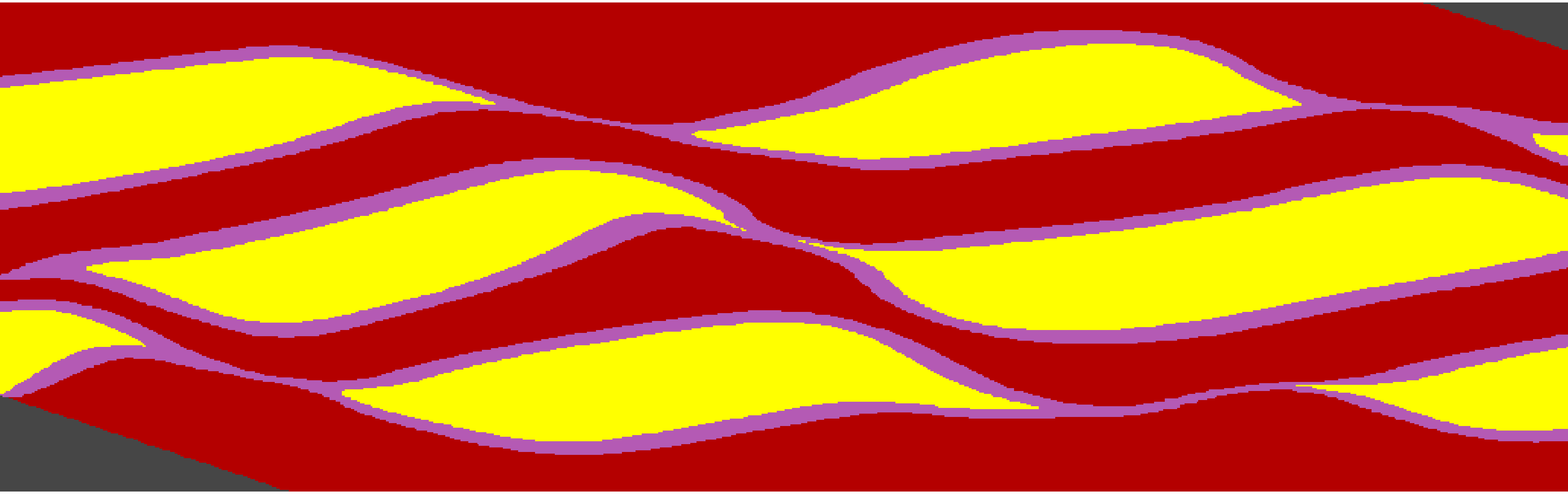

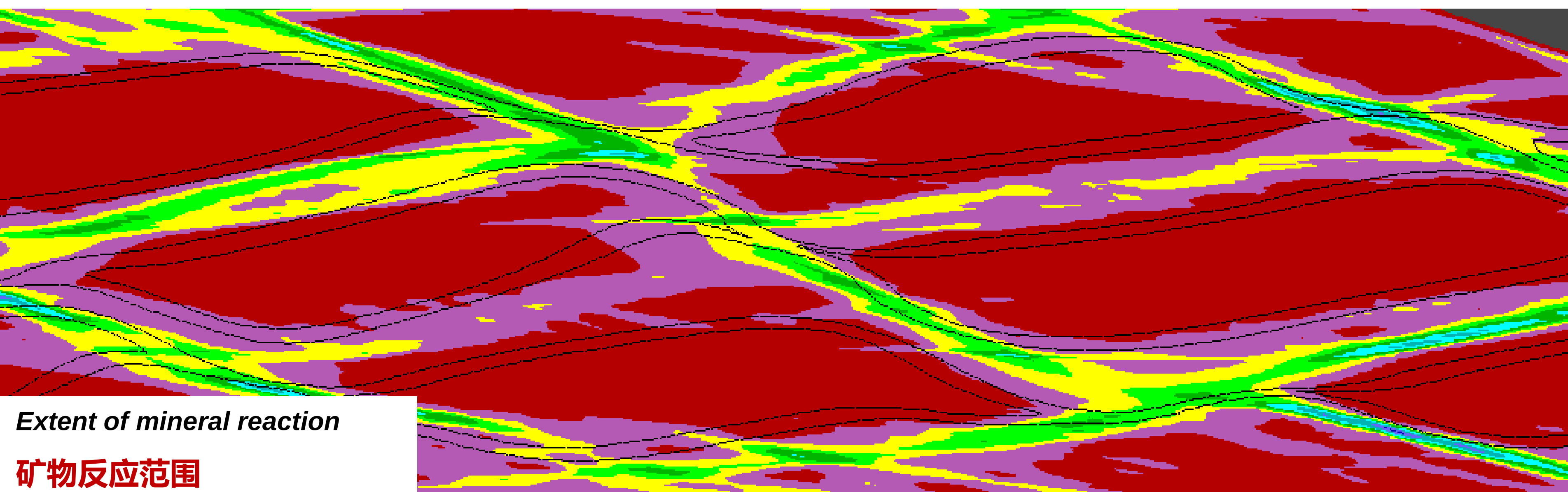

Brecciation

The process

角砾岩化

过程

PFC2D 3.10

Step 116000 15:50:44 Wed Feb 21 2007

View Size:
X: -2.188e-001 <=> 3.763e-001
Y: -1.000e-002 <=> 6.200e-001

Wall

Ball

FISH function crk_item

Fluid Velocity
Maximum = 7.302e+000
Linestyle

Job Title: P bonds: n,s strength 4.30000000000e+000, n,s stiff 5.70000000000e+0

View Title: Injecting Air 1.80000000000e-001 m/s

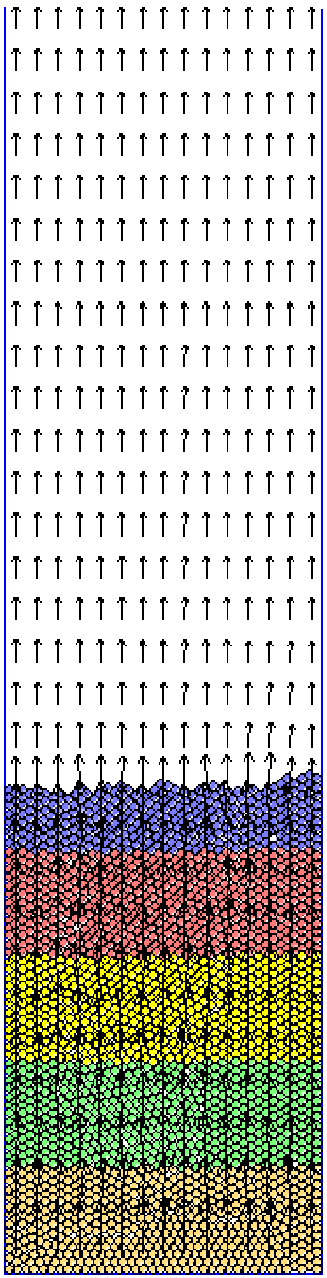

PFC2D 3.10

Step 116000 08:01:01 Wed Feb 14 2007

View Size:
X: -2.188e-001 <=> 3.763e-001
Y: -1.000e-002 <=> 6.200e-001

Wall

Ball

FISH function crk_item

Fluid Velocity
Maximum = 8.306e+001
Scale to Max = 1.000e+001
Linestyle

Job Title: P bonds: n,s strength 4.30000000000e+003, n,s stiff 5.70000000000e+0

View Title: Jet:Injecting Air 3.50000000000e+000 m/s

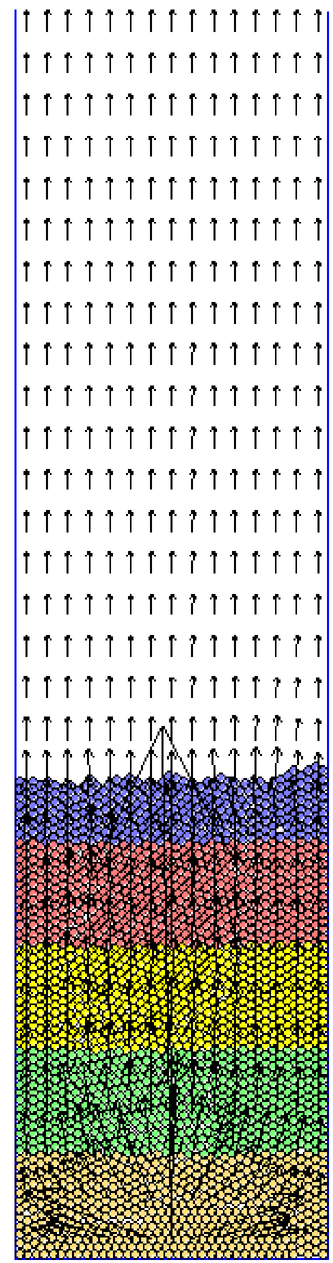

Method of fluid introduction affects migration patterns,

影响运移模式

with unfocused flow (left) resulting in sheet-like uniform motion,

与非汇聚流（左）导致片状匀速运动

& focused flow (right) encouraging turbulence and migration of fragments to the bottom of the box.

汇聚流（右）促使湍流和碎片迁移到盒子的底部

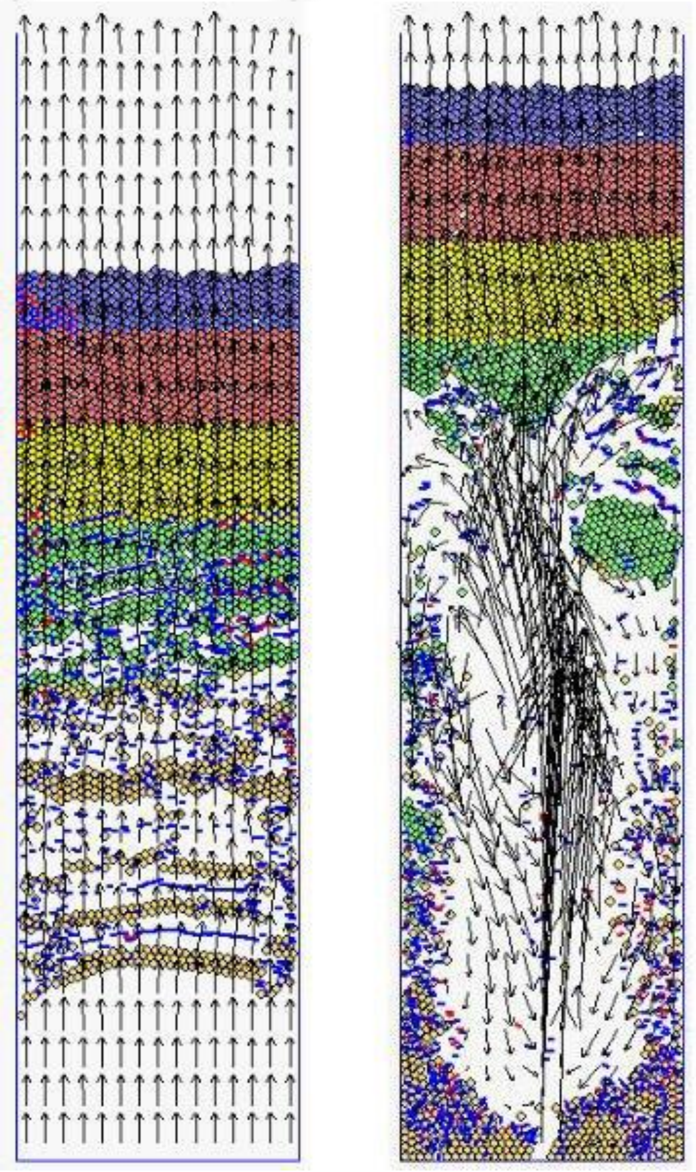

Parameters of Interest

- Fluid flow rate

  流体流率

- Rock strength

  岩石强度

- Fluid mechanism: introduced uniformly or from a point source.

  流体机制： 均匀或者来自点源

- Boundary conditions: unconfined or confined.

  边界条件：无限制及限制

Unfocused Flow 非汇聚流

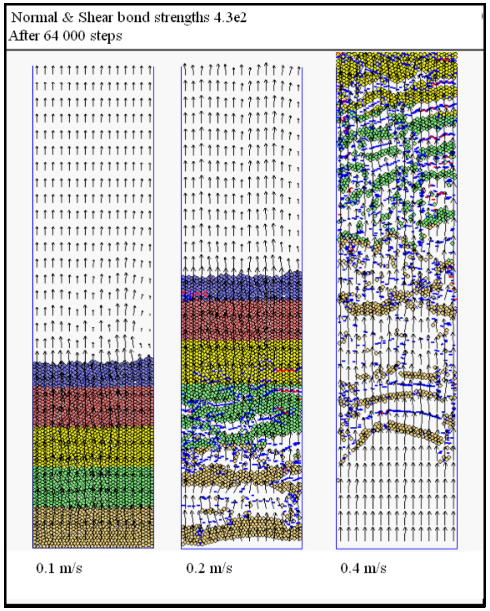

Example of the effect of varying fluid velocity through 0.1m/s, 0.2m/s, 0.4m/s.

改变流体速率：0.1米/秒，0.2米/秒，0.4米/秒

Behaviour map for unfocused fluid flow

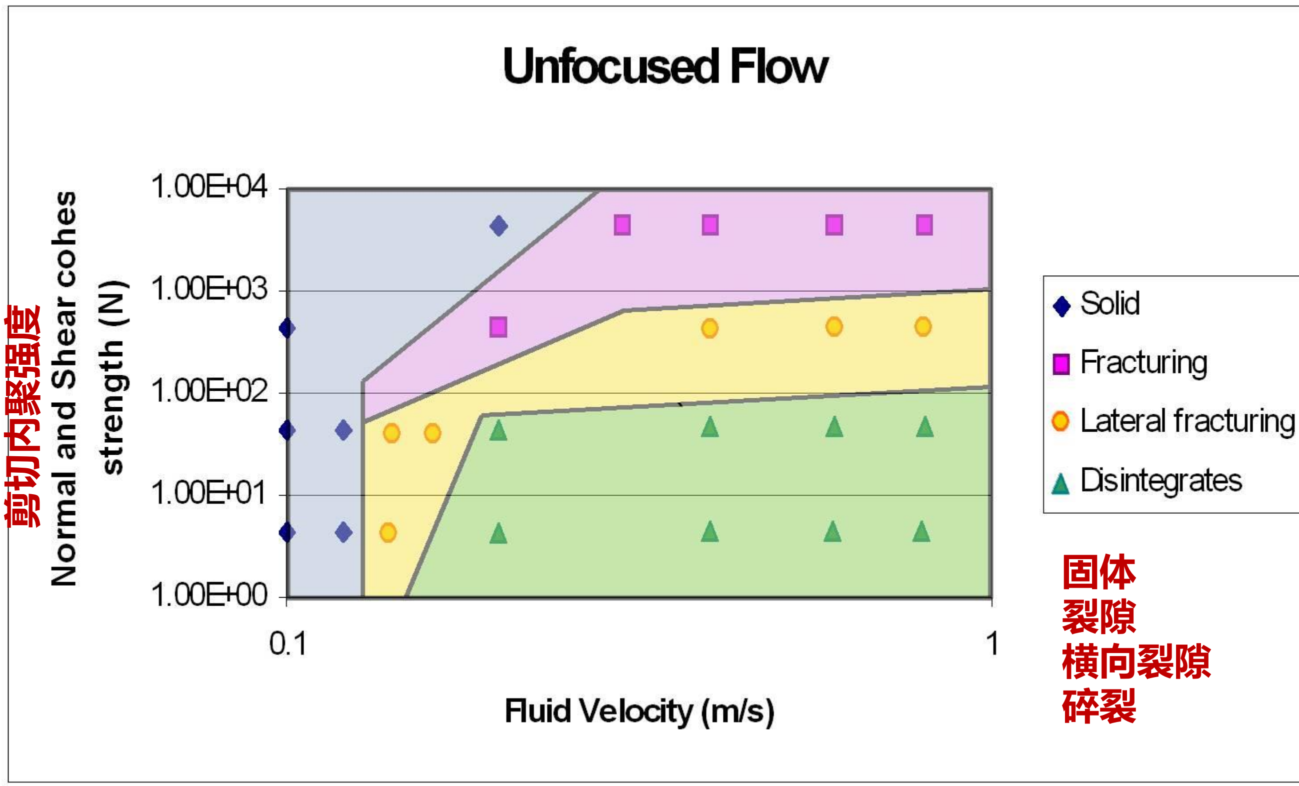

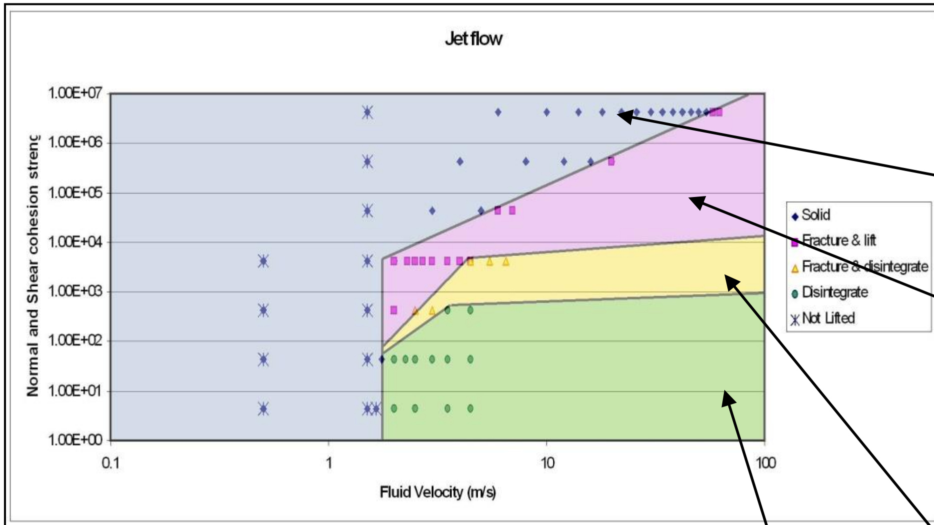

Unconfined Models

非限制模型

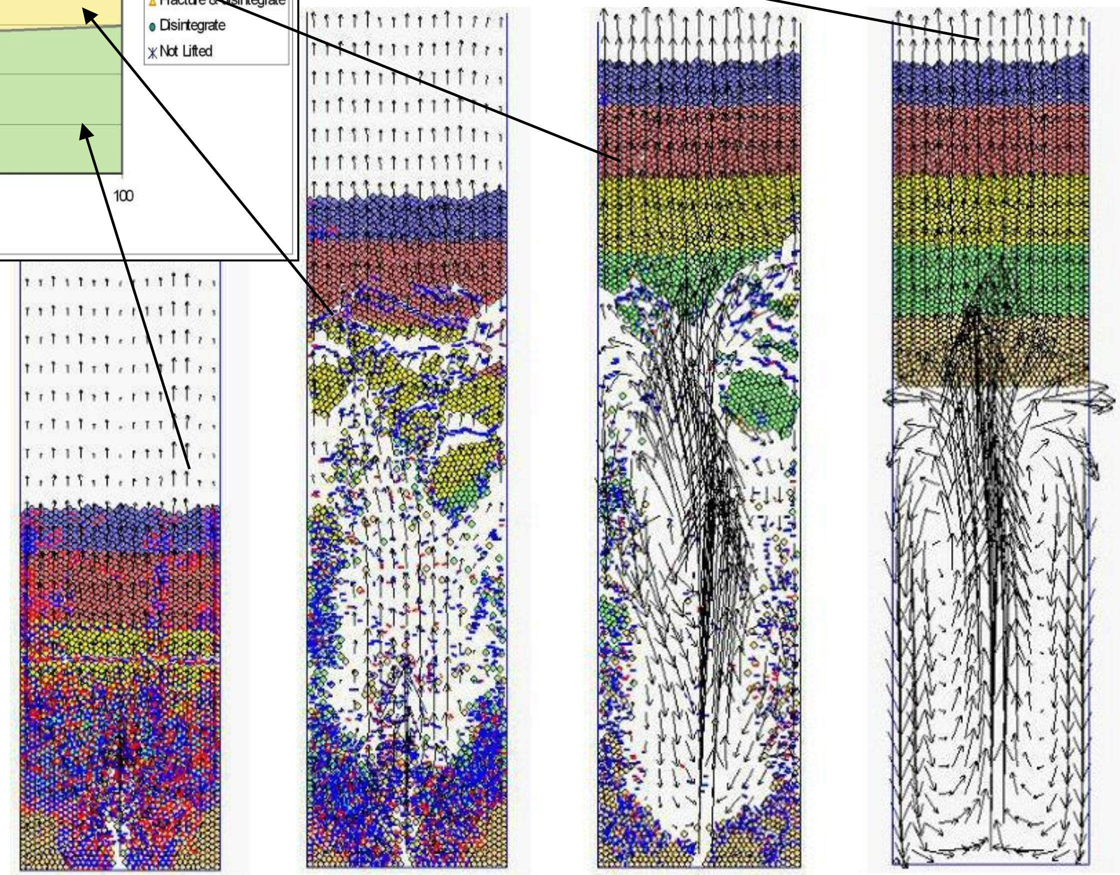

Investigations reveal a cohesion-fluid flow rate relationship where rock has the capacity to break into breccia-resembling pieces in terms of size and/or shape.

揭示内聚力-流体流率关系

岩石破碎为角砾岩-根据大小和

形态组成碎片

Disintegrates | Lifts & disintegrates | Fractures & lifts | Lifts solidly

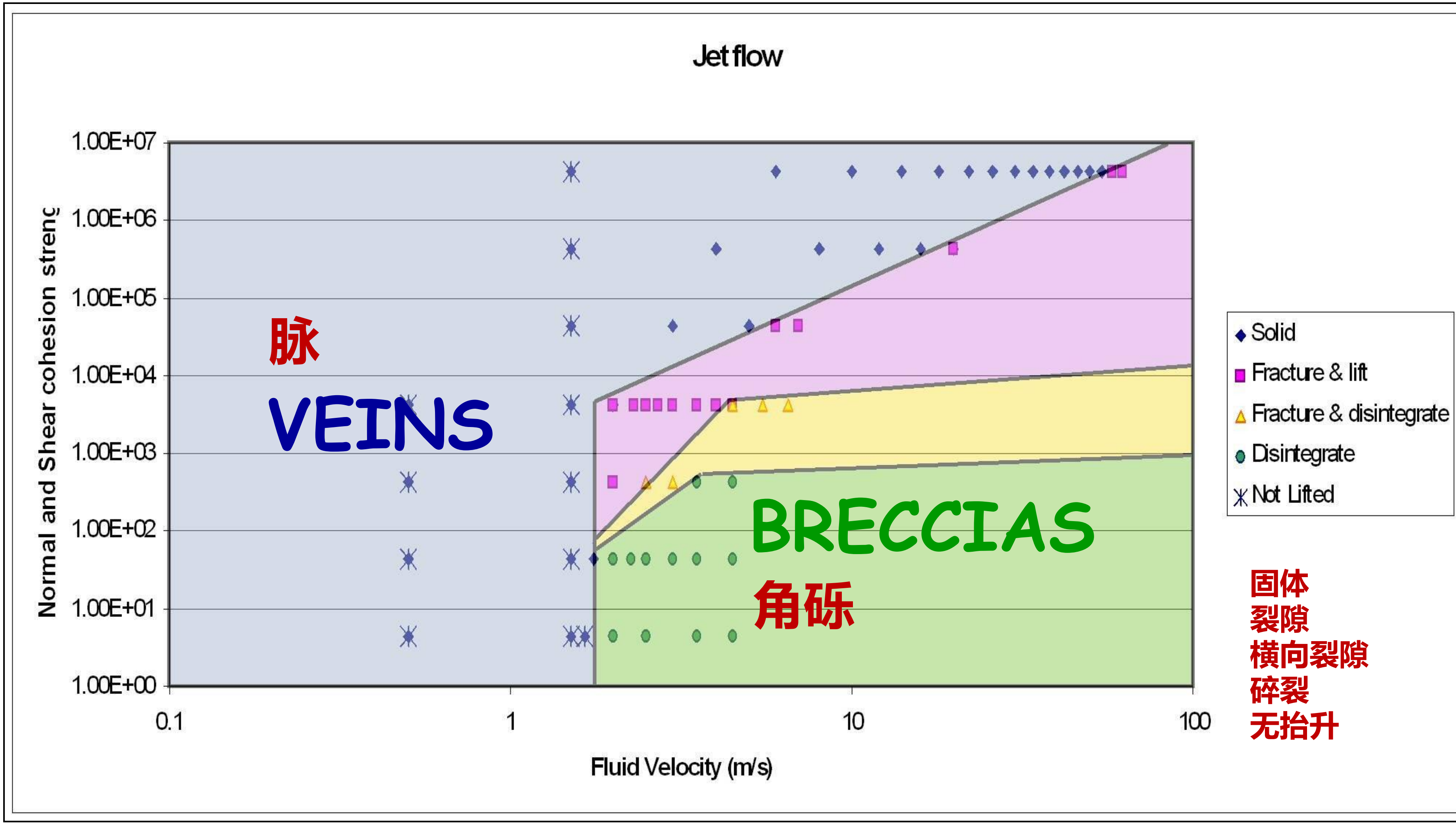

Figure demonstrates the consequences of the fluid flow being less than (veins) or greater than (breccias) the fluid flow predicted through Darcys Law for a given permeability and fluid pressure gradient.

在给定的渗透率和流体压力梯度下，流体流动的结果可以小于（脉）或者高于（角砾）通过达西定律预测的流体流动。

The preparation of such flow regime maps is fundamental to the interpretation of breccia textures in the field since one can position a particular texture within a rock strength/fluid velocity/porosity field on the map.

因为可以在一个岩石强度/流体速度/孔隙度场图中定位一个特殊的纹理，因此流型图是解释野外角砾岩纹理的基础

Application of an isolated pulse of over-pressured fluid to the base of the model

在模型底部施加一个孤立脉冲式的超压流体

Fracturing occurs ahead of the migrating fluid pulse with subsequent collapse of the fractured rock into the space left in the wake of the pulse

裂隙发育在流体迁移脉冲前，之后裂隙岩石紧随脉冲进入遗留空间

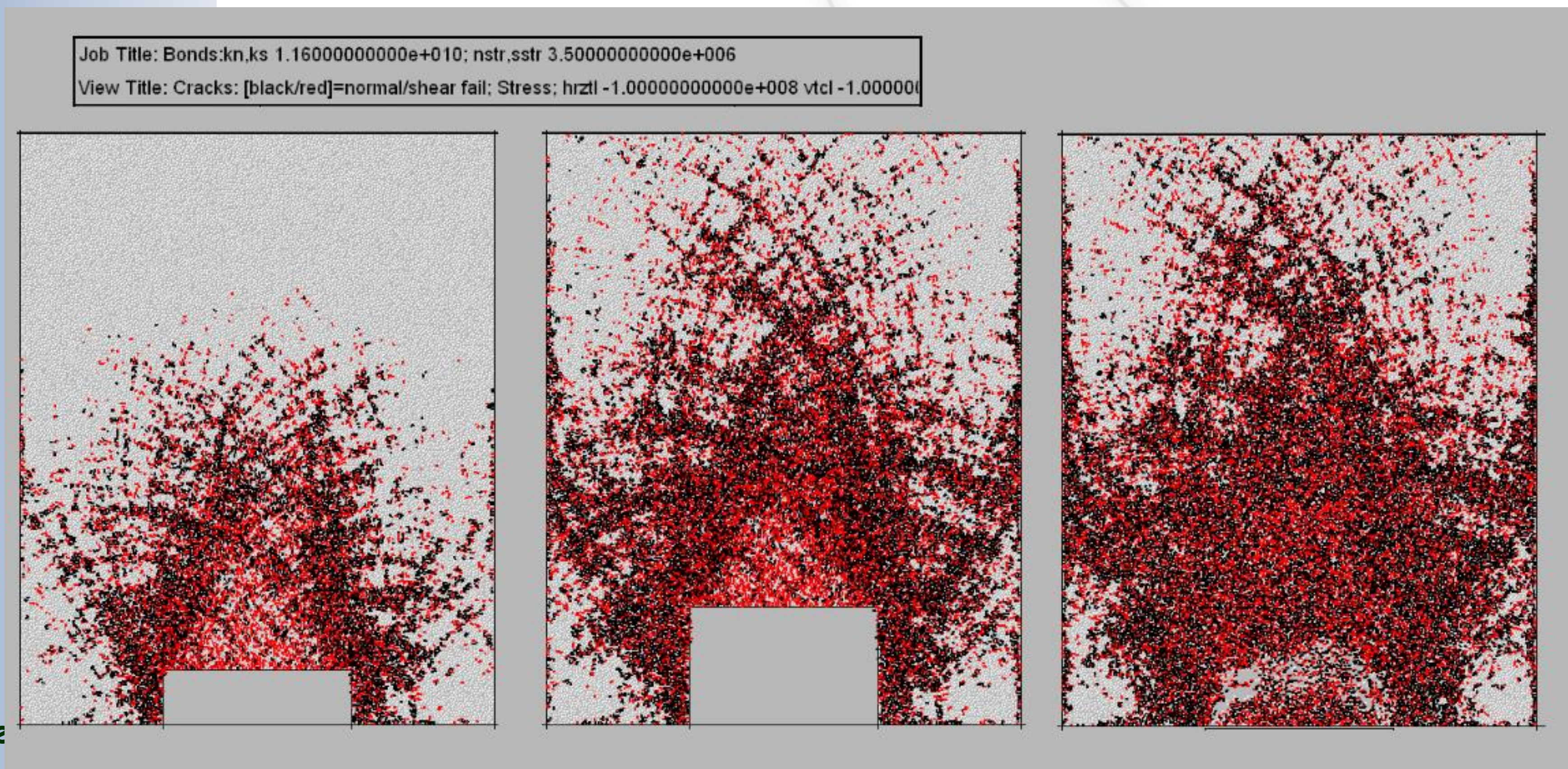

Hefe

Brecciation caused by upward migration of fluid pulse.

流体脉冲向上迁移引发角砾岩化

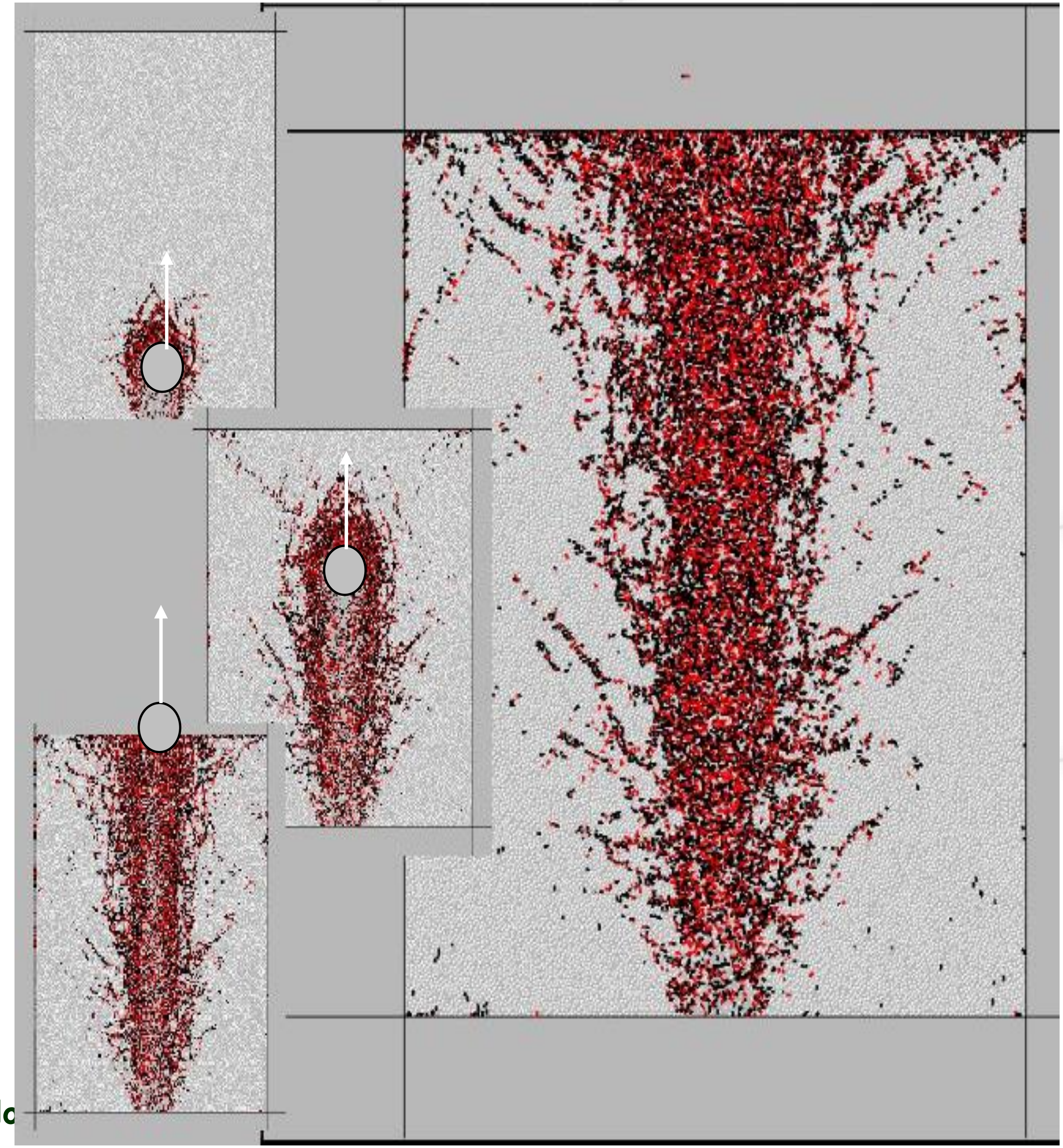

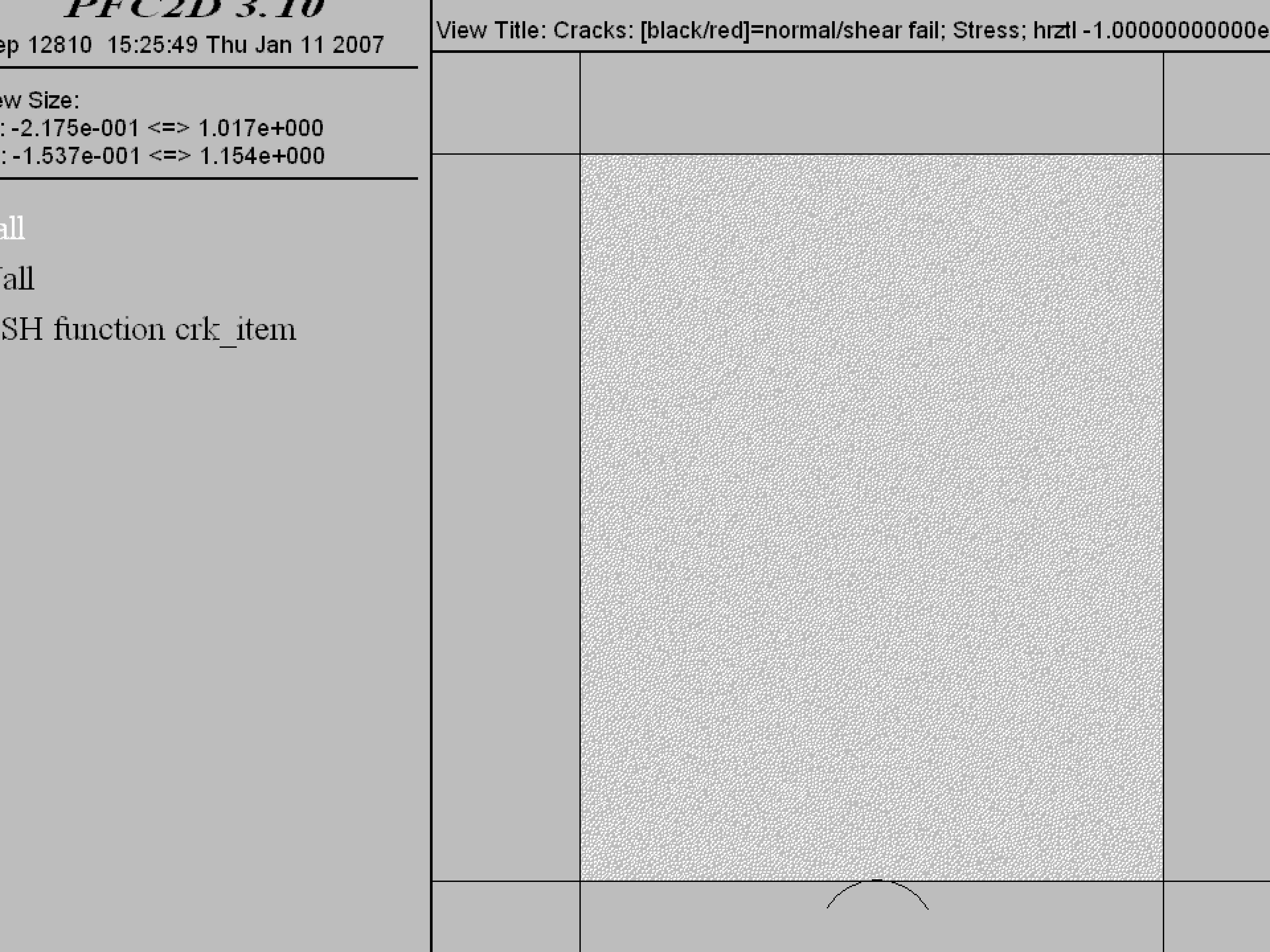
PFC2D 3.10
ep 12810 15:25:49 Thu Jan 11 2007
ew Size:
: -2.175e-001 <=> 1.017e+000
: -1.537e-001 <=> 1.154e+000
all
'all
SH function crk_item
View Title: Cracks: [black/red]=normal/shear fail; Stress; hrztl -1.00000000000e

Understanding an Evolving Orogen

–Olary-Broken Hill conceptual model **概念模型**

–numerical methods **数值方法**

–modelling results **建模结果**

Modelling Results

- dry models 干模型
- parameter experimentation 参数实验
- saturated 饱和的
- compare to conceptual model 与概念模型对比

Olary-Broken Hill Tectonic History

- large-scale extension
  大尺度伸展
- regional shortening
  区域压缩
- propagating overthrusting
  逆冲推覆
- fluid generation and migration
  产生流体并运移
- end of orogeny → melting, end of significant fluid generation and migration
  造山熔融终止，大规模流体产生及运移终止

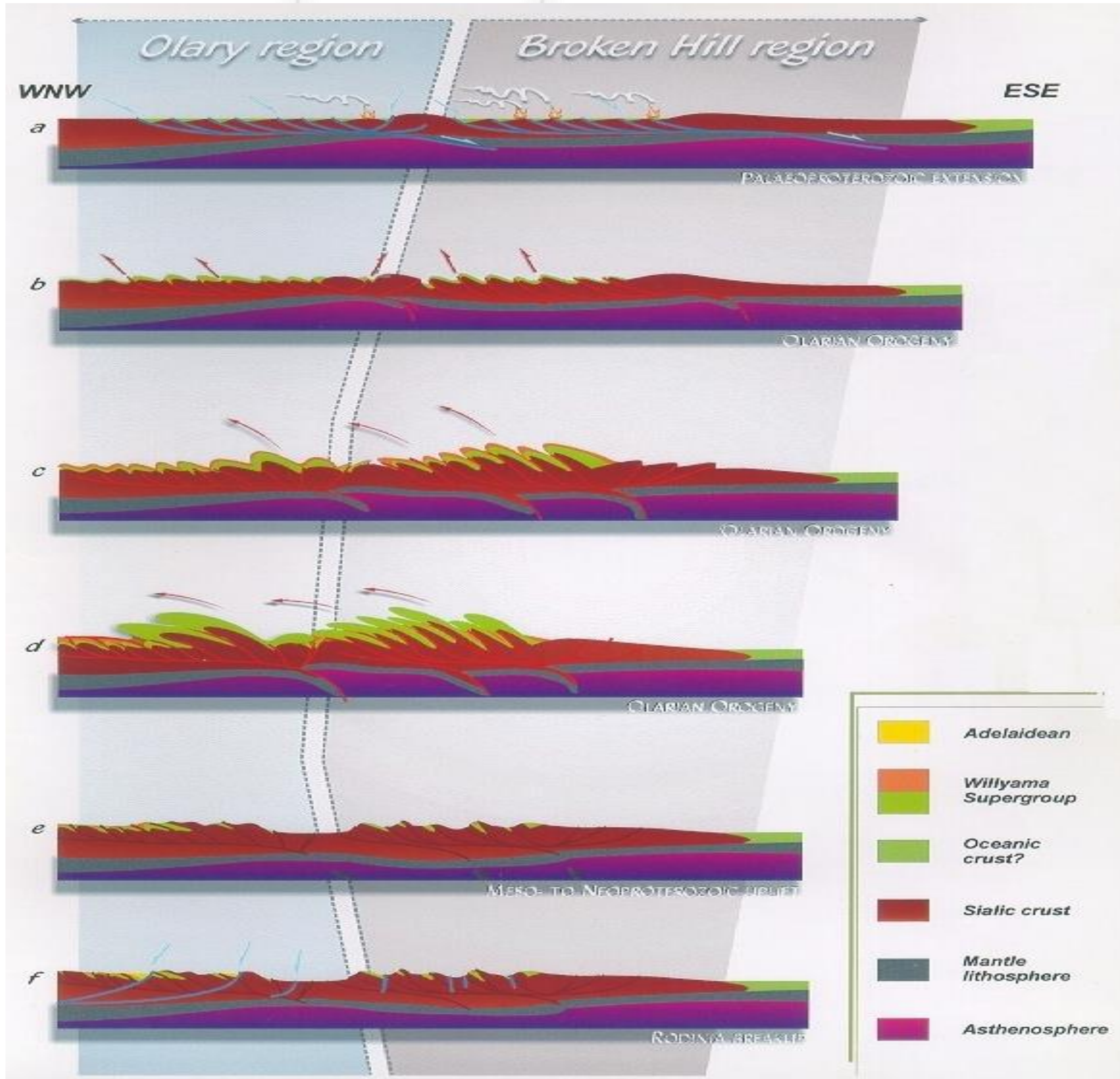

Olarian Orogeny

1570 Ma end

1600 Ma reworking

1630 Ma inversion

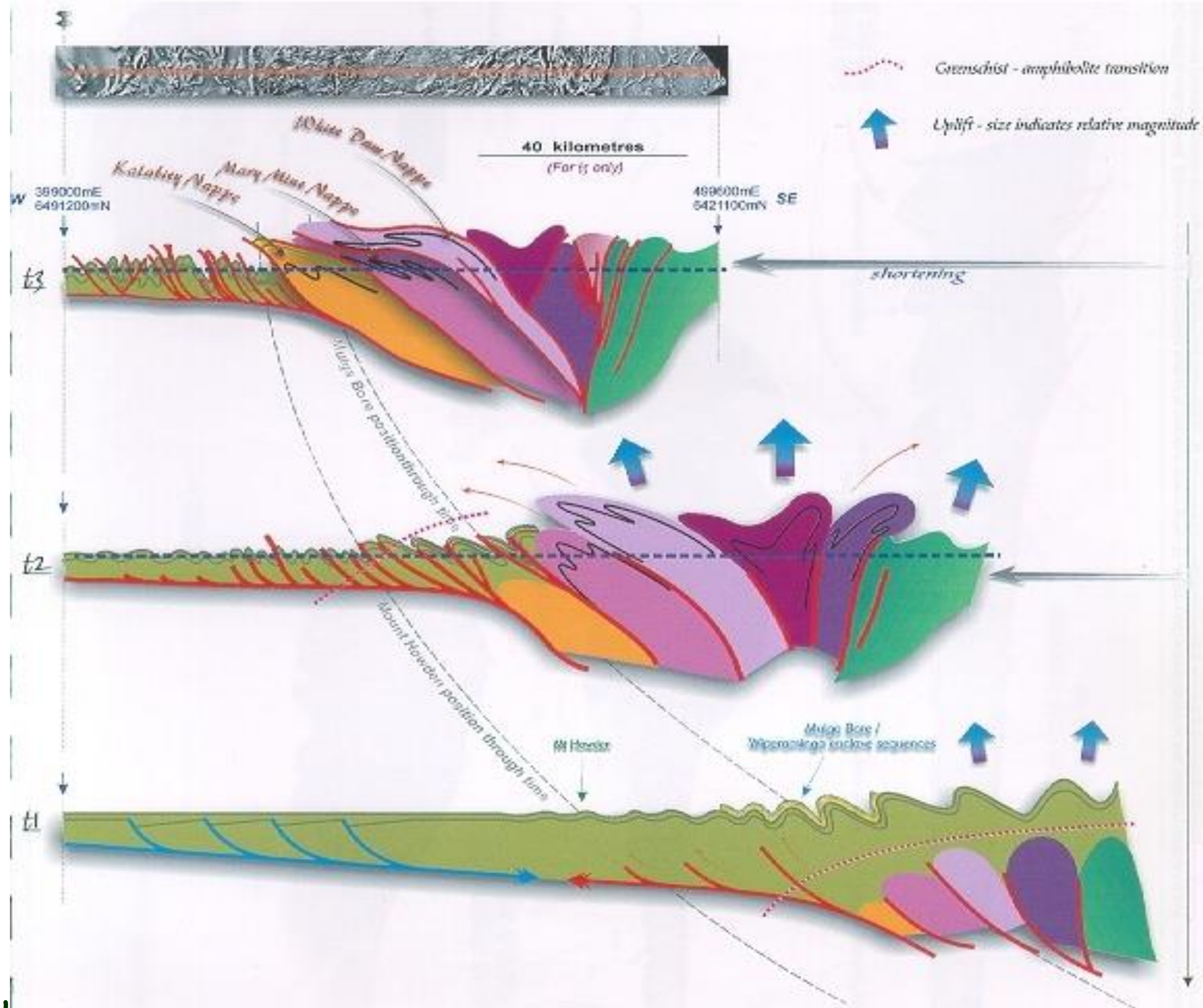

Numerical Code

- geodynamic processes (地球动力学进程)
  - **folding, thrusting, subduction** (褶皱，推覆，俯冲)
  - **partial melting of mantle** (地幔部分熔融)
  - **resultant fluid flow** (流体流动)
- large (unlimited) deformation (大/无限的变形)
  - **viscous fluid** (粘性流体)
  - **particle-in-cell-code solves finite element equations on a grid** (质点网格法求解基于网格的有限元方程)
  - **moveable integration points advect information** (移动积分点传导信息)

Experimental Box

- air layer**: negligible viscosity → no interference**
  空气层：粘度可忽略，无干预
- brittle upper crust**: high viscosity, yield law to simulate brittleness**
  脆性上地壳：高粘度，基于屈服准则模拟脆性材质
- plastic lower crust**: low viscosity, some stress dependence**
  塑性下地壳：低粘度，一定的应力依赖性

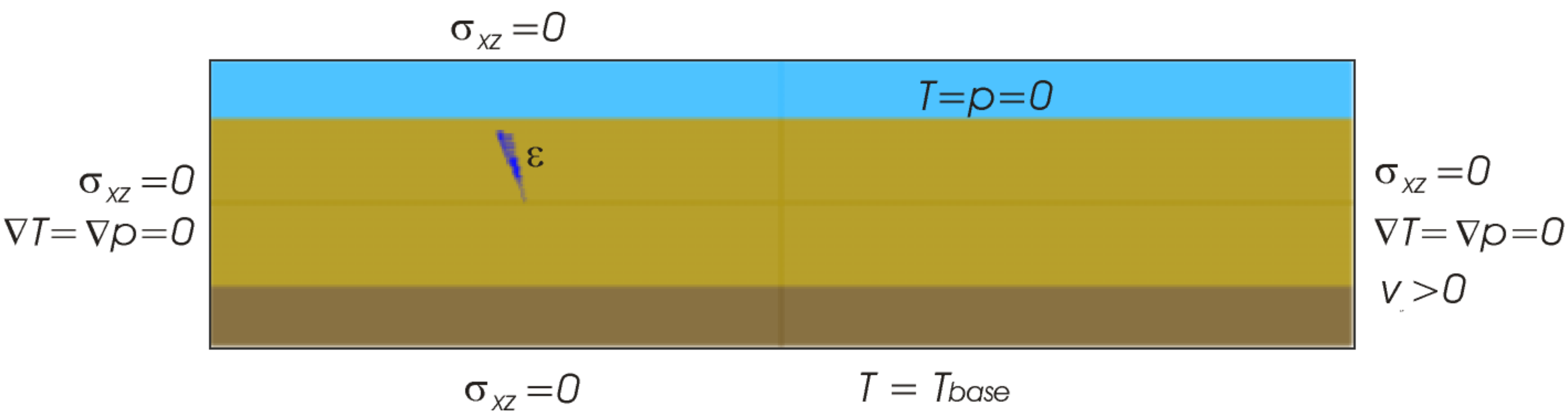

Experimental Box

– boundary conditions **(边界条件)**： **-shear stress 固体剪切应力**
-temperature 温度
-pore pressure 孔压
-initial strain perturbation 初始应变扰动

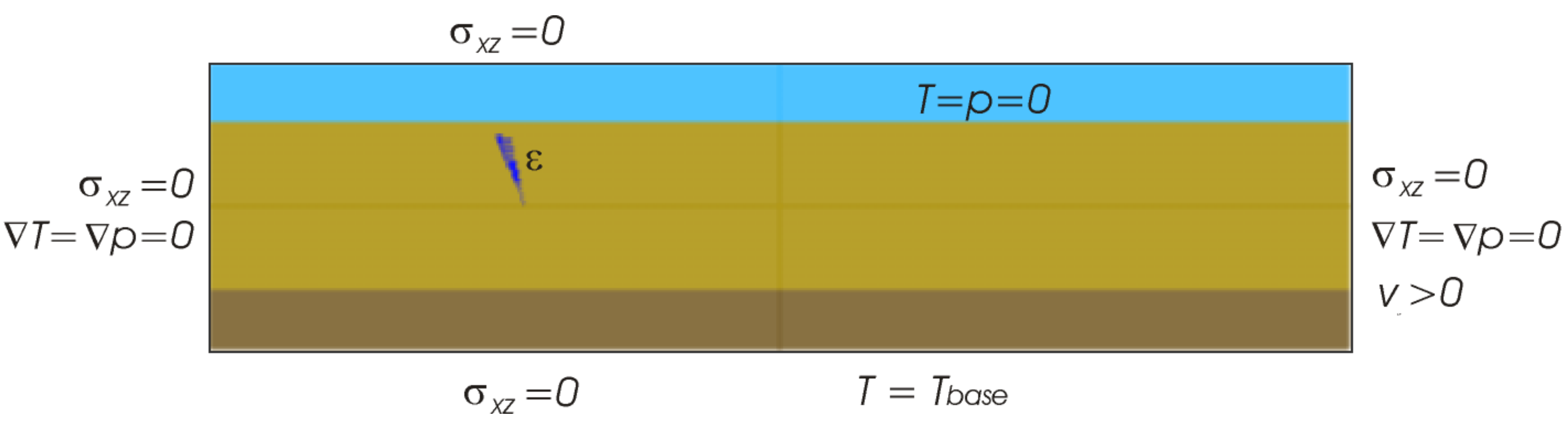

Crustal Strength

- *described by viscosity* **(粘度描述)**
  - **limited by yield curve → effective viscosity**
    受限于屈服曲线 → 有效粘度

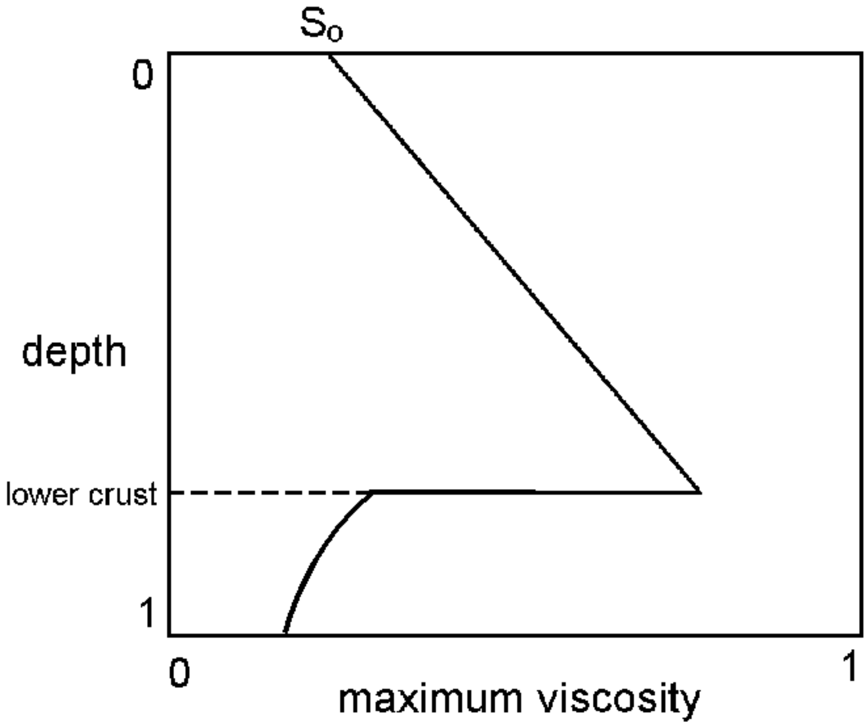

Dry Model Experiments

- **Low viscosity contrast between layers**
  层间低粘度比

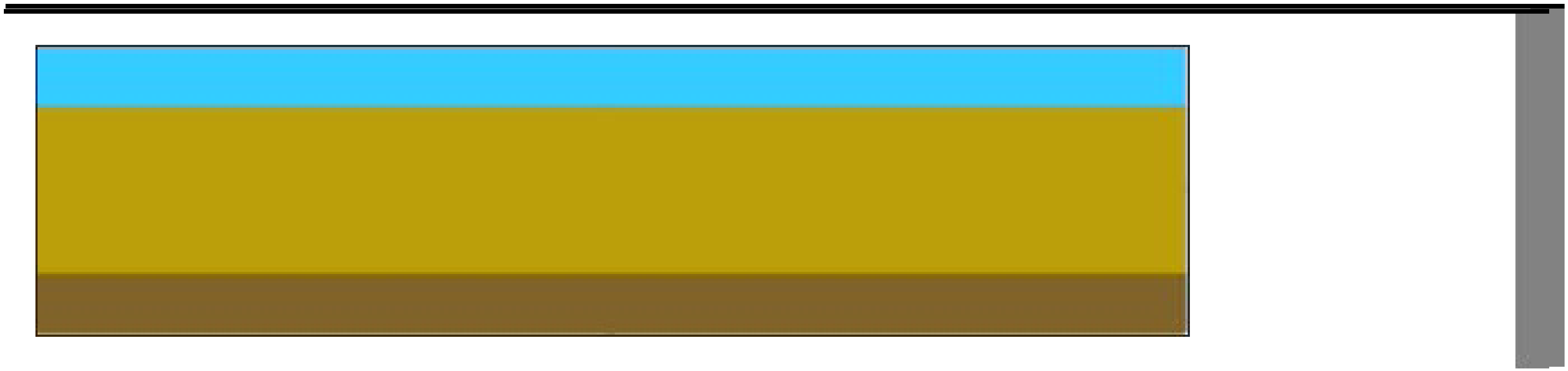

- **High viscosity contrast, high yield strength**
  高粘度比，高屈服强度

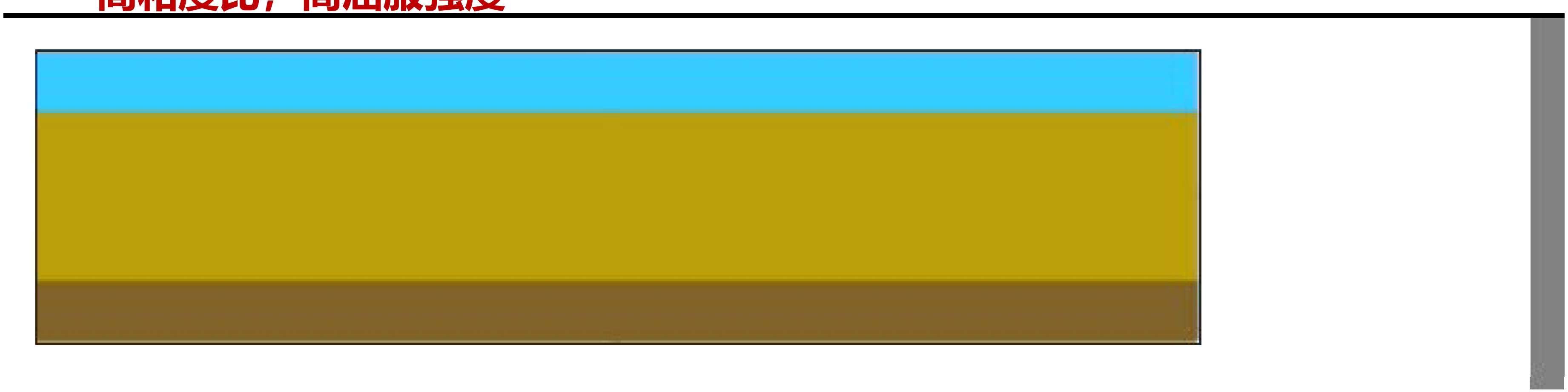

Dry Model Experiments

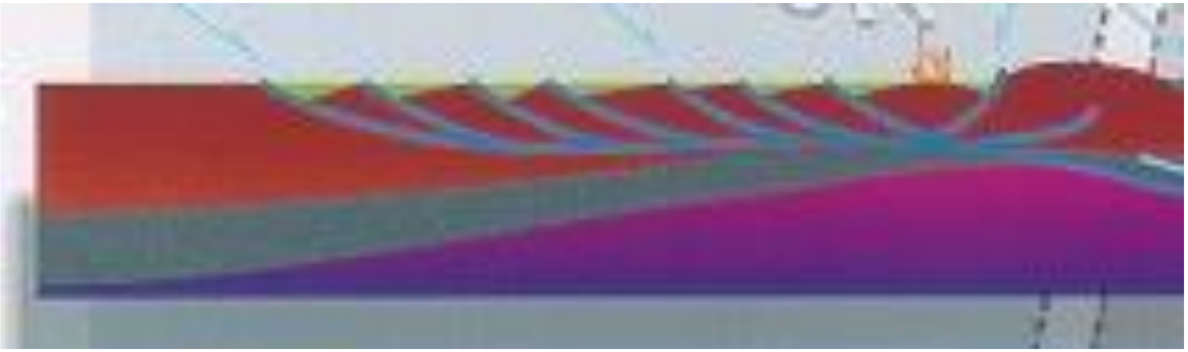

- **large viscosity contrast between crustal layers, lower yield viscosity (blue = shear zones)**
  地壳层间粘度比很高，低屈服粘度（蓝色 = 剪切带）

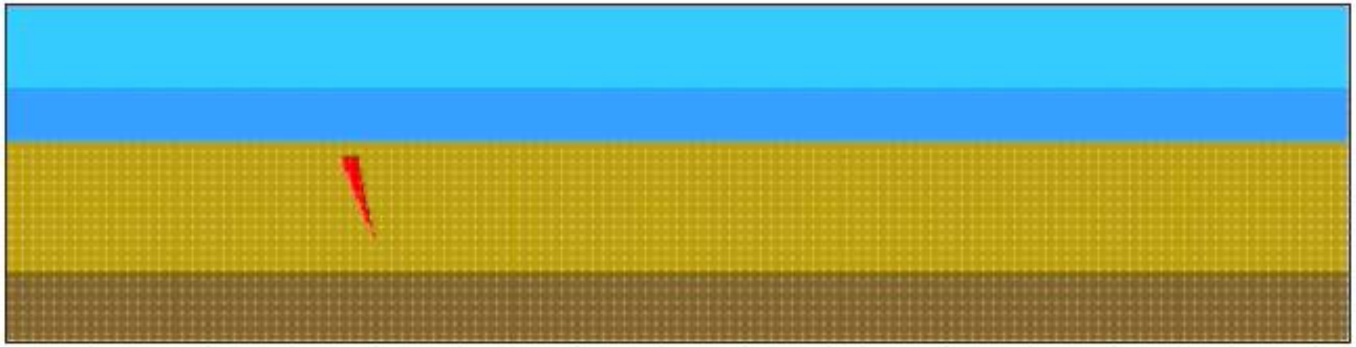

Addition of Pore Fluid

- effective stress　有效压力

solid stress + fluid stress

= solid stress + pore pressure

固体压力+流体压力

= 固体压力+孔隙压力

Addition of Pore Fluid

- porosity evolution 孔隙度演变

Porosity ϕ depends upon bulk solid volume changes

孔隙度Φ取决于固体体积变化

Addition of Pore Fluid

- permeability evolution **(渗透率演变)**

permeability k = k(ϕ , ε_p)

(plastic strain dependence → dilation angle)

(塑性应变依赖→ 膨胀角)

Physical Assumptions

- connected pore network 孔隙网骆相连
- saturated medium 饱和媒介
- fluid flows according to Darcy's Law 流体流动遵循达西定律
- ignore capillary pressures 忽略毛细管压
- incompressible solid

  固体不可压缩
- no thermal strains in the solid 固体中无热应变

Pore Flow

- extension + compression 伸展+挤压

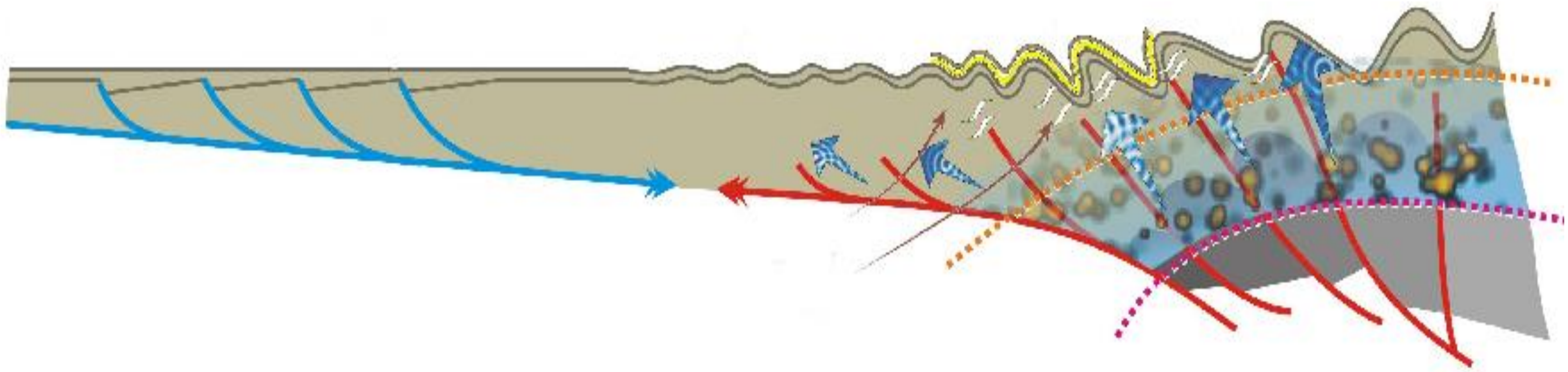

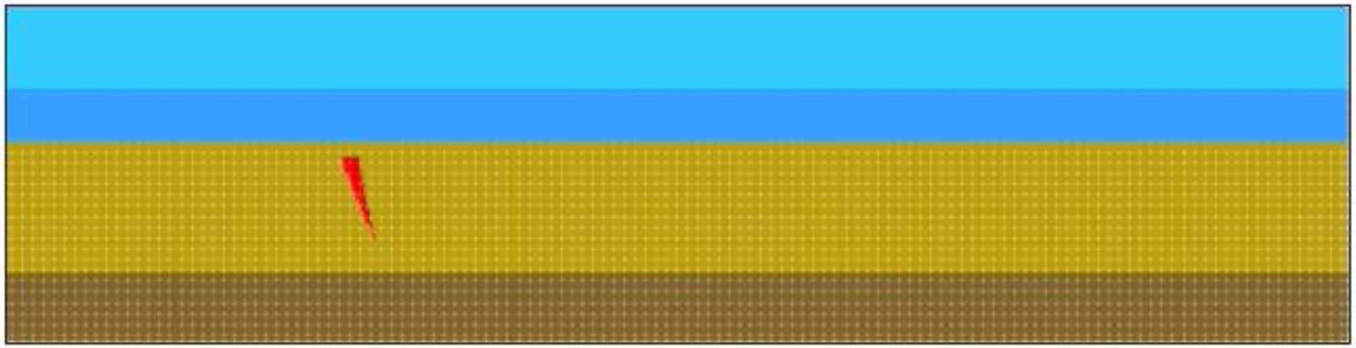

Pore Flow

- **extension + compression** **伸展+挤压**

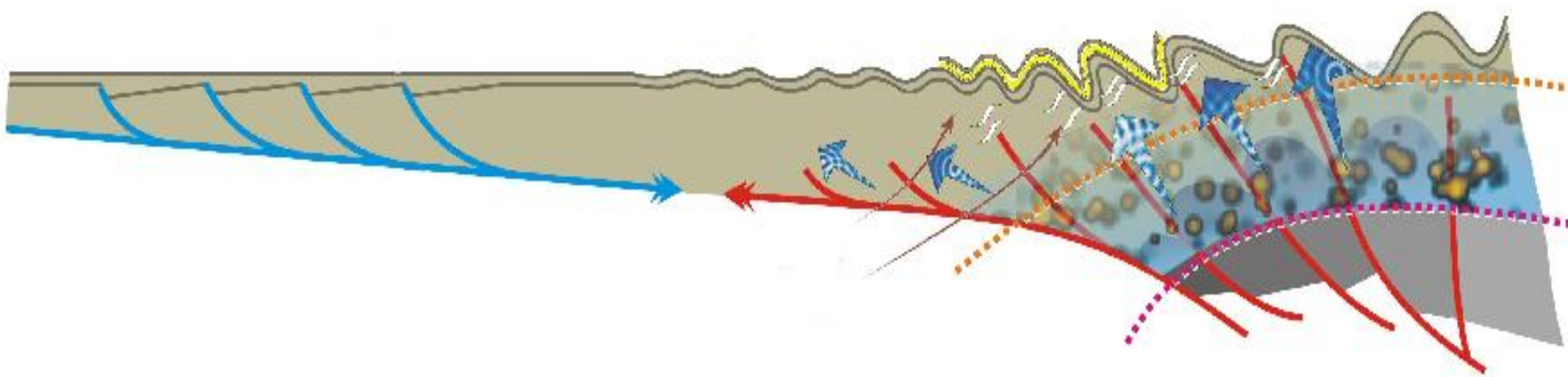

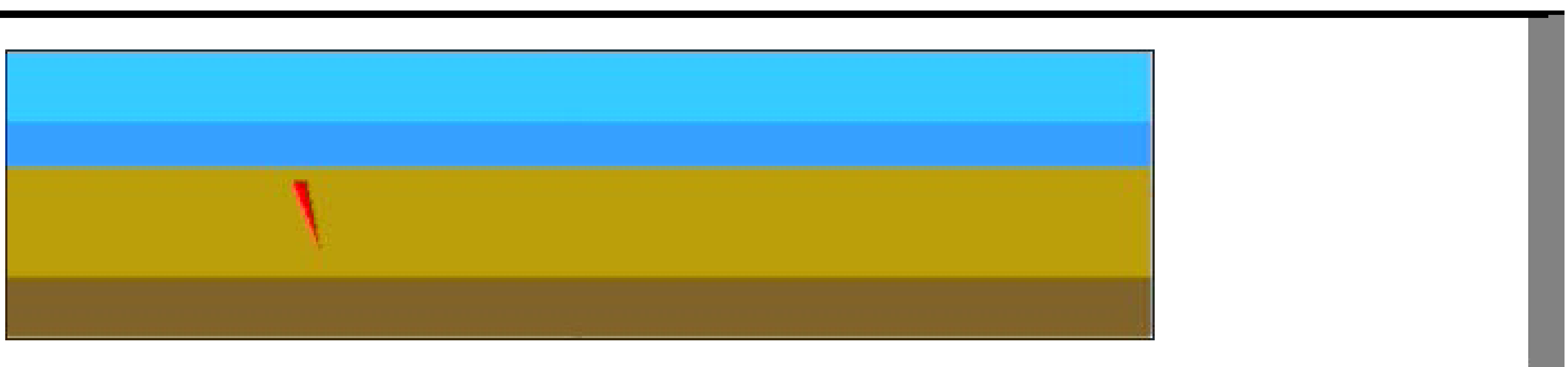

Weaker bottom layer (no flow vectors)

Pore Flow

- initial drawdown during extension
  - 伸展过程中，初始为向下流动

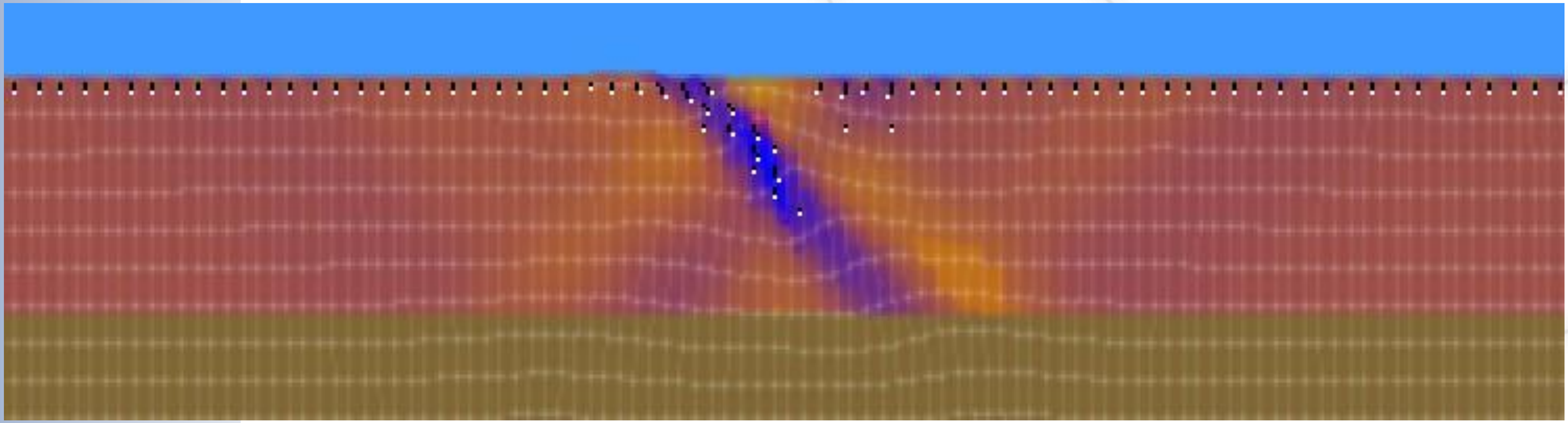

Pore Flow

- **flow down faults （blue）during extension**
  - **伸展过程中，向下流经断层**

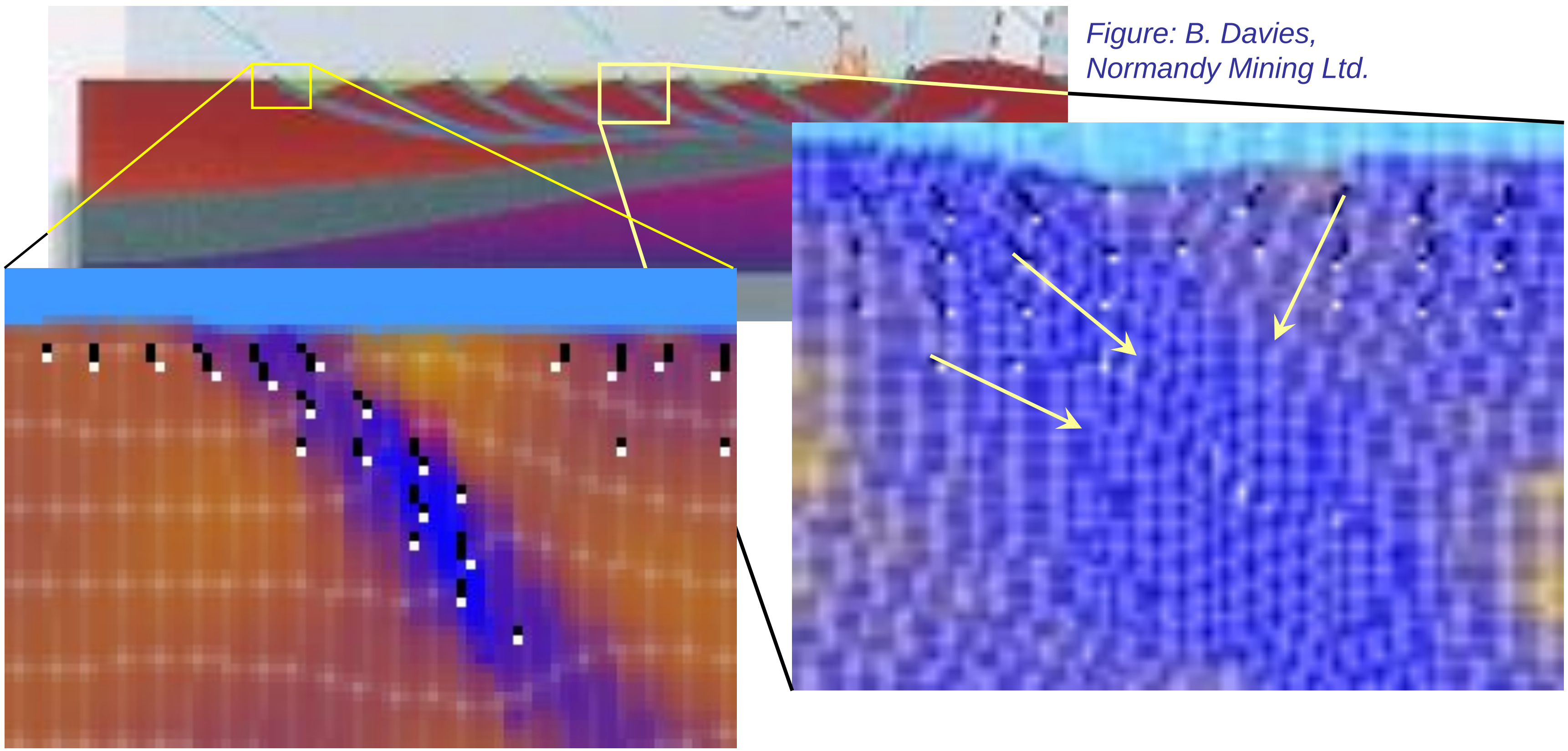

Figure: B. Davies, Normandy Mining Ltd.

Pore Flow

- **flow up (blue) faults during compression**

挤压过程中，流体经断层向上流动

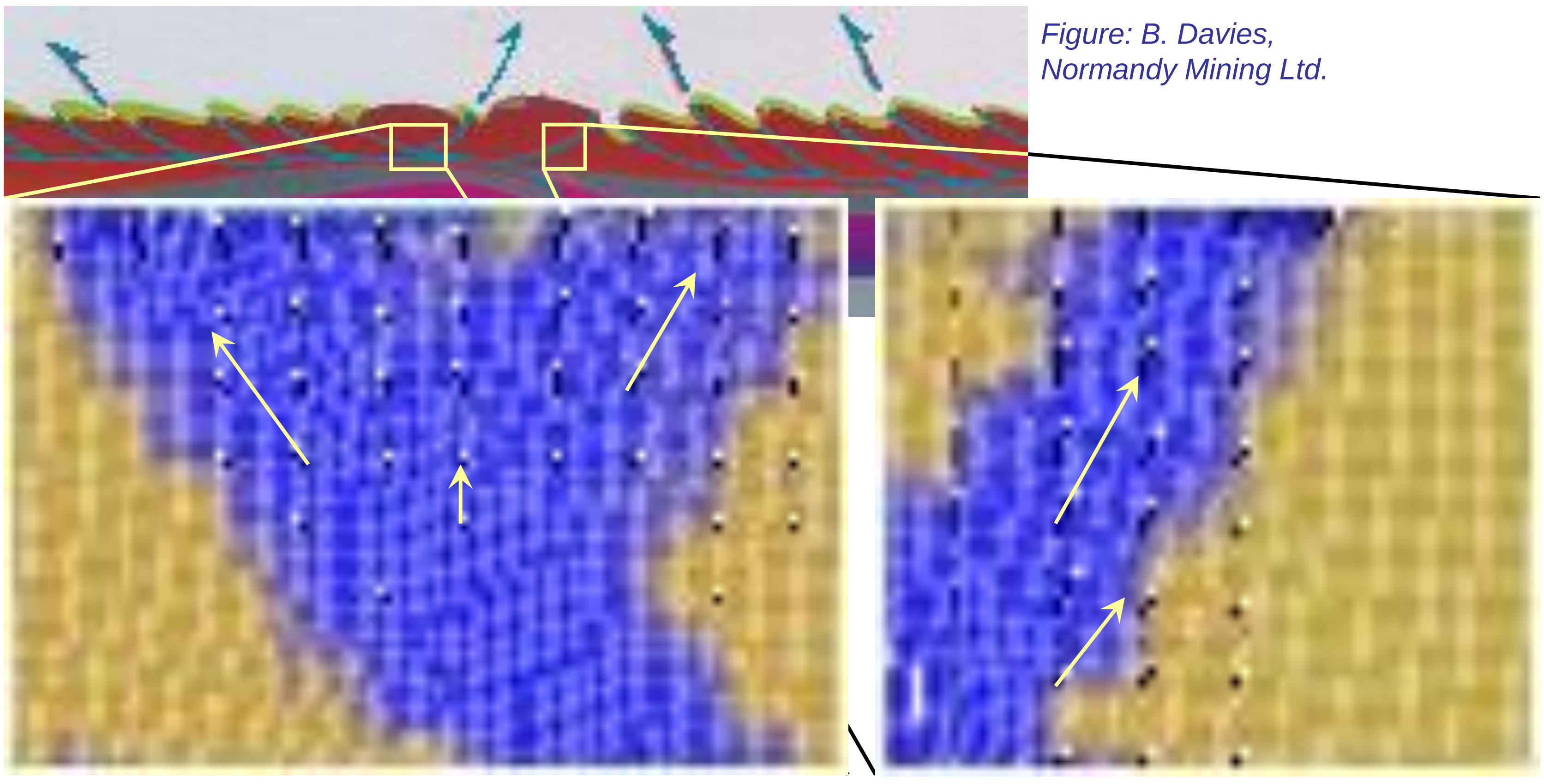

Figure: B. Davies, Normandy Mining Ltd.

Pore Flow

- **influence of topography**

受地势影响

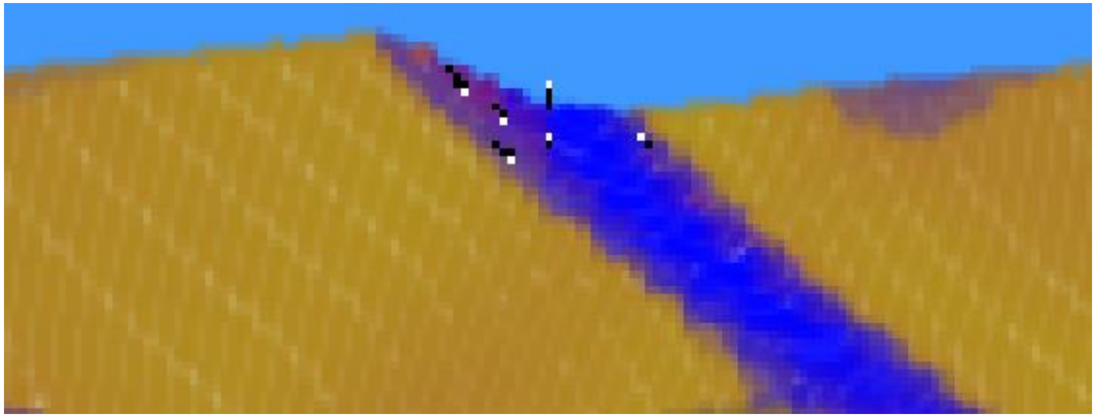

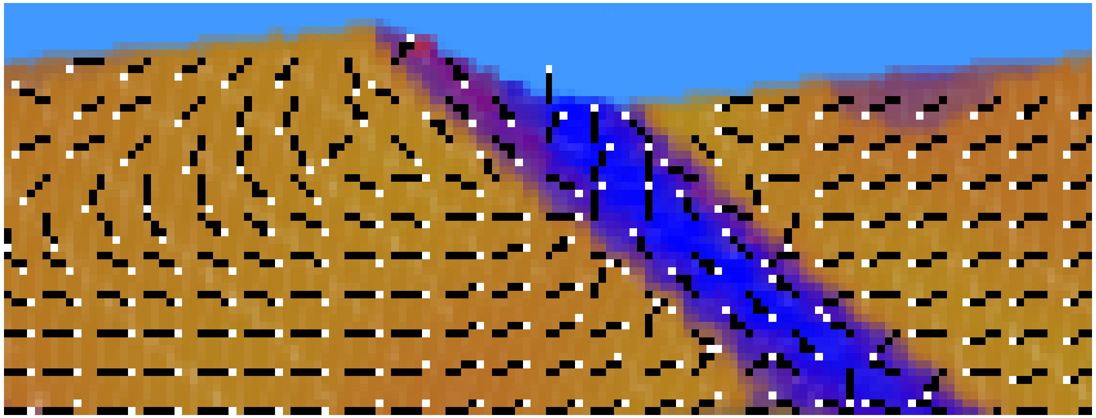

Competing effects of upward flow from compression and topographically driven downward flow

挤压导致的向上运动的流体与地势引起的向下运动的流体出现竞争效应

Next Steps

- anisotropic dilation angle effect

  各向异性膨胀角影响
- anisotropic permeability development in shear zones

  剪切带中的渗透率各向异性

  → fluid flow seals

  → 垂向流体流动封闭
- fluid boundary conditions need to be carefully considered

  细致考虑流体边界条件

Conclusions

- code is a tool

  代码是工具

- reproduces qualitative features of conceptual model

  重建概念模型中的定性特征

- extension - fluid channelled towards and down faults

  伸展 - 流体在断层中上下运移

- compression - fluid channelled up faults during reworking of domains

  挤压 -流体在断层中向上运移

Numerical technique:

- **Rheological model:** VISCO-EELASTO-PLASTIC

  流变模型：粘弹塑性

- **Stable mineral assemblages** are computed based o thermodynamic data and Gibbs free energy minimization (Connolly & Petrini, 2007) as a function of P and T

  稳定的矿物组合: 可根据热力学数据和最小吉布斯自由能（比如P和T的的函数）计算得到。

- **Hydration and water migration:** Dehydration reactions and associated water release are computed based on the physico-chemical conditions and the assumption of thermodynamic equilibrium. Expelled water is stored in a newly generated water marker that moves independently

  水合作用和水迁移：脱水反应和相关水的释放可基于物理化学条件和热力学平衡假设计算得到，释放的水储存在一个新生成的水环境中，并且能够独立移动

- **Changes in topography** - account for the effects of erosion and sedimentation

  地形改变：考虑侵蚀和沉积的影响

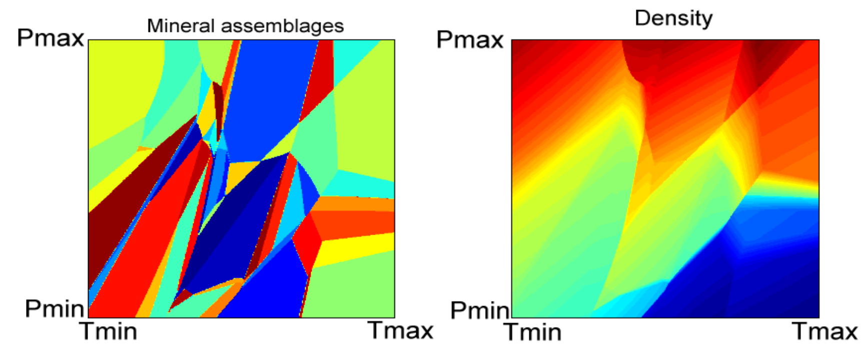

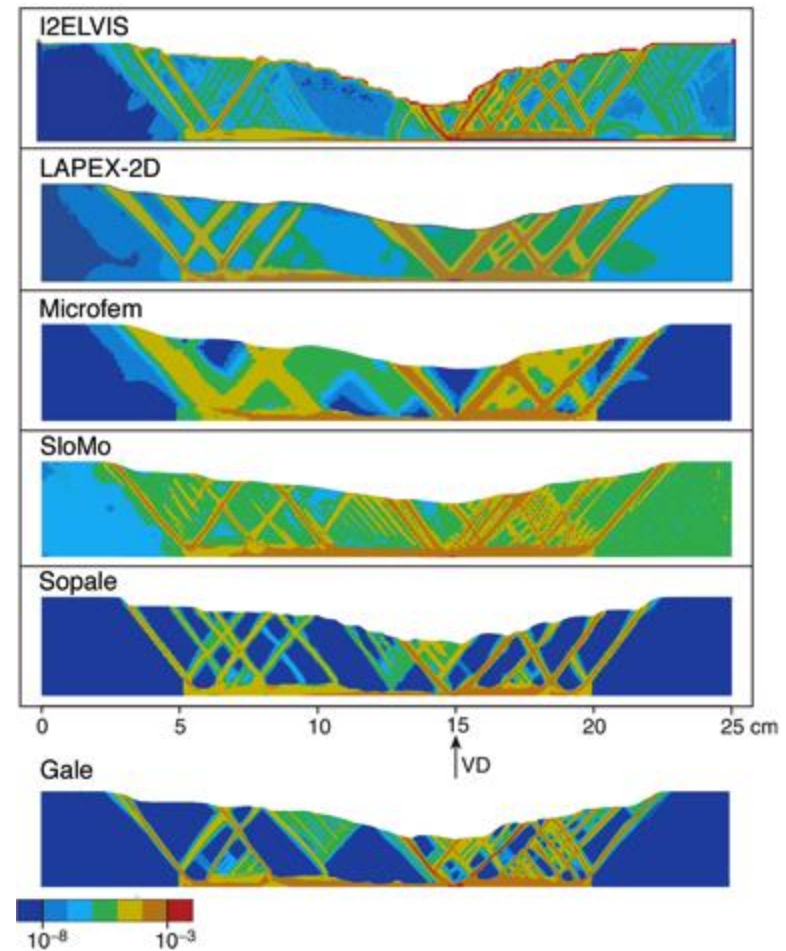

Numerical technique:

•**Partial melting** – For a given pressure and rock composition the volumetric degree of melting M_0 is:
部分熔融 - 对于给定的压力和 岩石组成，熔融的M0体积度是：

$$M_0 = 0 \quad \text{when } T < T_{solidus},$$

$$M_0 = (T - T_{solidus}) / (T_{liquidus} - T_{solidus}) \text{ when } T_{solidus} < T < T_{liquidus},$$

$$M_0 = 1 \quad \text{when } T > T_{liquidus},$$

•effective viscosity is calculated using:

$$\eta = \eta_0 \exp[2.5 + (1-M)(\frac{1-M}{M})^{0.48}]$$

$\eta_0 = 10^{13}$ Pa·s - molten mafic rocks,
$\eta_0 = 5\times10^{14}$ Pa·s - molten felsic rocks

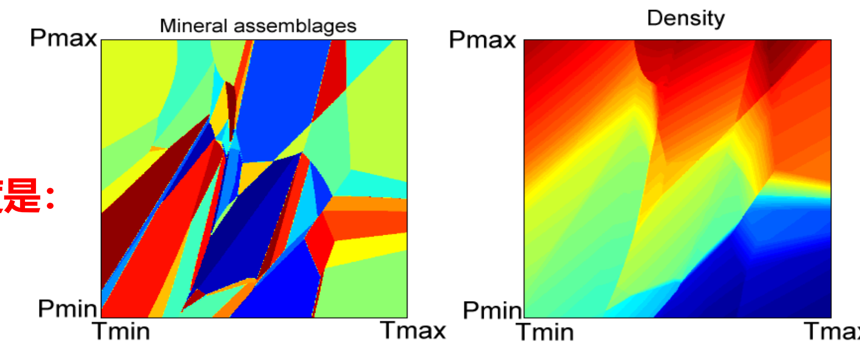

•**Melt extraction and intrusion** – when melt fraction exceeds 4%, only 4% remain in the source, markers track the amount of extracted melt. **熔体萃取和侵入- 当熔体超过4%，只有4%的熔体保留源中，标记能够对萃取的数量进行追踪。**

Extracted melt is transmitted instantaneously to emplacement areas: **萃取的熔体即时侵位**
intrusive rocks 80% of melt **侵入岩80%熔体**
extrusive rocks – 20 % of melt **喷出岩 – 20%熔体**

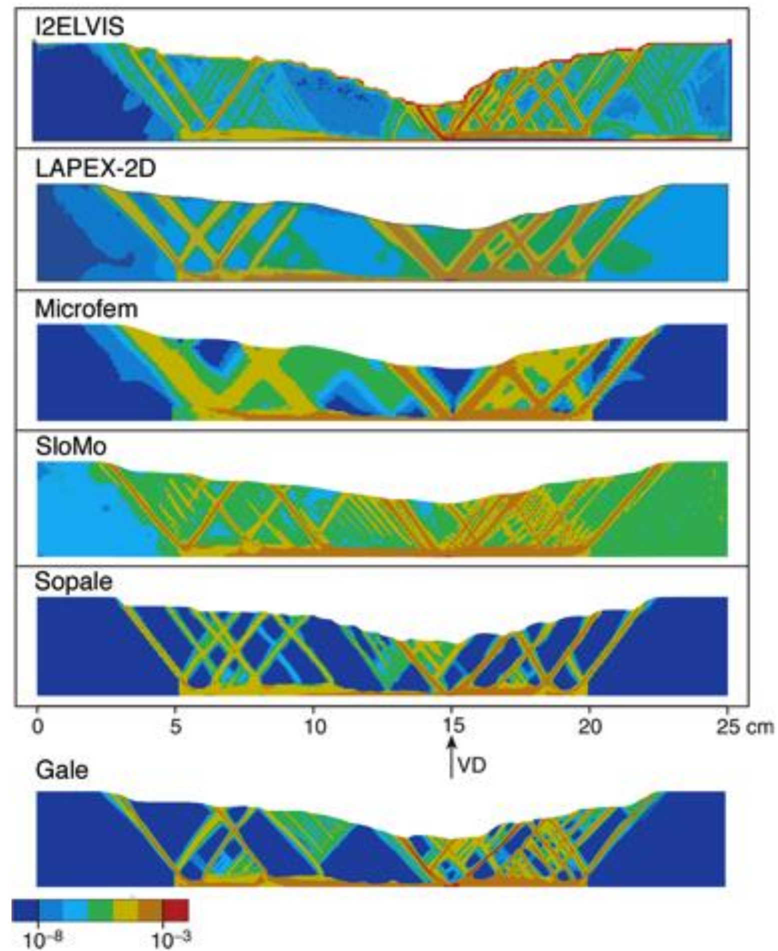

A movie demonstration of this software.

2 scenarios

1A: A weak zone dips to the left (movies 1 and 2)

1B: A weak zone dips to the right (movies 3 and 4)

The models have the same strength for the weak zones.

2: The strength of the lower crust is lower in the second and fourth movies.

下面的影片中具有相同强度的软弱区，但在第二个和第四个影片中，上地壳强度较小

Initial condition

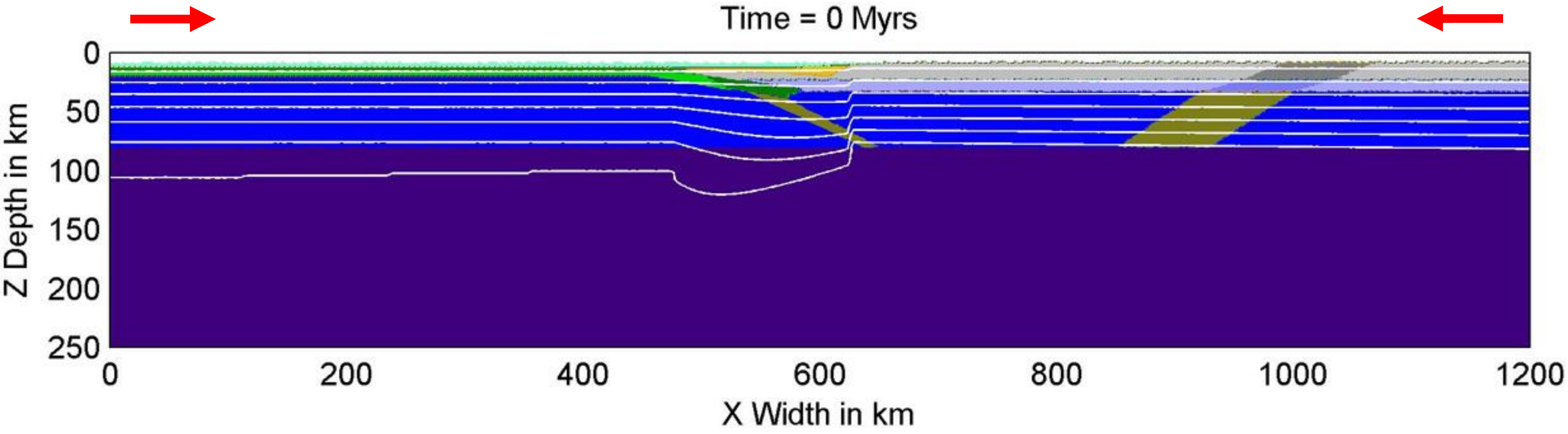

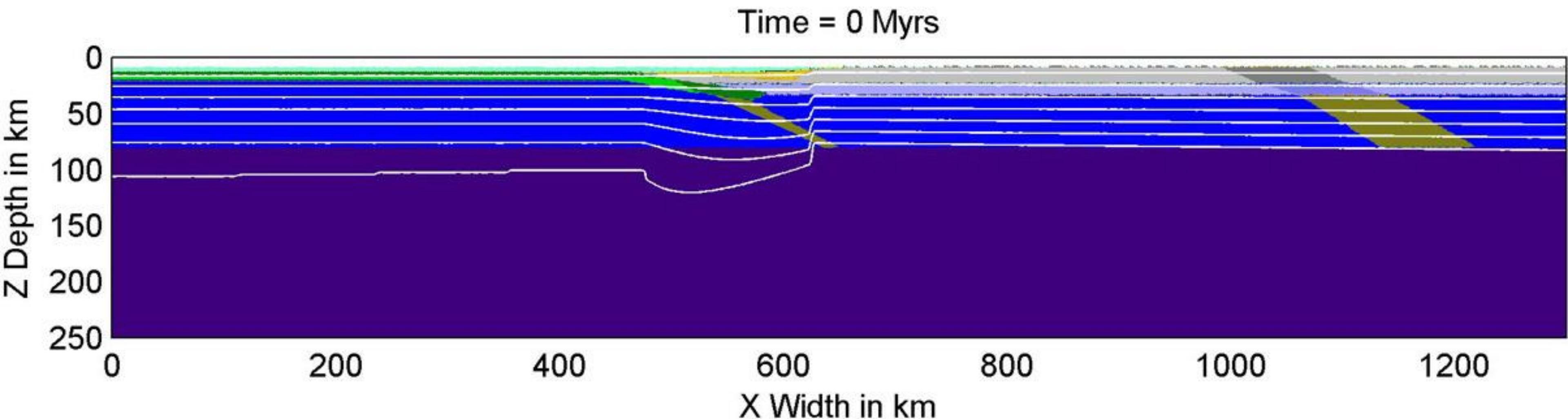

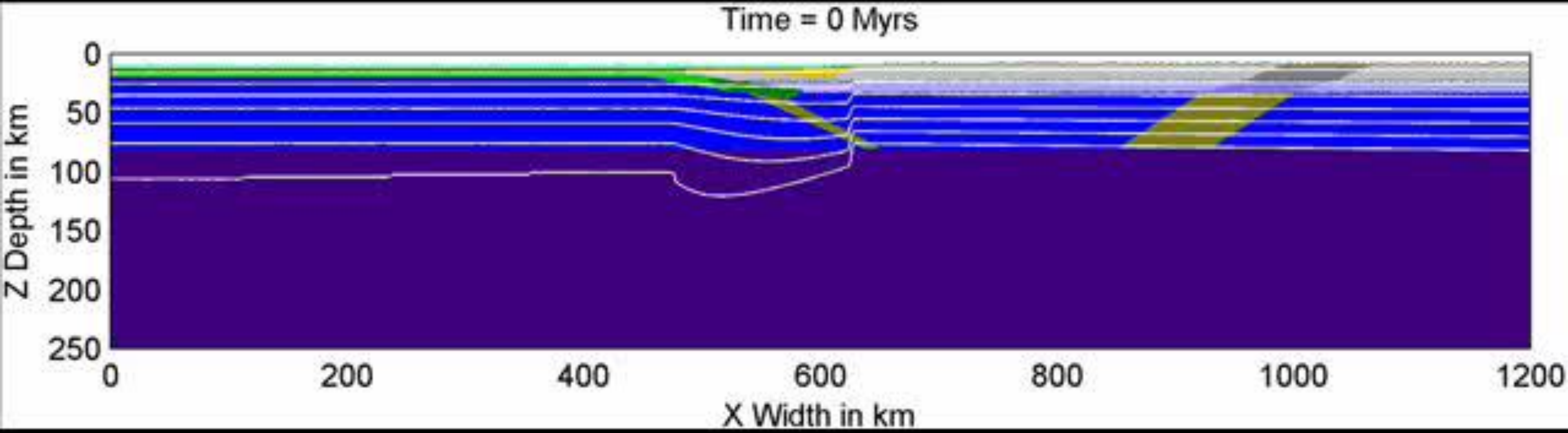

Time = 0 Myrs
0
50
100
150
200
250
Z Depth in km
0
200
400
600
800
1000
1200
X Width in km

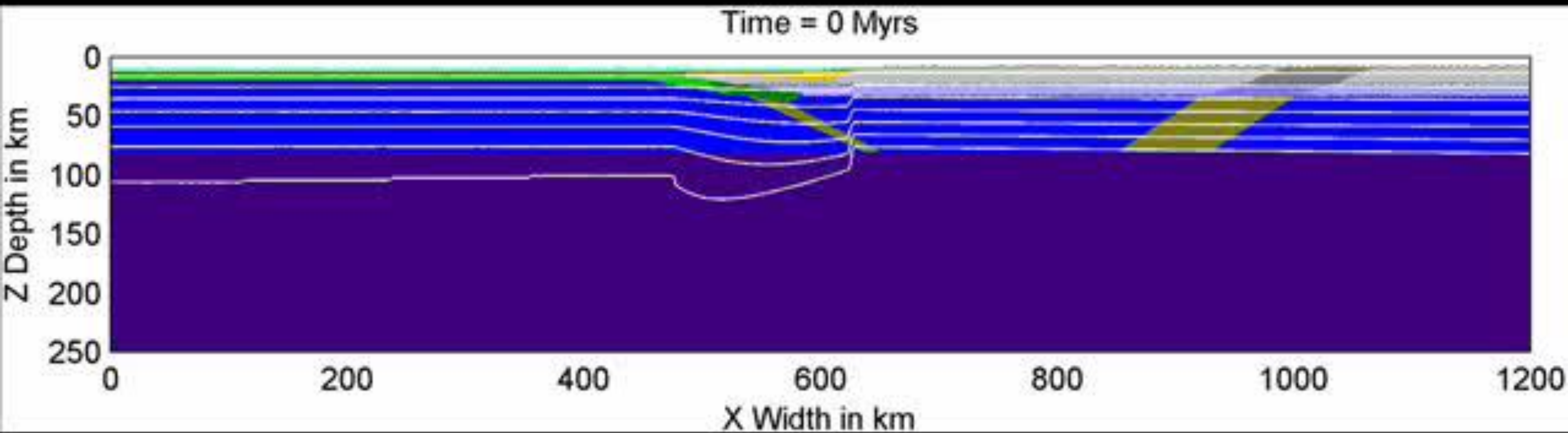

Time = 0 Myrs
Z Depth in km
0
50
100
150
200
250
0
200
400
600
800
1000
1200
X Width in km

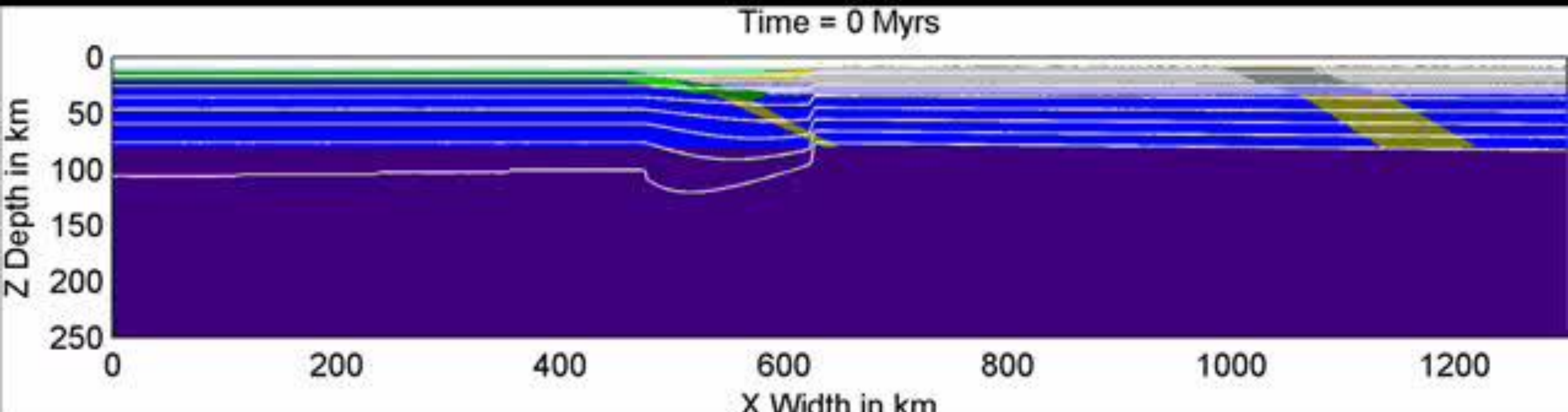
Time = 0 Myrs
0
50
100
150
200
250
Z Depth in km
0
200
400
600
800
1000
1200
X Width in km

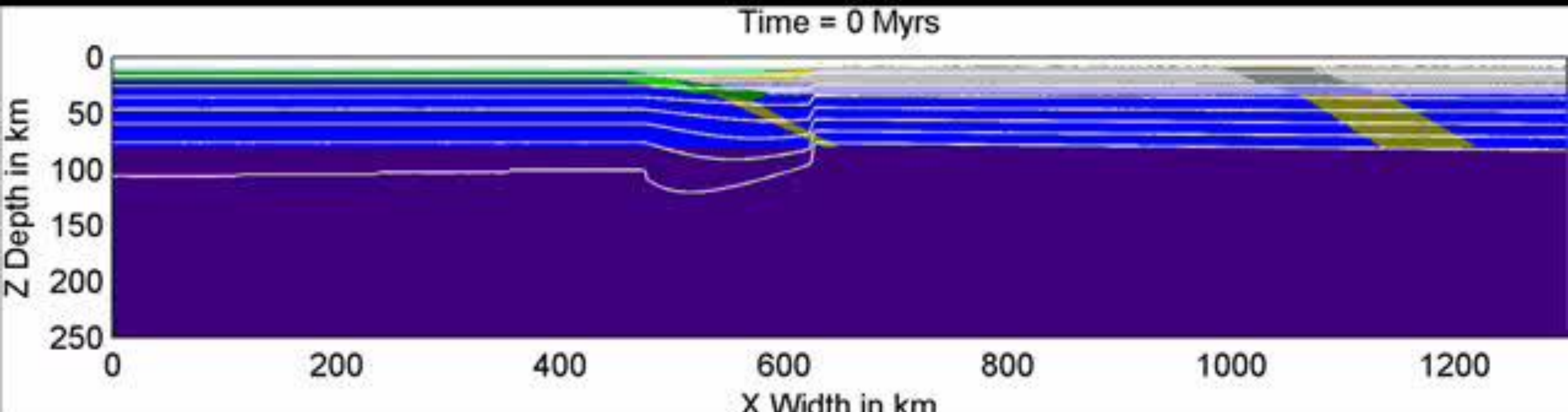

Time = 0 Myrs
Z Depth in km
0
50
100
150
200
250
0
200
400
600
800
1000
1200
X Width in km

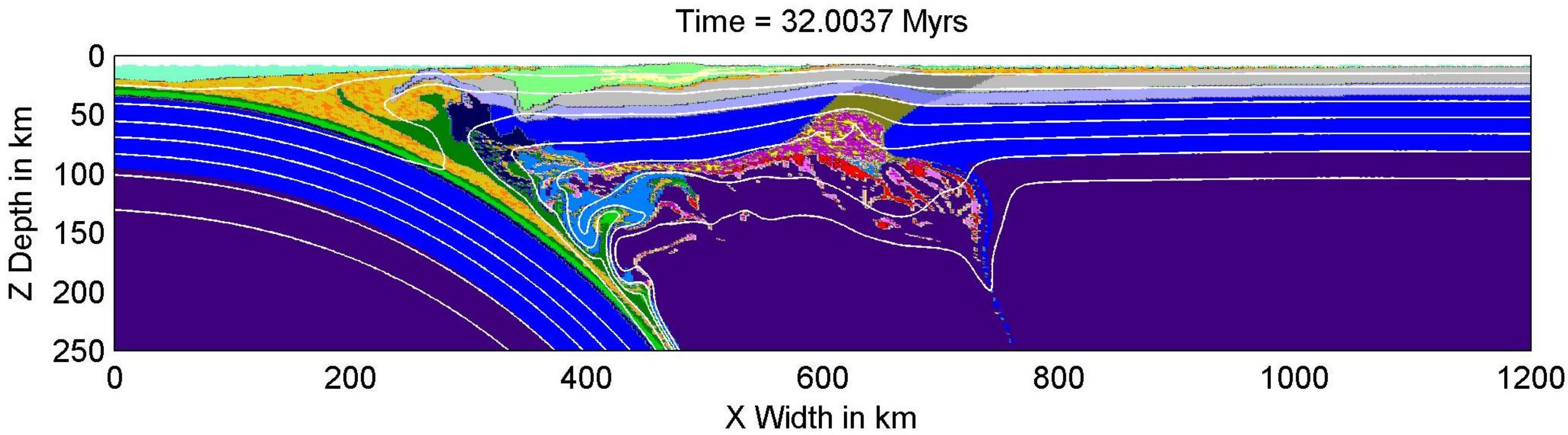
Time = 32.0037 Myrs
Z Depth in km
0
50
100
150
200
250
0
200
400
600
800
1000
1200
X Width in km

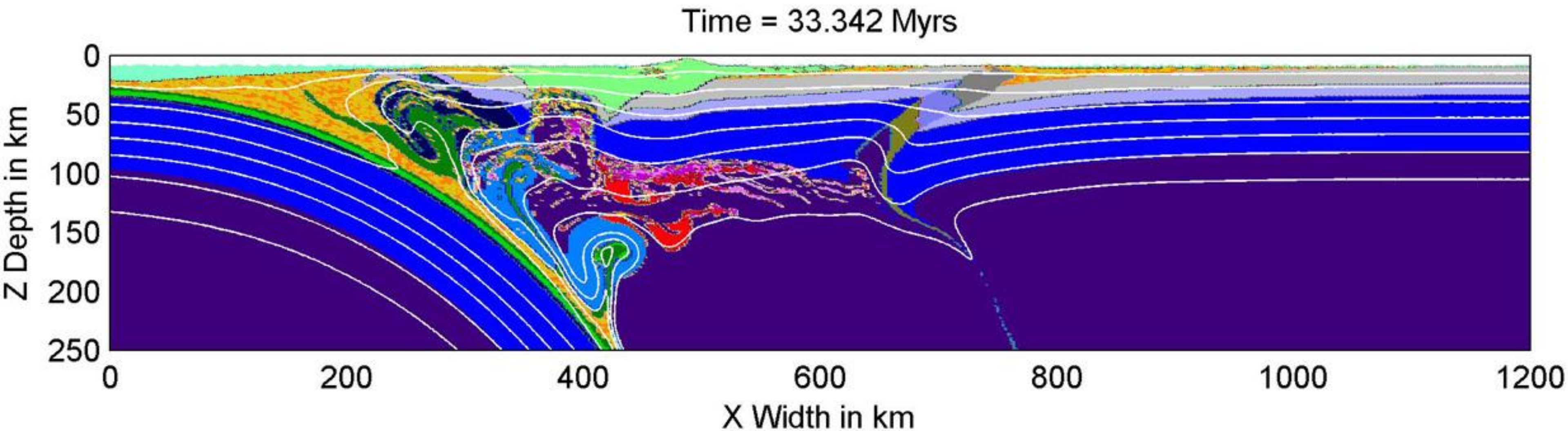
Time = 33.342 Myrs
Z Depth in km
0
50
100
150
200
250
0
200
400
600
800
1000
1200
X Width in km

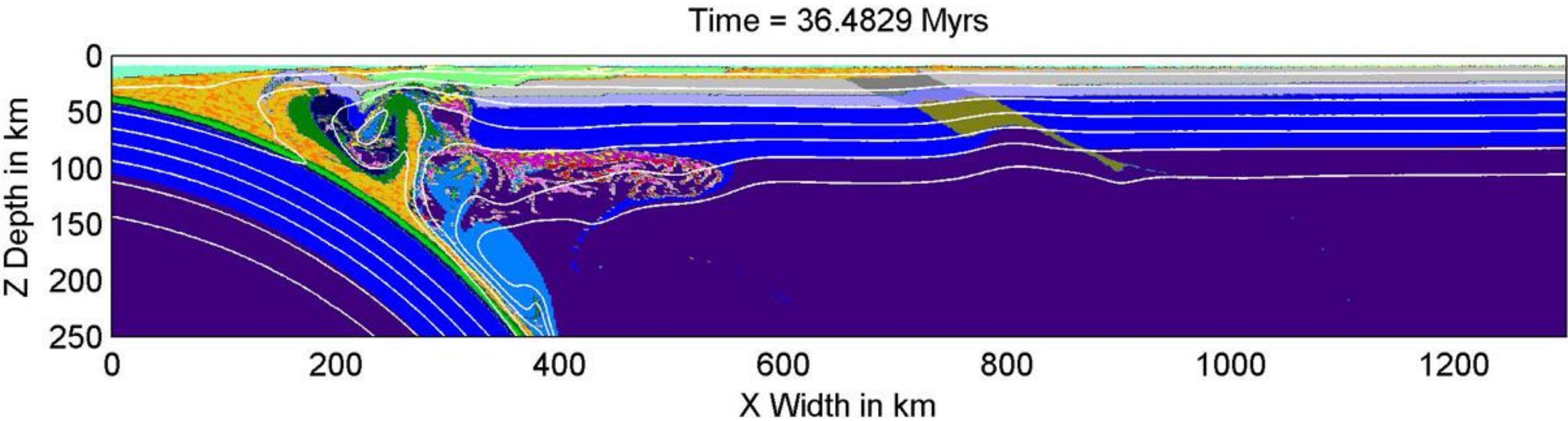

Time = 36.4829 Myrs
Z Depth in km
0
50
100
150
200
250
0
200
400
600
800
1000
1200
X Width in km

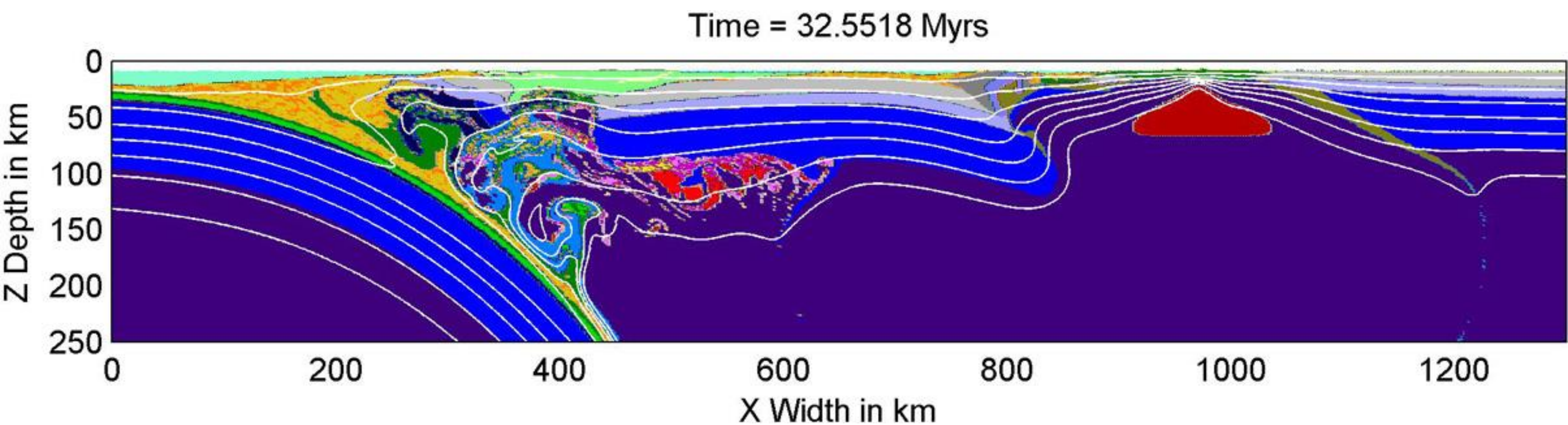

Time = 32.5518 Myrs
Z Depth in km
0
50
100
150
200
250
0
200
400
600
800
1000
1200
X Width in km

Initial setup:

Compression for 6Ma at rates: 0.5, 1, 2, 3 cm/a

Lithospheric thickness: 60, 80, 100, 200, 300 km

初始设置

6Ma压缩:

岩石圈厚度:

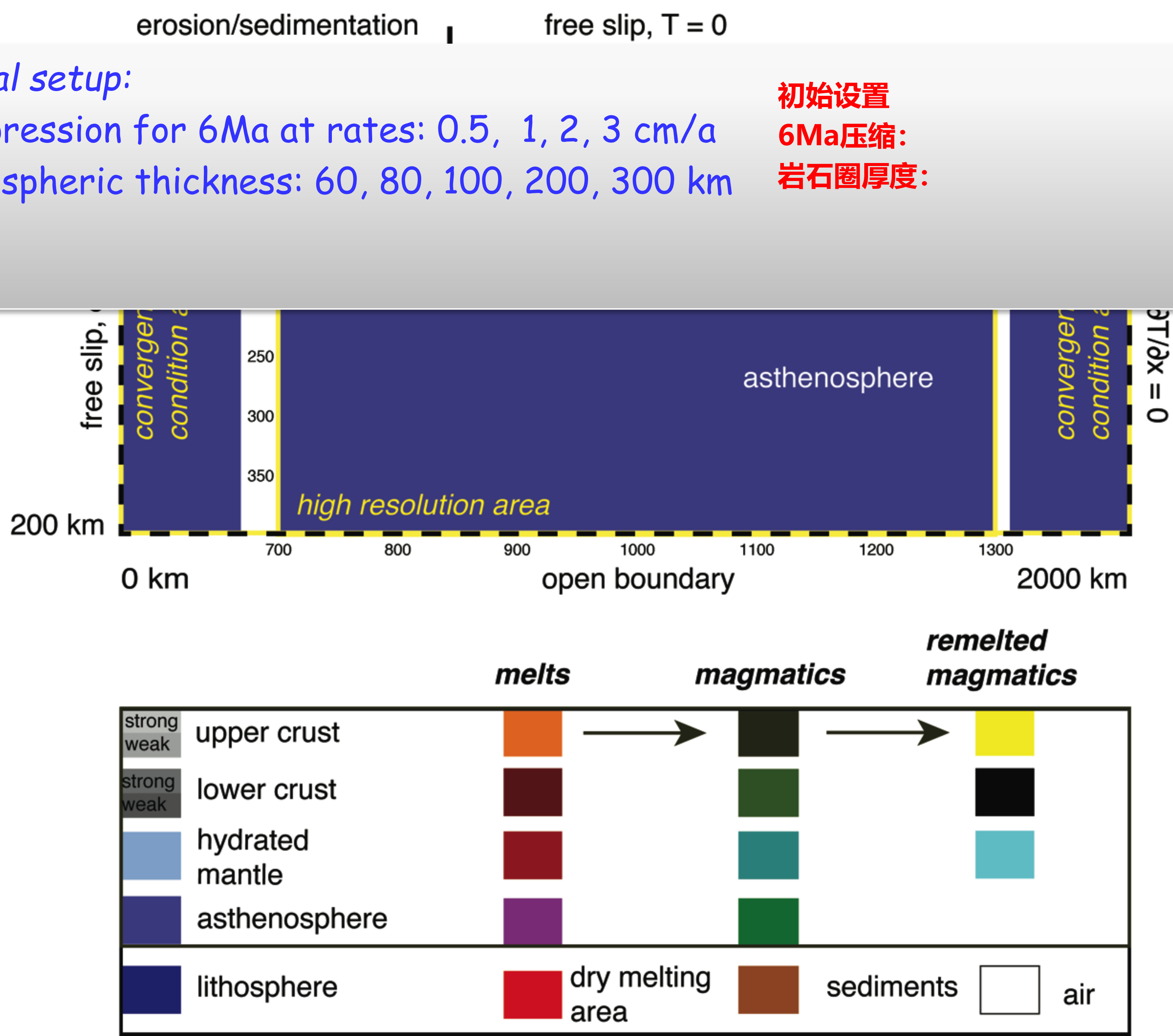

Intra-plate tectonics and magmatisim associated with it

板内构造与相关岩浆活动

Delamination

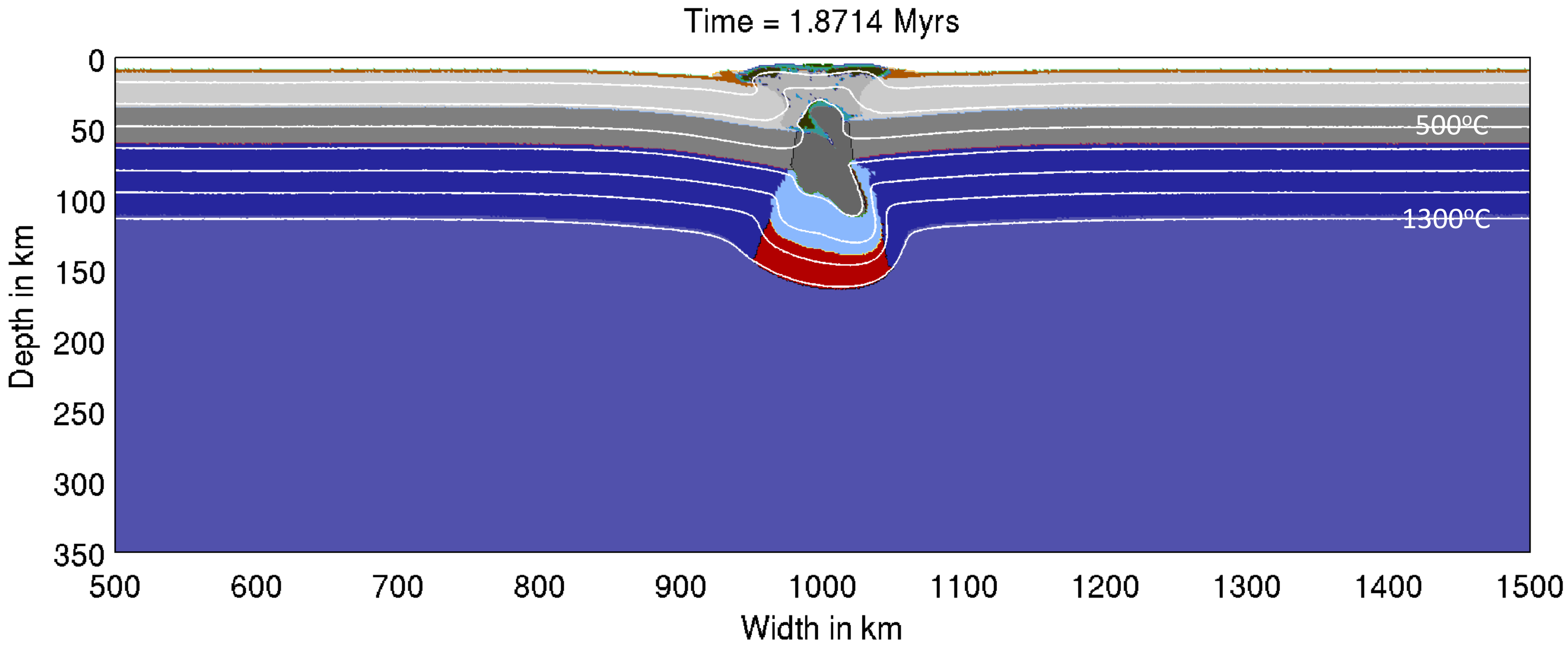

Delamination

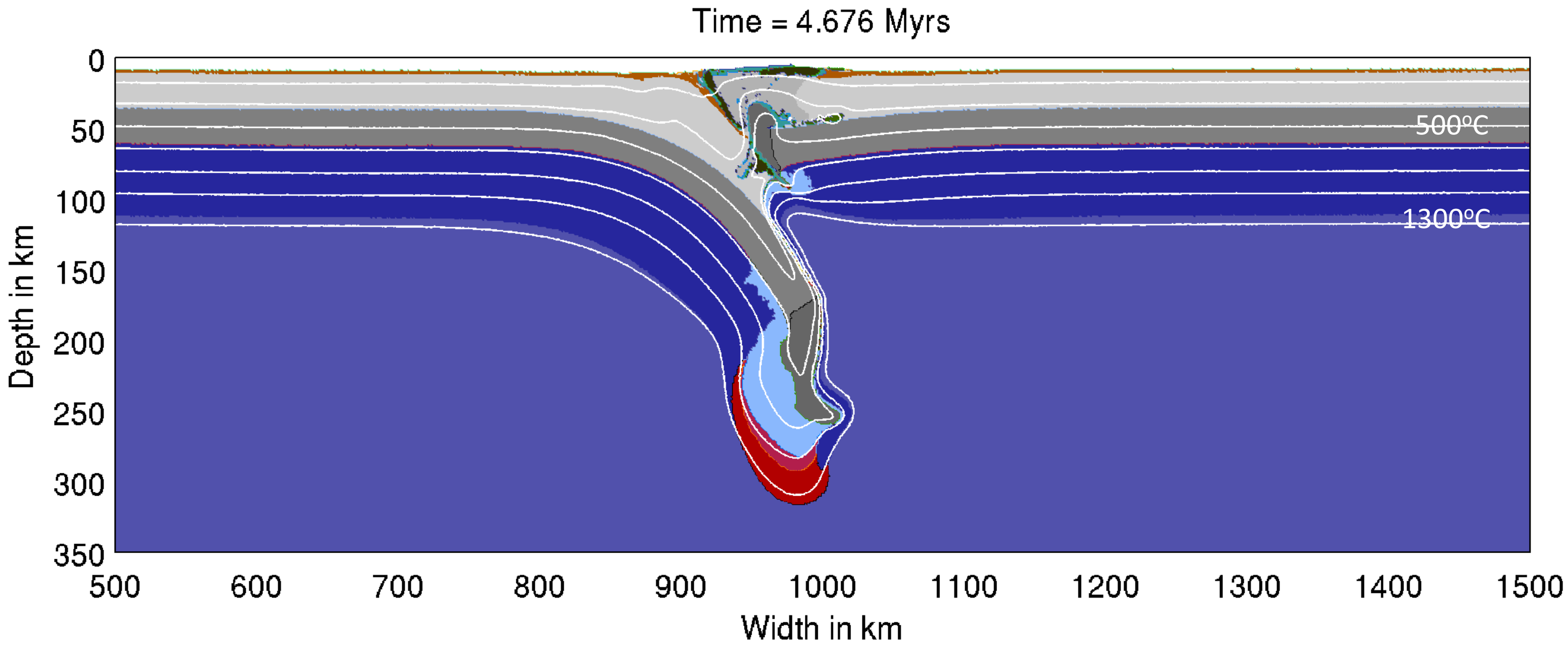

Delamination

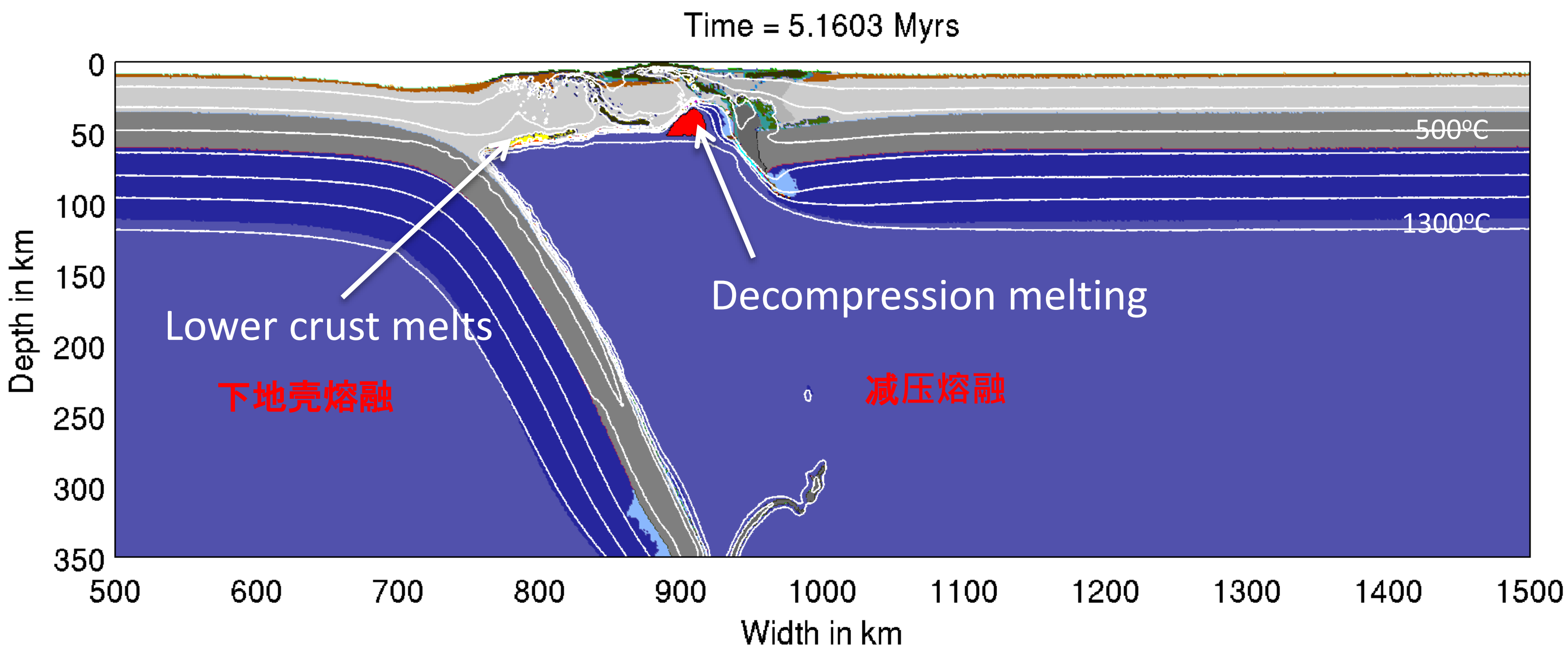

Delamination

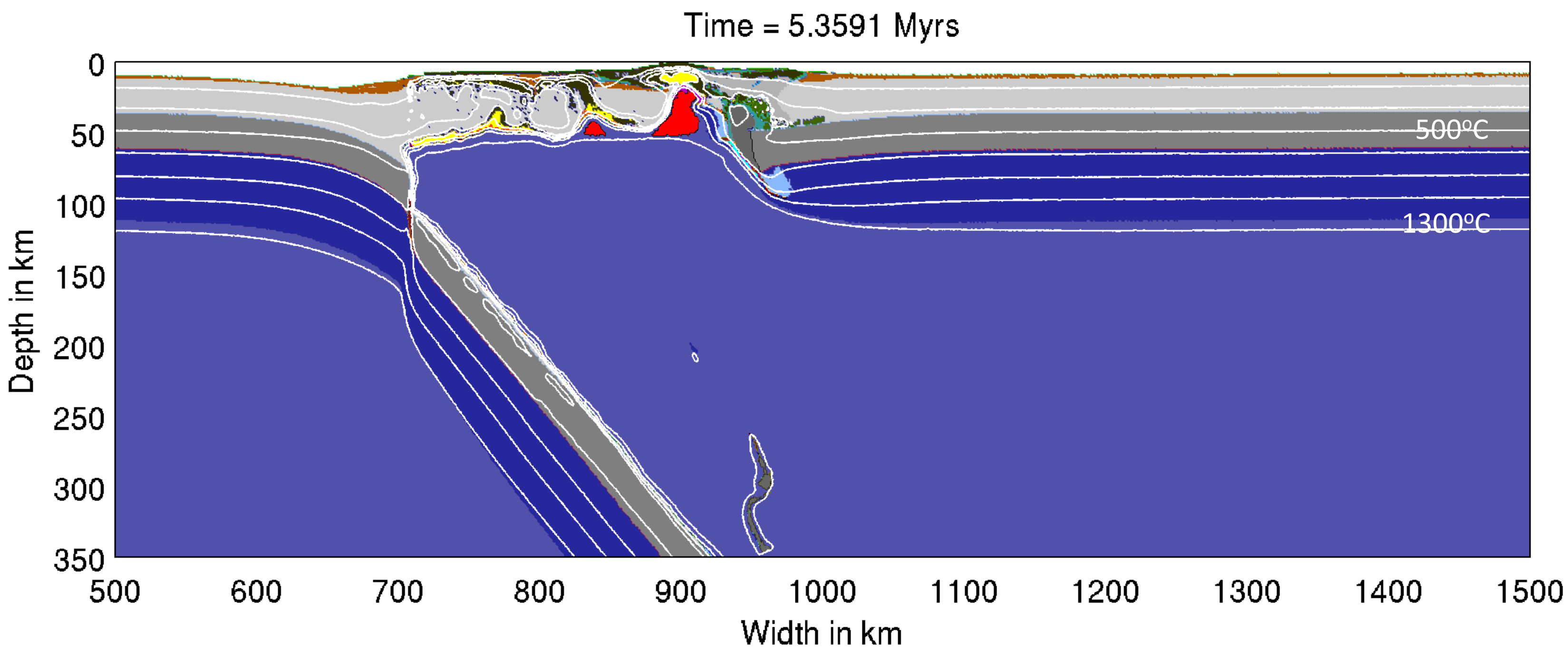

Delamination

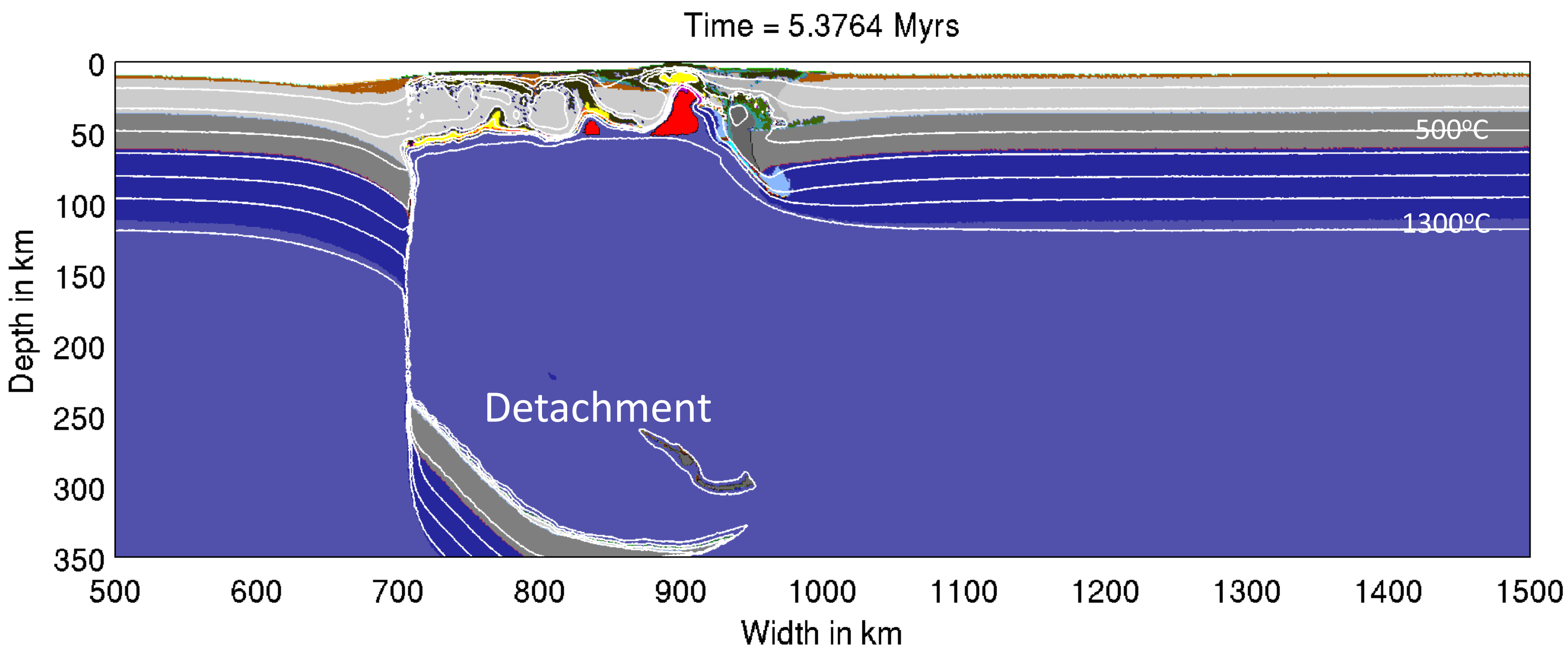

Delamination

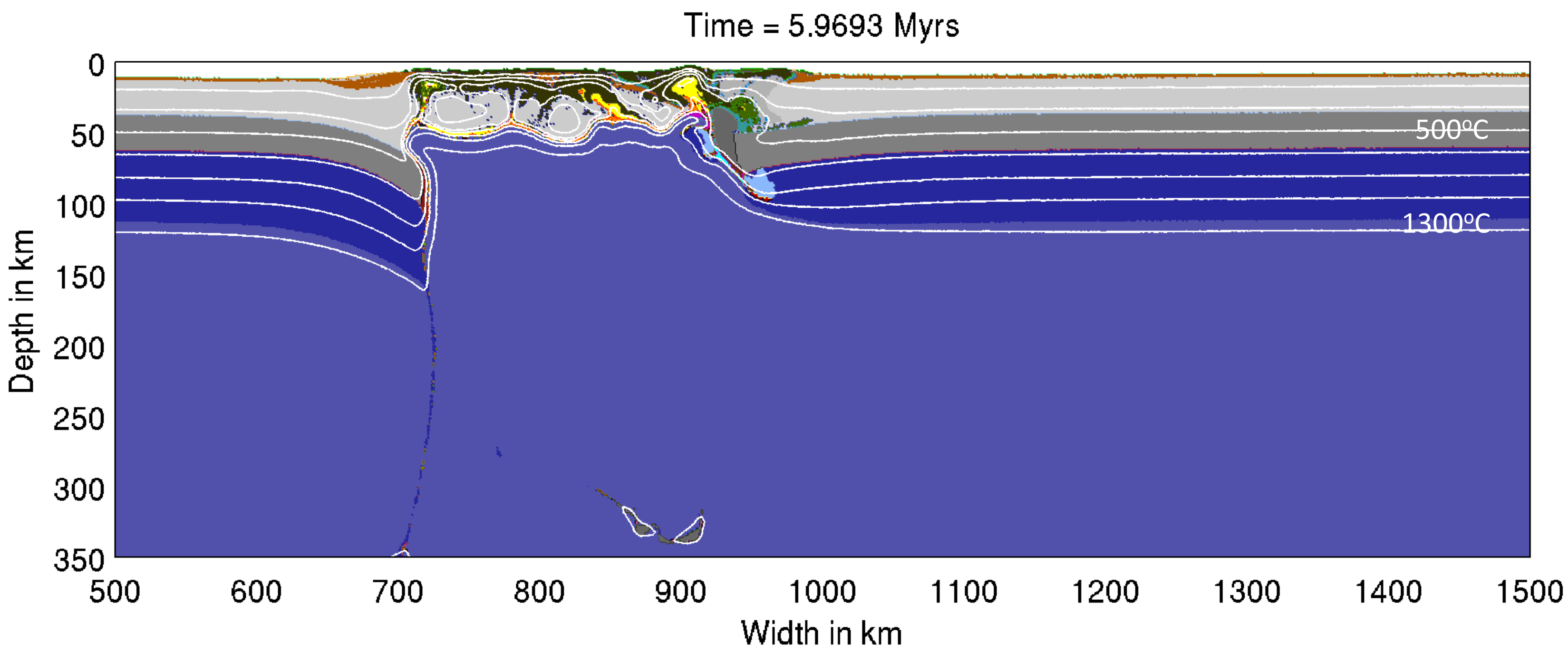

Delamination

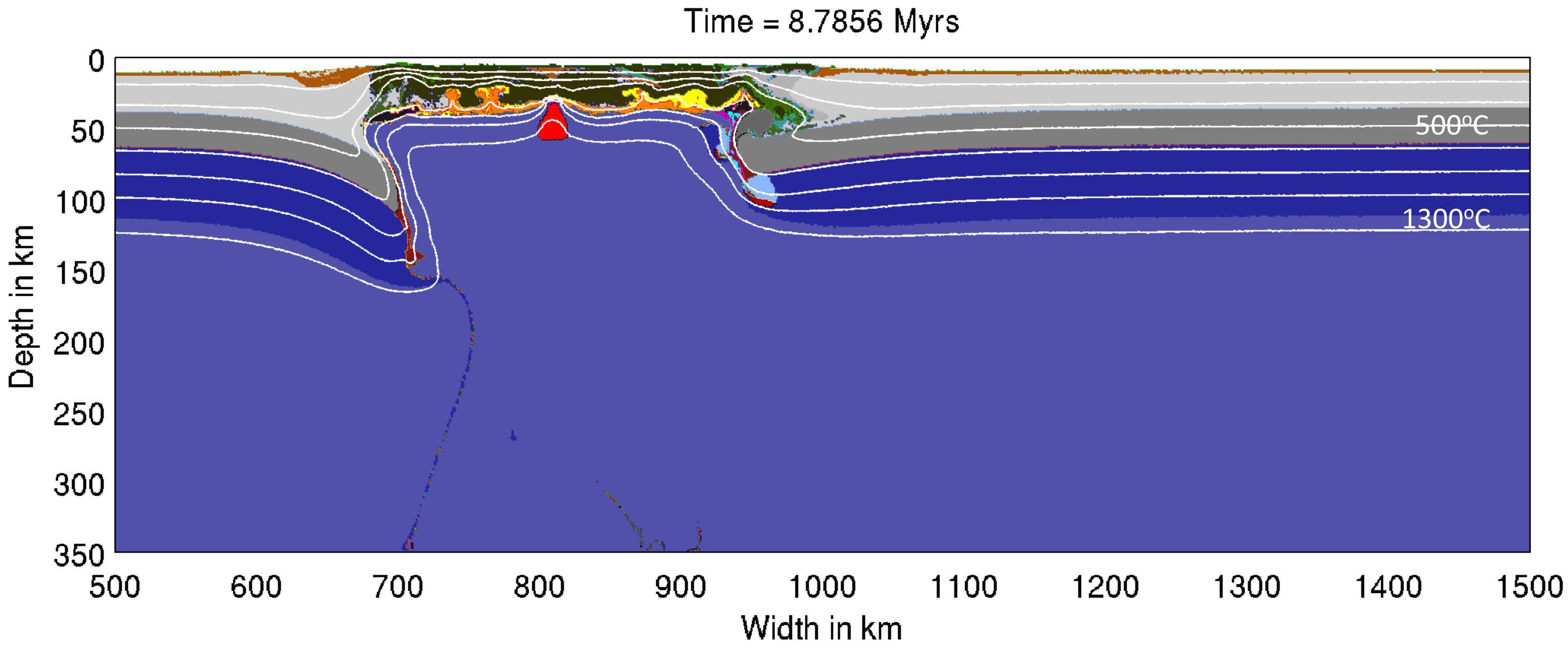

Delamination

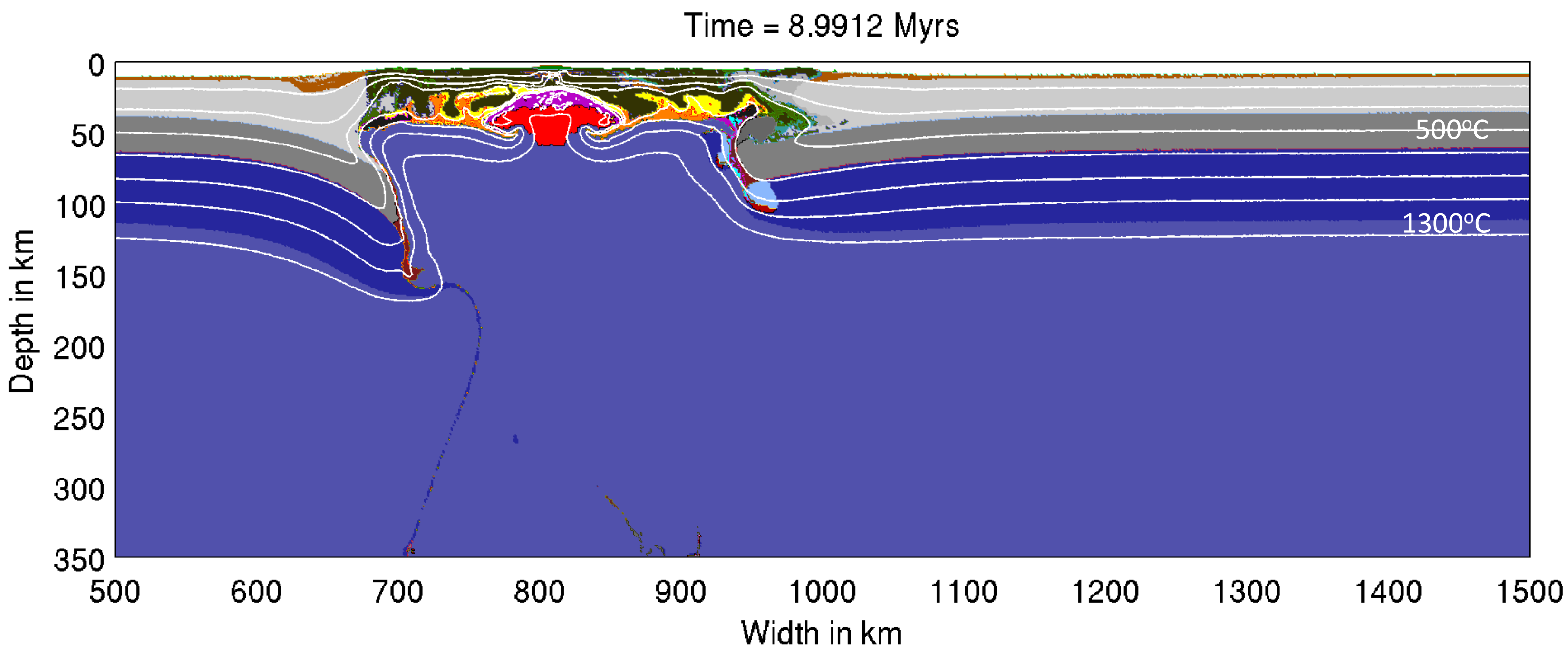

Delamination

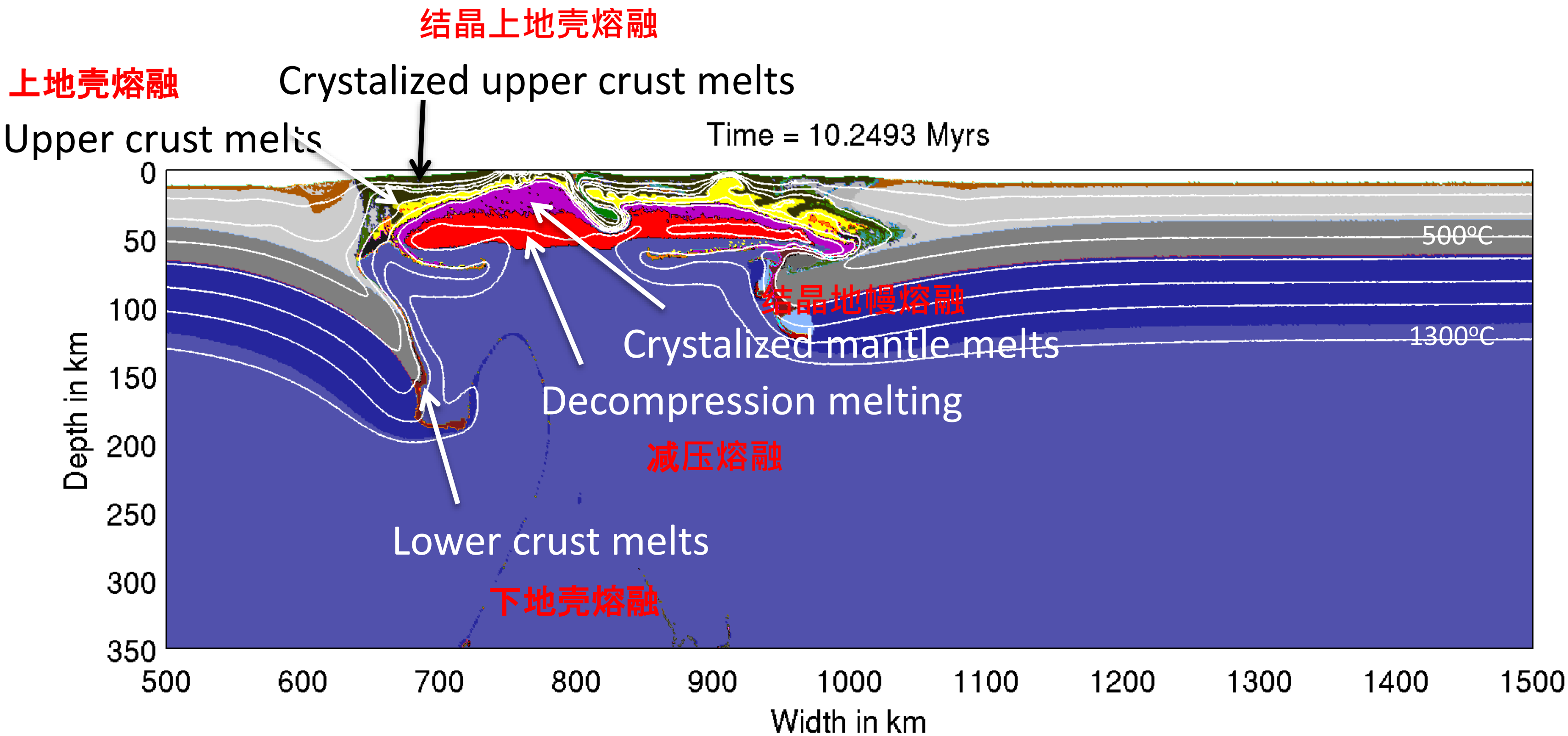

Delamination

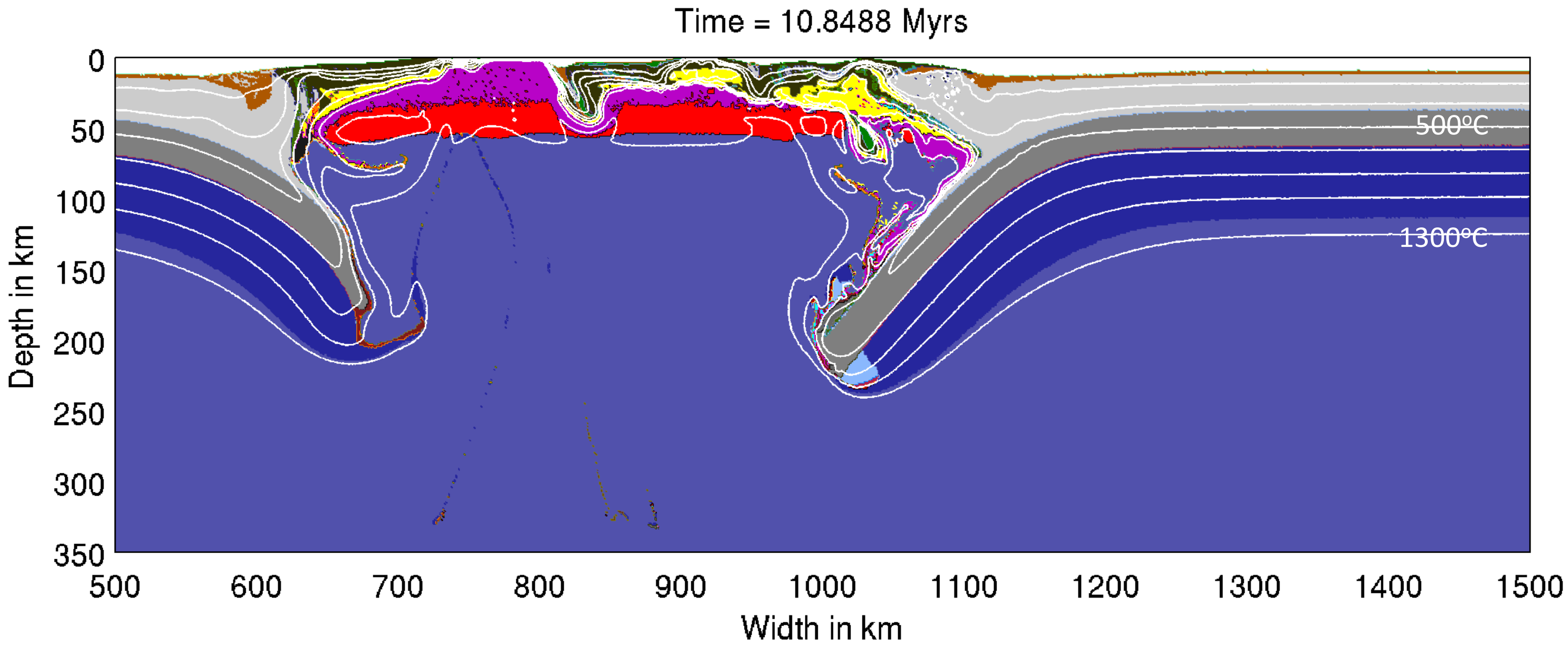

Delamination

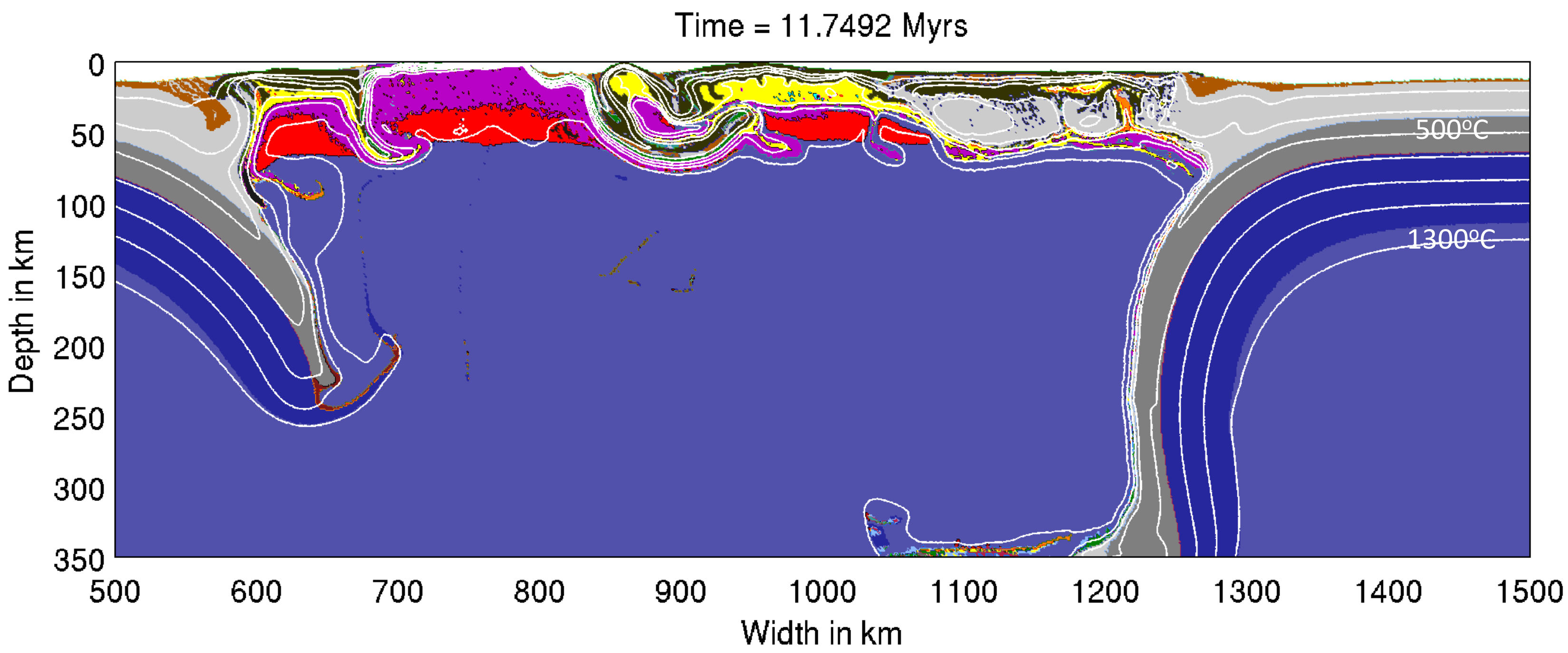

Delamination

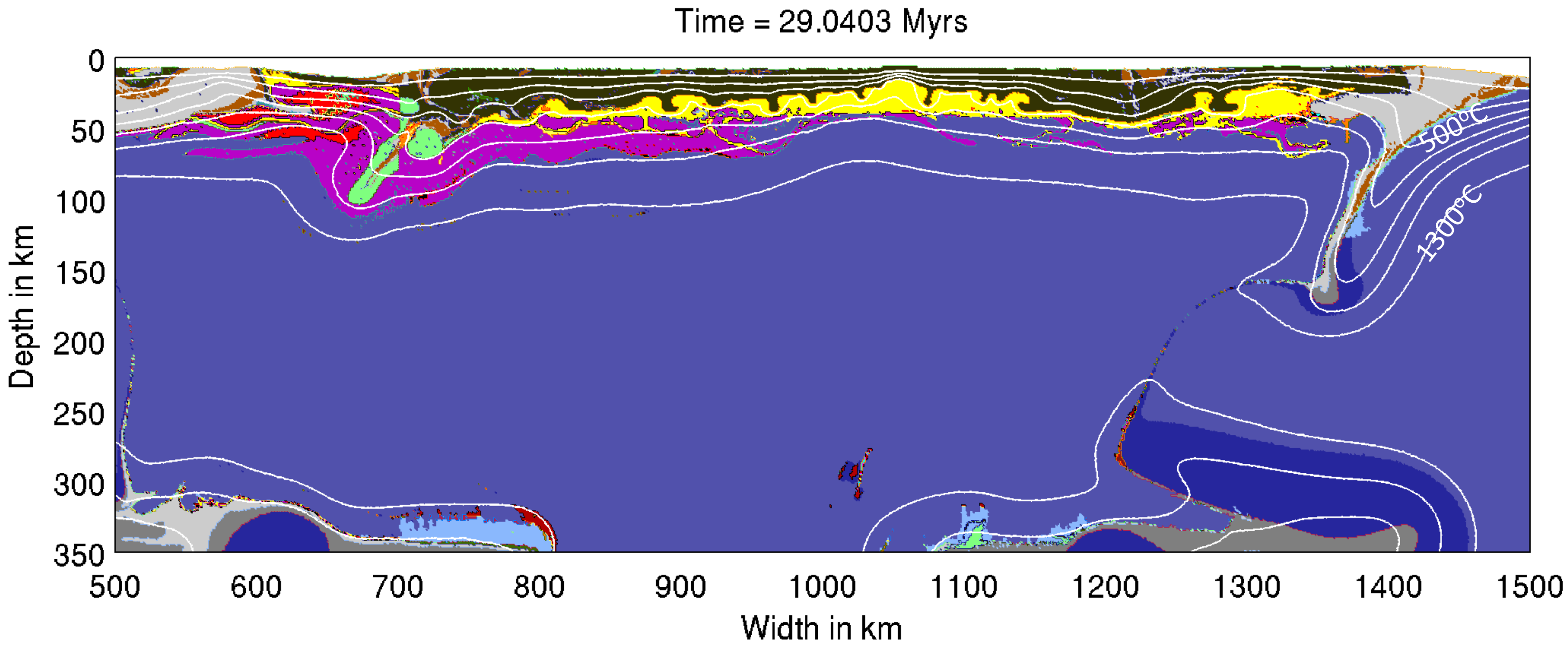

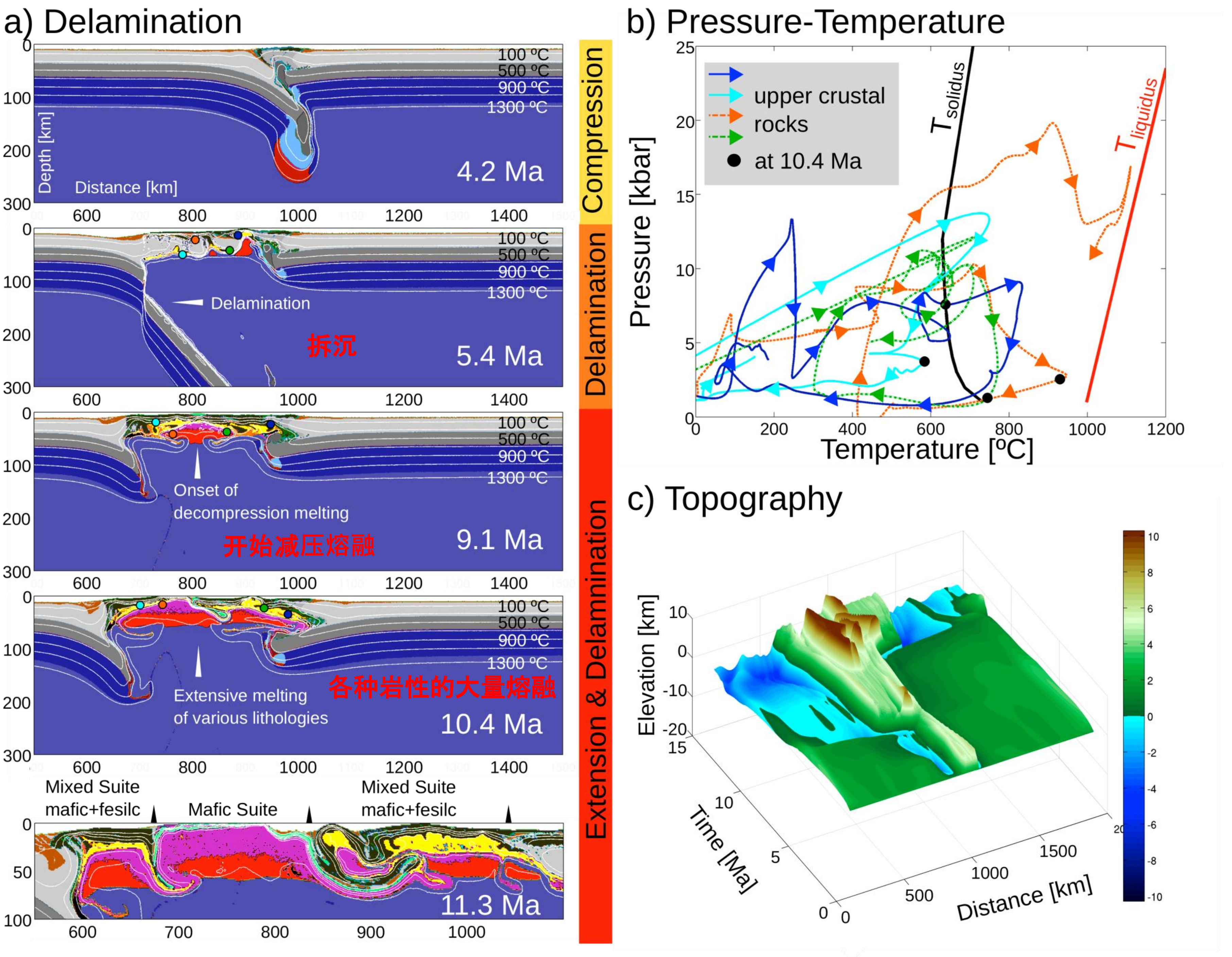
a) Delamination
b) Pressure-Temperature
c) Topography
Compression
Delamination
Extension & Delamination
Depth [km]
Distance [km]
100 ºC
500 ºC
900 ºC
1300 ºC
4.2 Ma
Delamination
拆沉
5.4 Ma
Onset of decompression melting
开始减压熔融
9.1 Ma
Extensive melting of various lithologies
各种岩性的大量熔融
10.4 Ma
Mixed Suite mafic+fesilc
Mafic Suite
Mixed Suite mafic+fesilc
11.3 Ma
upper crustal rocks
at 10.4 Ma
$T_{solidus}$
$T_{liquidus}$
Pressure [kbar]
Temperature [ºC]
Elevation [km]
Time [Ma]
Distance [km]

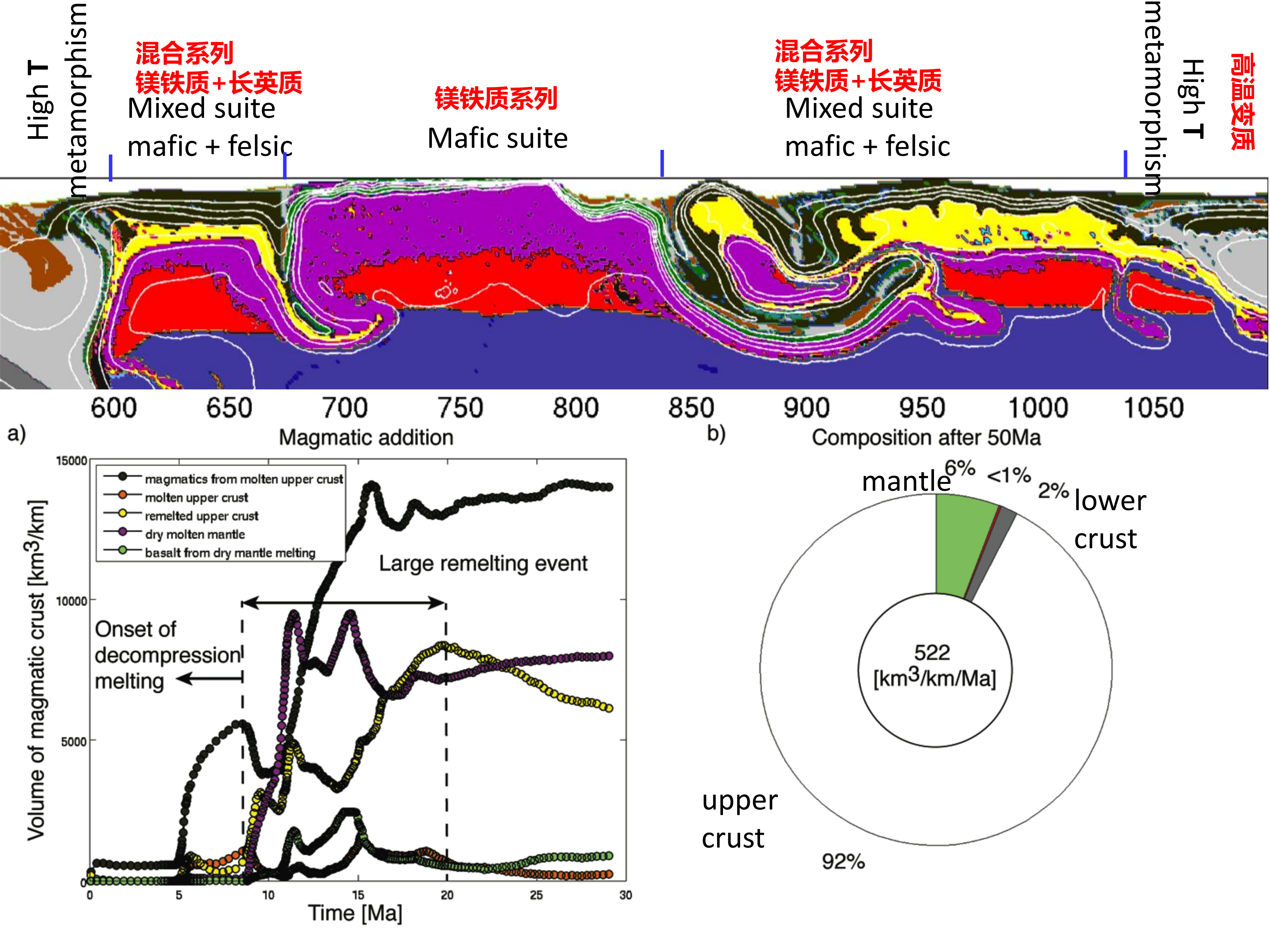

High T
metamorphism
混合系列
镁铁质+长英质
Mixed suite
mafic + felsic
镁铁质系列
Mafic suite
混合系列
镁铁质+长英质
Mixed suite
mafic + felsic
metamorphism
High T
高温变质
600
650
700
750
800
850
900
950
1000
1050
a)
Magmatic addition
b)
Composition after 50Ma
15000
10000
5000
0
Volume of magmatic crust [km3/km]
magmatics from molten upper crust
molten upper crust
remelted upper crust
dry molten mantle
basalt from dry mantle melting
Large remelting event
Onset of decompression melting
0
5
10
15
20
25
30
Time [Ma]
mantle
6%
<1%
2%
lower crust
522 [km3/km/Ma]
upper crust
92%

Modeling vs geology

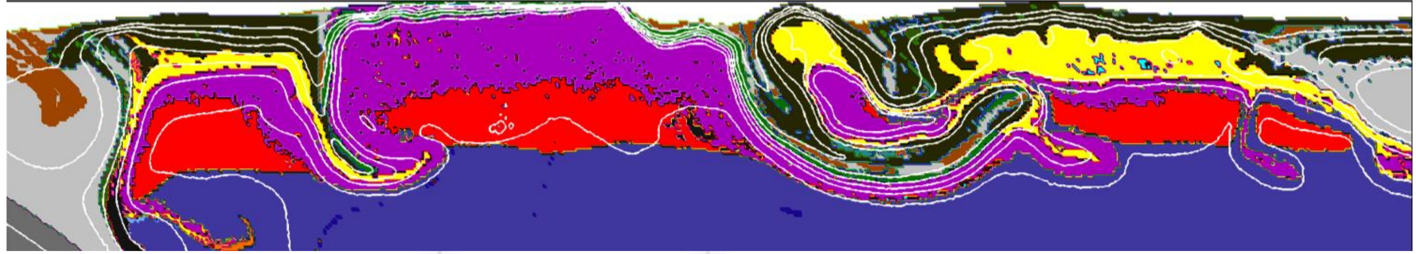

三叠纪晚期到中侏罗世
华北克拉通破坏

Possible scenario for destruction of the **North China Craton** During late Triasic to middle Jurassic

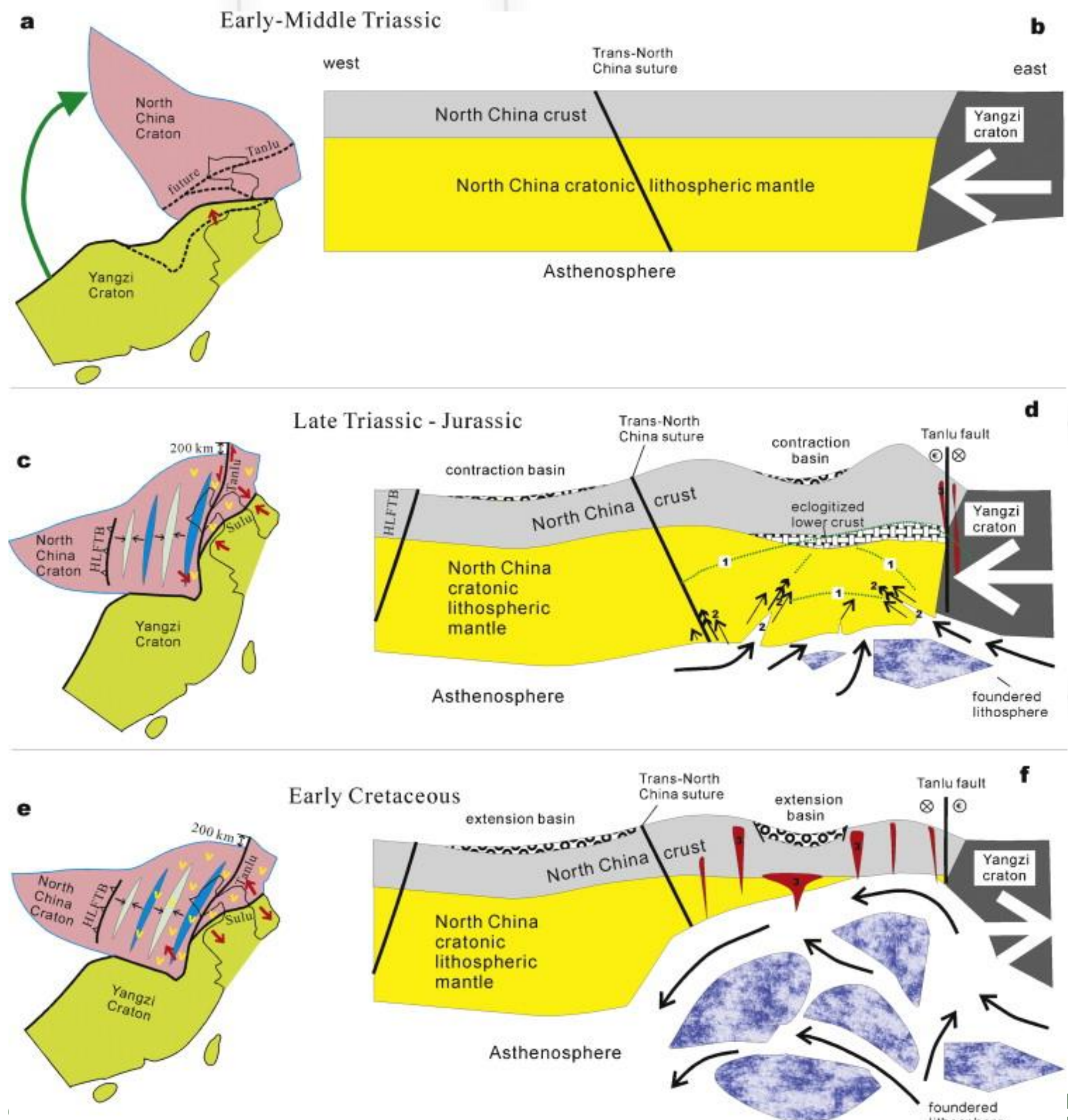

Initial setup:

Compression for 6Ma at rates: 0.5, 1, 2, 3 cm/a

Lithospheric thickness: 60, 80, 100, 200, 300 km

初始设置

6Ma压缩：

岩石圈厚度：

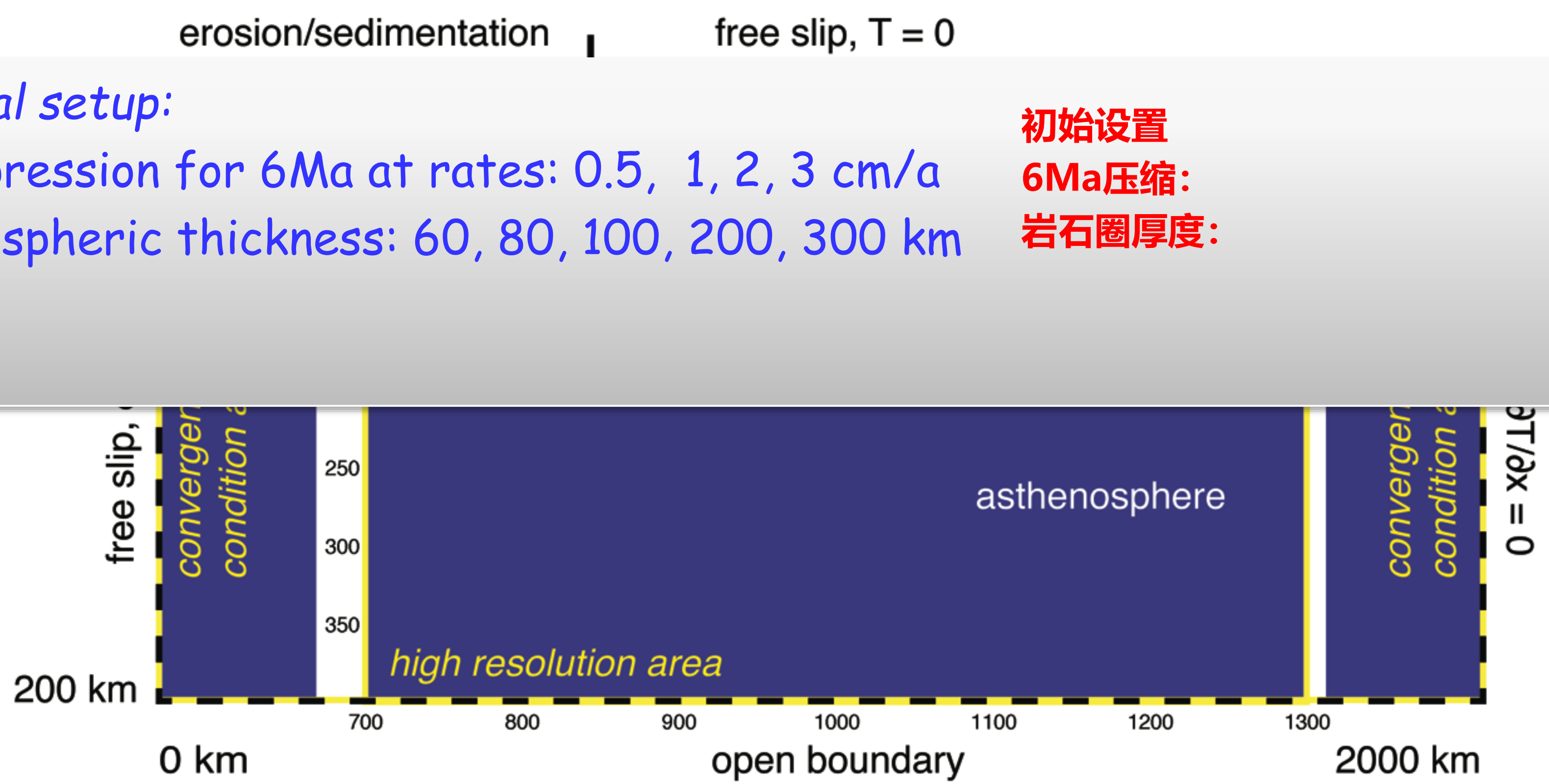

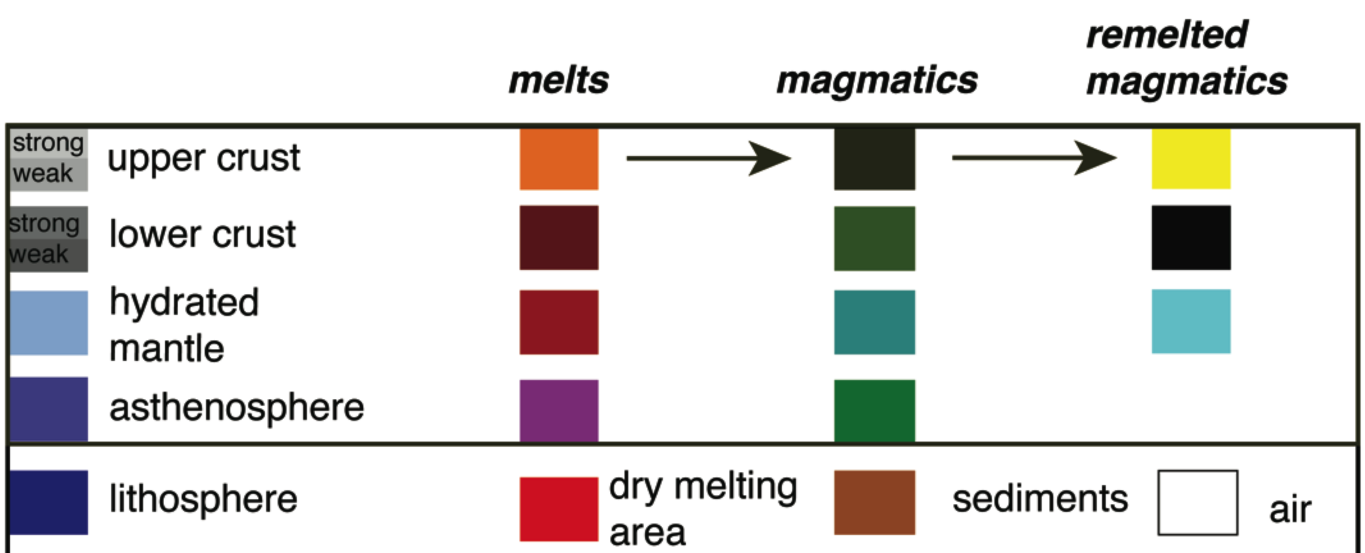

To conclude:

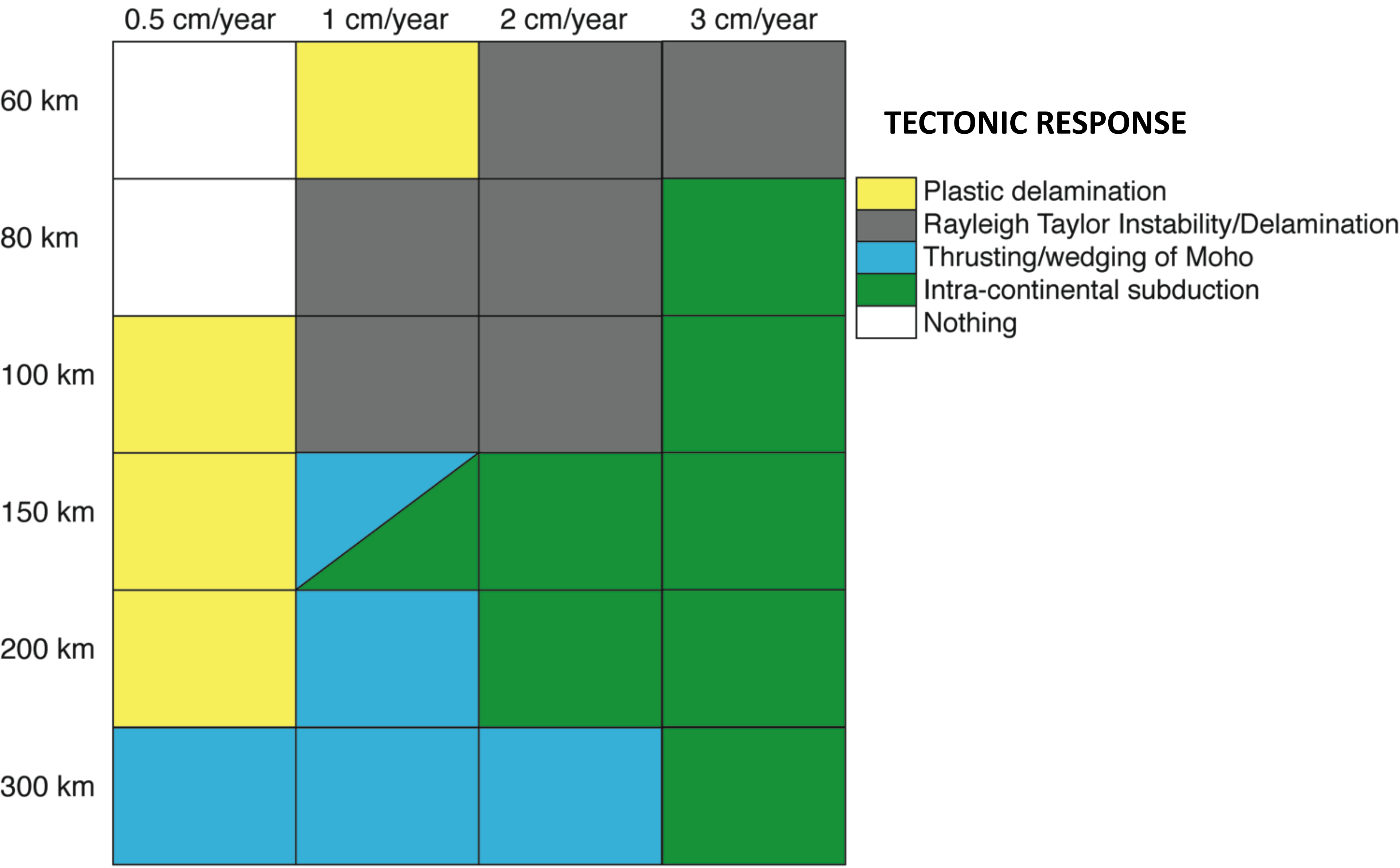
0.5 cm/year
1 cm/year
2 cm/year
3 cm/year
60 km
80 km
100 km
150 km
200 km
300 km
TECTONIC RESPONSE
Plastic delamination
Rayleigh Taylor Instability/Delamination
Thrusting/wedging of Moho
Intra-continental subduction
Nothing

To conclude:

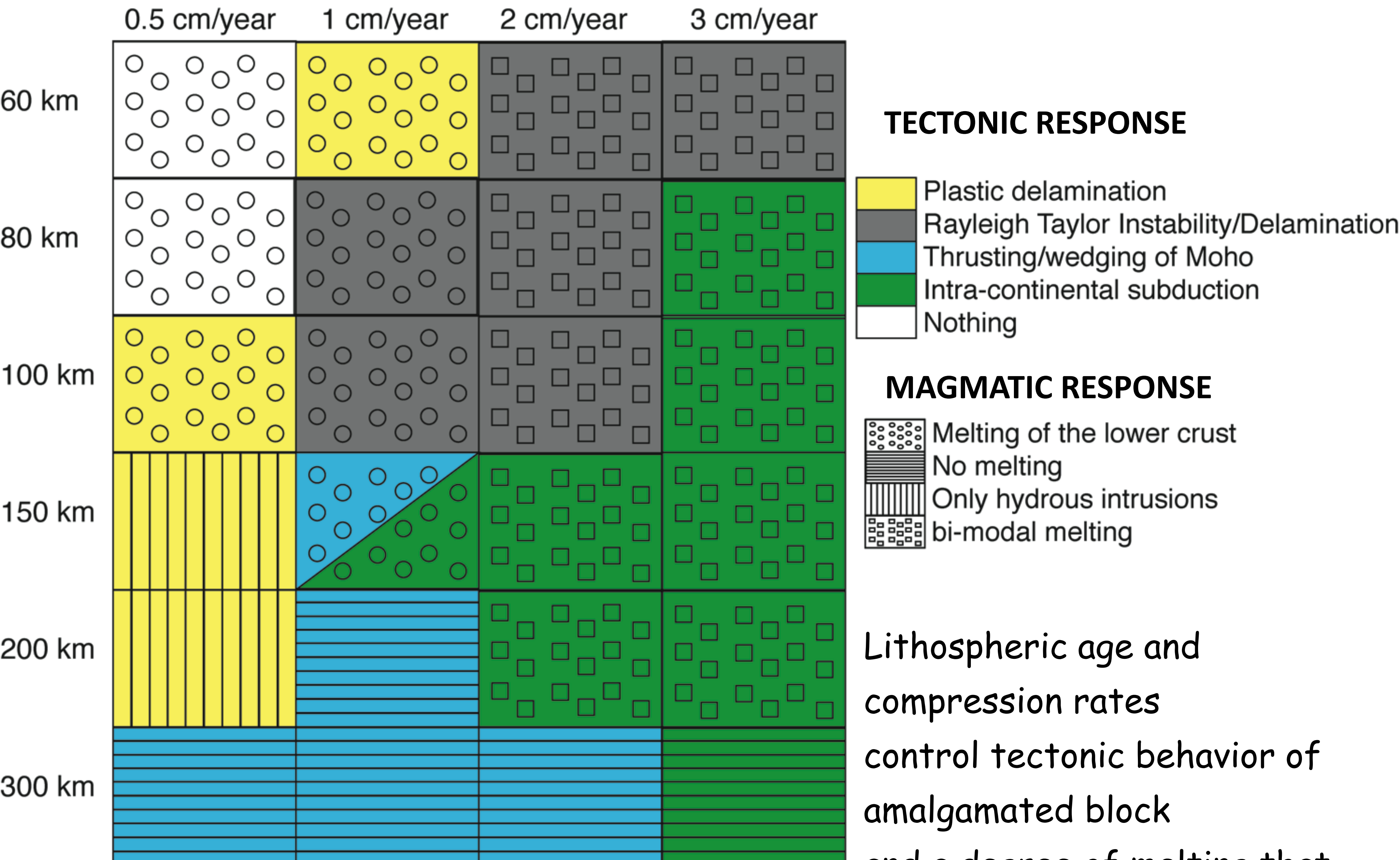

Lithospheric age and compression rates control tectonic behavior of amalgamated block and a degree of melting that occurs in these zones

岩石圈的年龄和压缩率控制构造行为特征。包括块汇聚，以及这些区域的一定程度熔融

3D

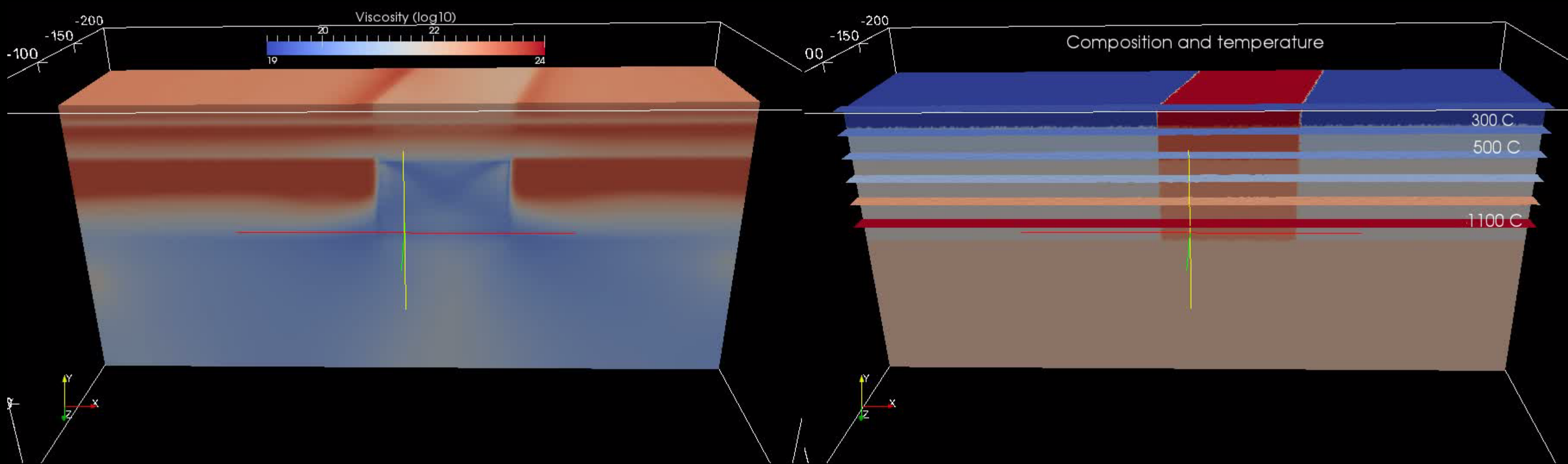

Viscosity (log10)
19
20
22
24
-200
-150
-100
Composition and temperature
300 C
500 C
1100 C

THE UNIVERSITY OF WESTERN AUSTRALIA

Thank you

Centre for EXPLORATION TARGETING

Australian Government
Australian Research Council

FIRST QUANTUM MINERALS LTD.

GEOLOGICAL SURVEY WESTERN AUSTRALIA

silverlake RESOURCES

ANGLOGOLD ASHANTI

SOUTH AUSTRALIA

Government of South Australia
Department of State Development

CSIRO

mriwa
Minerals Research Institute of Western Australia

Collaborators

Bruce Hobbs The University of Western Australia; CSIRO
Hans Muhlhaus The University of Queensland
Klaus Regenauer-Lieb University of New South Wales
Sarah Mikula CSIRO
Heather Sheldon CSIRO
Chris Wijns First Quantum Minerals
Brett Davies Normandy
Louis Moresi The University of Melbourne
Weronika Gorczyk The University of Western Australia
Klaus Gessner The Geological Survey of Western Australia